

NBSIR 82-2487

Hail Impact Testing Procedure for Solar Collector Covers

U.S. DEPARTMENT OF COMMERCE
National Bureau of Standards
National Engineering Laboratory
Center for Building Technology
Materials Division
Washington, DC 20234

April 1982

Prepared for
U.S. Department of Energy
Office of Solar Heat Technologies
Active Heating and Cooling Division
Washington, DC 20585

QC
100
U56
82-2487
1982
c. 2

NBSIR 82-2487

HAIL IMPACT TESTING PROCEDURE FOR SOLAR COLLECTOR COVERS

David R. Jenkins
Robert G. Mathey

U.S. DEPARTMENT OF COMMERCE
National Bureau of Standards
National Engineering Laboratory
Center for Building Technology
Materials Division
Washington, DC 20234

April 1982

Prepared for
U.S. Department of Energy
Office of Solar Heat Technologies
Active Heating and Cooling Division
Washington, DC 20585



U.S. DEPARTMENT OF COMMERCE, Malcolm Baldrige, *Secretary*
NATIONAL BUREAU OF STANDARDS, Ernest Ambler, *Director*

NATIONAL BUREAU
OF STANDARDS
LIBRARY

MAY 14 1982

Not recd

Q114

, USB

no. 82-2487

1982

C.2

HAIL IMPACT TESTING PROCEDURE FOR SOLAR COLLECTOR COVERS

by

David R. Jenkins* and Robert G. Mathey**

ABSTRACT

This report presents laboratory test results which simulate hail impact on solar collector covers. The general objective of the work is to contribute to the development of a test method for evaluating the resistance of solar collector covers to this type of loading. A procedure for such testing is described as well as results obtained with ice balls impacting four typical collector cover materials. Aspects which are discussed include the preparation of ice balls, the design and operation of a launcher for ice ball propulsion, the method of mounting cover panel specimens, the selection of ice ball velocity and impact location, and techniques for failure or damage assessment.

The research results show that ice balls of consistent diameter and mass can be prepared in the laboratory. Further, both analysis and results tend to show that acceptable simulation for evaluation or testing can be achieved with normal impacts of ice balls traveling at a resultant velocity which is the vector sum of the terminal velocity and a horizontal wind component. Results for a variety of impact locations are presented and for comparison purposes, arbitrarily selected points near the collector cover boundaries appear to be a reasonable choice. Finally, it is shown that for some collector cover materials, more than one kind of failure must be considered when evaluating test results. Test data for two types of tempered glass, semirigid fiber reinforced plastic, and flexible thin plastic film covers are presented.

Key Words: hail damage, hail impact testing, hail launcher, simulated hail testing, solar collector covers, test method development.

* Professor of Engineering, University of Central Florida, Orlando, Florida, on assignment to the National Bureau of Standards from September 1978 to September 1980 under provisions of the Intergovernmental Personnel Act.

** Center for Building Technology, National Bureau of Standards, Washington, DC.

ACKNOWLEDGMENT

This report was prepared under the sponsorship of the DoE Active Heating and Cooling Division, Office of Solar Heat Technologies.

The authors wish to acknowledge with thanks the contribution of Mr. Jessie C. Hairston of the National Bureau of Standards (NBS) for conducting the laboratory tests and for the fabrication of some of the test apparatus. The authors also recognize the contribution of David Waksman, Elmer R. Streed, Thomas W. Reichard, and Louis E. Cattaneo of NBS for the development of the first draft of a standard for use in the evaluation of the hail impact resistance of solar collector covers. This draft standard was published in National Bureau of Standards Report NBSIR 78-1305A, "Provisional Flat Plate Solar Collector Testing Procedures: First Revision," June 1978.

In addition, the authors are grateful for valuable comments provided by Ms. Elizabeth J. Clark of NBS regarding the selection of cover materials for test and for information pertaining to a proposed standard for evaluation of hail impact resistance of solar collector covers which was under consideration by ASTM E44.04.02 Cover Plate Task Group. This proposed standard was approved by ASTM in June 1981 and is designated as ASTM E822-81, "Practice for Determining Resistance of Solar Collector Covers to Hail by Impact with Propelled Ice Balls."

TABLE OF CONTENTS

	<u>Page</u>
ABSTRACT	iii
ACKNOWLEDGMENT	iv
LIST OF TABLES	vii
LIST OF FIGURES	x
CONVERSION FACTORS FOR METRIC (SI) UNITS	xii
1. INTRODUCTION AND PURPOSE	1
1.1 COVER MATERIALS AND FUNCTION	1
1.2 BACKGROUND	1
1.3 PURPOSE	2
1.4 SCOPE	2
2. HAIL TESTING CONCEPTS AND VARIABLES	4
2.1 MAJOR PARAMETERS	4
2.2 IMPACT LOADINGS AND STRESSES	5
2.3 SIMULATED HAIL TESTING BY OTHER INVESTIGATORS	6
2.4 LABORATORY TESTING	8
3. PREPARATION OF ICE BALLS	9
3.1 SIMULATION	9
3.2 THE SPLIT MOLD APPROACH	9
3.3 CASTING PROCEDURE	11
4. LAUNCHER	14
4.1 COMPRESSED AIR GUN	14
4.2 INTERCHANGEABLE BARRELS	14
4.3 TIMING RANGE	20
4.4 OPTICAL POINTER	20
5. MOUNTING OF COVER SPECIMENS	23
5.1 COVER SUPPORT FRAMES	23
5.2 PLACING SPECIMENS IN THE FRAMES	23
5.3 SUPPORT FRAME POSITIONER	25
6. ICE BALL VELOCITY AND IMPACT POINTS	32
6.1 ALTERNATIVE LABORATORY VELOCITIES	32
6.2 VALUES OF TERMINAL VELOCITY AND WIND VELOCITY	32
6.3 MAGNITUDE OF THE NORMAL VELOCITY	34
6.4 IMPACT LOCATIONS ..	38
7. FAILURE OR DAMAGE ASSESSMENT	40
8. TEST PROCEDURE	48

TABLE OF CONTENTS (Continued)

	<u>Page</u>
9. TEST RESULTS	49
9.1 GENERAL	49
9.2 TEMPERED GLASS, TEXTURED SIDE EXPOSED	51
9.3 TEMPERED GLASS, BOTH SIDES SMOOTH	52
9.4 SEMIRIGID FIBER REINFORCED PLASTIC SHEET	52
9.5 FLEXIBLE THIN PLASTIC FILM	53
9.6 TEMPERED GLASS MOUNTED IN SOLAR COLLECTORS	54
10. CONCLUSIONS	57
11. REFERENCES	58
APPENDIX A IMPACT TEST DATA	A1

LIST OF TABLES

		<u>Page</u>
Table 1.	Interchangeable Barrel Materials and Dimensions	17
Table 2.	Ice Ball Parameters for Laboratory Testing	33
Table 3.	Summary of Ice Ball Impact Test Results	50
Table A-1	Tempered Glass Exposed Side Textured 1/8 in. Thick	A2
Table A-2	Tempered Glass Exposed Side Textured 1/8 in. Thick	A2
Table A-3	Tempered Glass Exposed Side Textured 1/8 in. Thick	A2
Table A-4	Tempered Glass Exposed Side Textured 1/8 in. Thick	A3
Table A-5	Tempered Glass Exposed Side Textured 1/8 in. Thick	A3
Table A-6	Tempered Glass Exposed Side Textured 1/8 in. Thick	A3
Table A-7	Tempered Glass Exposed Side Textured 1/8 in. Thick	A3
Table A-8	Tempered Glass Exposed Side Textured 1/8 in. Thick	A4
Table A-9	Tempered Glass Exposed Side Textured 1/8 in. Thick	A4
Table A-10	Tempered Glass Exposed Side Textured 1/8 in. Thick	A4
Table A-11	Tempered Glass Exposed Side Textured 1/8 in. Thick	A4
Table A-12	Tempered Glass Both Sides Smooth 1/8 in. Thick	A5
Table A-13	Tempered Glass Both Sides Smooth 1/8 in. Thick	A5
Table A-14	Tempered Glass Both Sides Smooth 1/8 in. Thick	A5
Table A-15	Tempered Glass Both Sides Smooth 1/8 in. Thick	A6

LIST OF TABLES (continued)

		<u>Page</u>
Table A-16	Tempered Glass Both Sides Smooth 1/8 in. Thick	A6
Table A-17	Tempered Glass Both Sides Smooth 1/8 in. Thick	A6
Table A-18	Tempered Glass Both Sides Smooth 1/8 in. Thick	A7
Table A-19	Tempered Glass Both Sides Smooth 1/8 in. Thick	A7
Table A-20	Tempered Glass Both Sides Smooth 1/8 in. Thick	A7
Table A-21	Tempered Glass Both Sides Smooth 1/8 in. Thick	A7
Table A-22	Tempered Glass Both Sides Smooth 1/8 in. Thick	A8
Table A-23	Reinforced Plastic Polyester Resin With Glass Fiber Mat 0.040 in. Thick	A8
Table A-24	Reinforced Plastic Polyester Resin With Glass Fiber Mat 0.040 in. Thick	A8
Table A-25	Reinforced Plastic Polyester Resin With Glass Fiber Mat 0.040 in. Thick	A9
Table A-26	Reinforced Plastic Polyester Resin With Glass Fiber Mat 0.040 in. Thick	A9
Table A-27	Reinforced Plastic Polyester Resin With Glass Fiber Mat 0.040 in. Thick	A9
Table A-28	Reinforced Plastic Polyester Resin With Glass Fiber Mat 0.040 in. Thick	A10
Table A-29	Reinforced Plastic Polyester Resin With Glass Fiber Mat 0.040 in. Thick	A10
Table A-30	Poly(Vinyl Fluoride) Film 0.004 in. Thick	A10
Table A-31	Poly(Vinyl Fluoride) Film 0.004 in. Thick	A11
Table A-32	Poly(Vinyl Fluoride) Film 0.004 in. Thick	A11
Table A-33	Poly(Vinyl Fluoride) Film 0.004 in. Thick	A11
Table A-34	Poly(Vinyl Fluoride) Film 0.004 in. Thick	A12
Table A-35	Poly(Vinyl Fluoride) Film 0.004 in. Thick	A12

LIST OF TABLES (continued)

		<u>Page</u>
Table A-36	Poly(Vinyl Fluoride) Film 0.004 in. Thick	A12
Table A-37	Poly(Vinyl Fluoride) Film 0.004 in. Thick	A13
Table A-38	Tempered Glass Both Sides Smooth 1/8 in. Thick Mounted in Solar Collector	A13
Table A-39	Tempered Glass Both Sides Smooth 1/8 in. Thick Mounted in Solar Collector	A13
Table A-40	Tempered Glass Both Sides Smooth 1/8 in. Thick Mounted in Solar Collector	A14
Table A-41	Tempered Glass Both Sides Smooth 1/8 in. Thick Mounted in Solar Collector	A14
Table A-42	Tempered Glass Both Sides Smooth 1/8 in. Thick Mounted in Solar Collector	A14
Table A-43	Tempered Glass Both Sides Smooth 1/8 in. Thick Mounted in Solar Collector	A14

LIST OF FIGURES

	<u>Page</u>
Figure 1. Cross Section of Metal Mold Pattern for Making Rubber Molds Used to Cast Ice Balls	10
Figure 2. Silicone Rubber Ice Ball Molds	12
Figure 3. Overall View of Launcher System	15
Figure 4. Compressed Air Gun	16
Figure 5. Interchangeable Barrels for the Compressed Air Gun	18
Figure 6. Installation of Barrel in the Compressed Air Gun	19
Figure 7. Optical Pointer for the Hail Gun	21
Figure 8. Schematic of the Optical Pointer	22
Figure 9. Sketch of Assembled Support Frame	22
Figure 10. Typical Support Frame Cross Sections	24
Figure 11. Corner Strap for Support Frames	24
Figure 12. Tensioning of Film Cover Material	26
Figure 13. C-Clamp Weights Attached to Film Cover Material	27
Figure 14. Hole in Film Cover Material to Permit Bolt Passage	28
Figure 15. Transverse Loading of Film Cover to Check Consistency of Tensioning	29
Figure 16. Lift Truck Modified as a Support Frame Positioner	31
Figure 17. Three-Dimensional Relationship of Resultant Velocity and Normal Component of Resultant Velocity	35
Figure 18. Two-Dimensional Relationship of the Hailstone Velocity Components and the Normal Velocity Component for Wind Direction Perpendicular to the Horizontal Edge of An Inclined Collector	35
Figure 19. Assumed and Actual Normal Velocity Values for Various Terminal Velocities	37
Figure 20. Layout of Impact Points	39

LIST OF FIGURES (continued)

	<u>Page</u>
Figure 21. Overall View of a Textured Surface Tempered Glass Cover Specimen After Fracture	41
Figure 22. Hole in Tempered Glass Cover Specimen Caused by Impact of an Ice Ball	42
Figure 23. Localized Cracking Failure in Reinforced Plastic Cover Caused by Impact of an Ice Ball	43
Figure 24. Cylinder Sealed to Reinforced Plastic Material for Leak Testing	44
Figure 25. Tearing and Penetration Through Reinforced Plastic Cover Material Caused by Impacting Ice Ball	45
Figure 26. Indentations in Plastic Film Cover	47
Figure 27. Puncture Failures of Plastic Film Cover	47
Figure 28. Detail of Solar Collector Edge Support	56

CONVERSION FACTORS FOR METRIC (SI) UNITS

Physical Quantity	To Convert From	To	Multiply By
Length	ft	m	3.048×10^{-1}
Length	in	m	2.54×10^{-2}
Force	lbf	N	4.448
Mass	lbm	kg	4.536×10^{-1}
Force/length	lbf/ft	N/m	1.459×10
Velocity	ft/s	m/s	3.048×10^{-1}
Temperature	°F	°C	$t^{\circ}\text{C} = (t^{\circ}\text{F} - 32) / 1.8$
Energy	ft-lbf	J	1.356
Momentum	lbf-s	N-s	4.448

1. INTRODUCTION AND PURPOSE

1.1 COVER MATERIALS AND FUNCTION

This report presents testing procedures and test results for flat plate solar collector cover materials subjected to simulated hail impact. The cover materials examined are representative of the three classes normally encountered, namely, rigid, semirigid, and flexible. Tempered glass is a typical rigid cover, fiber reinforced plastic is a typical semirigid cover, and polymeric thin film is a typical flexible cover.

In a solar collector, the cover plate (or cover plates since double covers are often used) in addition to protecting the interior of the collector from the weather has at least three functions which affect collector efficiency. Most importantly, the cover permits transmission of solar energy to the absorber plate and consequently its transmittance should be as high as possible. Secondly, the cover may suppress infrared reradiation from the absorber plate. Thirdly, by maintaining a confined air space between the cover and the absorber plate, the cover plate tends to reduce convective heat loss from the absorber plate. Thus, cover failure can substantially degrade the operation of the entire system. Failure of a collector cover by hail impact can occur by several means. Unquestionably, complete rupture of the cover material where the cover plate is destroyed is one type of failure. Also, extensive crazing, fine crack development, or surface distortion which substantially reduce transmission could be looked upon as failure. Further, local rupture of the cover material which allows air exchange from inside to outside may be considered to be a failure. Such a local rupture may also permit moisture penetration into the collector which could cause degradation of the absorber plate and insulation and result in a decrease in thermal performance of the collector. It is noted that cover plate failures affect the function or serviceability of collectors and are not in general a safety problem. A possible exception to this could be with annealed glass or other materials which break in a similar manner and could give off large flying shards.

1.2 BACKGROUND

Laboratory evaluation of hail impact resistance may be performed for several reasons: (1) to evaluate impact resistance of a single material or collector; (2) to compare the impact resistance of several materials or collectors; (3) to provide a common basis for selection of cover materials or collectors for use in various geographic areas; or (4) to evaluate changes in impact resistance due to environmental factors such as weather. The purpose of the testing may influence the choice of testing parameters. If the purpose of the testing is to determine the minimum size hail ball causing damage, testing will proceed with progressively larger ice balls until the cover material sustains damage. However, if the purpose of the testing is to determine whether a collector could be used in a specific geographic region, it would be necessary to test the cover using ice balls of the selected size and corresponding velocity

for satisfactory service in that region. Simiu and Cattaneo [1]* proposed maximum hailstone sizes corresponding to a 20-year mean recurrence interval for various regions of the United States. An appropriate hailstone size and corresponding velocity can be selected from reference [1] or from a similar governing or advisory document [2].

Prior to the approval of the American Society for Testing and Materials Standard designated as ASTM E 822-81 in June 1981, "Standard Practice for Determining Resistance of Solar Collector Covers to Hail by Impact with Propelled Ice Balls," there was no standard method available to evaluate the impact resistance of covers. The early Department of Housing and Urban Development (HUD) Minimum Property Standards [3] and the Interim Performance Criteria prepared by National Bureau of Standards (NBS) for Department of Energy (DoE) and HUD, respectively [4, 5], had requirements for testing such as hail ball size for geographic regions, but did not have a test method.

1.3 PURPOSE

The primary purpose of the research reported here is to contribute to the development of a test method for simulating hail impact on solar collector covers. For some time now, the general outlines of a test method have been in existence [6, 7], namely to propel ice balls or other hail simulators with a known velocity at a target consisting of the material to be evaluated. The broad requirements for the test method were that the laboratory procedure provide good simulation of hail storm events and that the method be a practical one that can be reproduced by a number of laboratories at reasonable cost.

Consequently, the work reported herein has emphasized the refinement of testing procedures and data evaluation procedures rather than the accumulation of extensive additional data on hail impact resistance of specific solar collector cover materials.

1.4 SCOPE

The hail impact test procedure for covers used in flat plate solar collectors was based on many factors. Most importantly were those dealing with the velocities of ice balls used to simulate hail, impact loads caused by falling hail and propelled ice balls, impact locations on the collector cover, support conditions for the covers, and failure or damage assessment of collector covers caused by impacting ice balls.

Other factors considered were the procedures, techniques, equipment, and methods of test and fabrication for the different phases of the hail impact testing procedure. A procedure is given for the preparation of ice balls which includes a method for making ice ball molds. A launcher for propelling ice balls is described along with a timing device for measuring their velocity. An optical pointer technique for alignment of the barrel of the launcher on a

* Numbers in brackets indicate references listed in section 11.

selected target area on the solar collector cover is described. Also, a method for mounting the cover material in a cover support frame is given together with a method to position the cover support frame during testing.

Test results are presented for the impact resistance of rigid, semirigid, and flexible cover materials mounted in cover support frames and for tempered glass mounted in flat plate solar collectors. This testing was performed to evaluate the test method. It was not intended to develop a comprehensive data base that could be used to determine the suitability of specific products. Since the properties of a specific product are highly dependent on the formulation, method of manufacture, and other variables it is not possible to draw conclusions for generic classes of materials.

Based upon the laboratory impact testing experience at the National Bureau of Standards (NBS) a standard for use in evaluation of hail impact resistance of solar collector covers was drafted and submitted to ASTM Committee E44 on Solar Energy Conversion, Subcommittee E44.04 on Materials Performance. The ASTM Cover Plate Task Group, E44.04.02, prepared the standard practice designated as ASTM E822-81, "Practice for Determining Resistance of Solar Collector Covers to Hail by Impact with Propelled Ice Balls." During the conduct of this study to develop a hail impact testing procedure for solar collector covers, information was provided by NBS to the Task Group for consideration for their draft standard. The laboratory work described in this report supports and explains the major elements of the ASTM standard.

2. HAIL TESTING CONCEPTS AND VARIABLES

2.1 MAJOR PARAMETERS

When evaluating the damage risk which hail presents to solar collector installations, a number of parameters must be considered. Only a brief overview of the significant parameters will be presented. The parameters pertaining to hail which will be discussed are frequency of occurrence, size, specific gravity, speed, angle of velocity vector with collector surface, and kinetic energy. Other parameters to be considered are the mounting method of the cover and the location of hail impact. Simiu and Cattaneo [1] have presented a summary of published data applicable to hail load determination. As is true for loadings associated with most natural phenomena, randomness suggests a statistical rather than deterministic approach. The frequencies of occurrence of storms containing hail and the hailstone diameter distribution vary with the region of the United States. Hail frequency maps are available which show the average number of days with hail in various areas. In recent years, the availability of increased hail data and the use of more sophisticated statistical analyses has made it possible to estimate the maximum size of hail to be expected under various conditions [1].

Specific gravity of hail is an important consideration since it appears to be less than that of ice due to air entrapped in the hailstone as it freezes [1]. However reported values often do not show a great variation from solid ice having a specific gravity of 0.92 and thus the use of ice balls in simulating hail impact does not seem to be excessively conservative [8, 9].

The speed at which a hailstone strikes an object is also a critically important parameter. Much attention has been devoted to this subject by other investigators and their work is discussed in section 6.2. In general it has been observed that hailstones fall at a terminal velocity which occurs when the weight of the hailstone equals the drag force. Since most hailstones are accompanied by wind it seems reasonable to add vectorially a horizontal wind component to the vertical terminal velocity component. For this research program, a resultant velocity was used which was based on a 66 ft/s horizontal wind velocity and the appropriate terminal velocity for a given hailstone diameter (section 6.2). The angle which the velocity vector makes with the collector surface is another important consideration and the conservative assumption of normal impact at terminal or at a resultant velocity is usually made in testing (section 6.3).

Finally, the kinetic energy of a hailstone,

$$\text{Kinetic energy} = 1/2 mV^2 \quad (1)$$

where: m = mass of hailstone
 V = velocity of hailstone,

while it is a combination of other parameters, is one measure of the intensity of impact on the cover surface. Since kinetic energy is not conserved when the ice ball or hailstone hits the cover, part of the kinetic energy is consumed

in fracturing of the ice ball, part goes into work done to deform the cover, and part is used by the ice ball or its fragments which rebound from the cover surface.

An alternate measure of the intensity of impact on the cover surface is the momentum of the hailstone, that is,

$$\text{Momentum} = mV \quad (2)$$

where m and V are as defined above. While momentum is conserved in the impact, this fact is not easy to exploit since the masses and flight paths of all hail ball fragments after impact are difficult to determine.

It has been shown experimentally that the method of mounting a cover (i.e., its support condition) and the location at which ice balls impact the cover affect its resistance to impact. As an example, the corners are in general the most critical impact points (see section 6.4).

2.2 IMPACT LOADINGS AND STRESSES

The exact nature of the impact loading, or impulse loading, which occurs when the cover is struck by an ice ball is complex and may be difficult to fully define. Impulse is by definition, the load versus time history at the point of impact. This aspect of hail impact has not yet been well studied and might be an appropriate subject for future investigation. The exact nature of the impulse depends on the deformation of the ice ball and of the cover material while they are in contact, on whether fragmentation of the ice ball occurs during the contact period, and on whether fracture of the cover material occurs during this period. Consequently, it is extremely difficult to experimentally define the load-time curve for the full duration of the impulse. Alternatively, it is possible to determine the duration of the impulse or the length of time the ice ball and cover are in contact and it may be possible to determine the total impulse or area under the load-time curve since total impulse is equal to the change in momentum of the impacting objects, that is

$$\int_{t_1}^{t_2} F \, dt = \Sigma \Delta m_i \cdot \Delta v_{i2} - m V_1 + \text{Cover momentum} \quad (3)$$

where:

- F = normal force
- t = time
- m = mass of ice ball
- Δm_i = mass of pieces of ice ball
- V_1 = velocity of ice ball, initial
- Δv_{i2} = velocity of pieces of ice ball, final.

The duration of the impulse is $t_2 - t_1$. When the duration of the impulse is compared to the natural period of vibration of the plate-like collector cover, characterizing the impact response can sometimes be simplified. For example,

an approximate analysis of dynamic load response for a single degree of freedom system indicates that, if the duration of the impulse is short relative to the natural period of the structure, then the maximum displacement amplitude and consequently the maximum stress depend only on the impulse height or magnitude [10]. Impulse durations were not determined in this research program.

If the form of the impulse can be approximated, the relationship between the time varying forces and the stresses in the cover material may be clarified by the use of structural mechanics. Since the collector cover can in most cases be considered as a thin plate by structural mechanics definition and since the rapid loading probably assures elastic material behavior up to failure, dynamic elastic plate analysis may give reasonable predictions of cover deflections and stresses. The largest stresses in a plate would be normal to its cross section at the plate surfaces. The technique of modal analysis would seem to be appropriate and would be applicable to point impact loadings [11]. However, the edge support conditions of a cover in a solar collector or in a laboratory support frame are not usually the same as the simply supported edges assumed in most published analysis. By definition a simple support is one in which there is no vertical deflection of the plate and there is unrestrained rotation at the supports about lines parallel to the edges of the plate. This uncertainty in the support conditions of covers in collectors could bring into question the validity of quantitative predictions made by dynamic plate theory. Qualitatively this analytical technique may be used to compare the stress levels produced by impacts at various points on the plate. Later it is noted that failure appears to initiate on the "back" side of the cover, that is the surface opposite to the contact surface. This suggests that plate action may predominate.

Mechanics analysis may also provide some insight into the localized stresses caused by contact between the spherical ice ball and the flat cover plate. These so-called contact stresses were originally calculated by Hertz [12] and tend to cause failure below the contact surface due to large shearing stresses in that region. Again, elastic material behavior of the cover plate and ice balls is assumed. The radius of curvature of the spherical ice ball would affect the stress level produced as would the instantaneous value of the load acting between the two bodies.

To summarize this discussion of impact stress prediction, several possibly significant parameters can be added to those already mentioned in section 2.1. These include the duration of the impulse, the total impulse, the support conditions of the cover in its supporting frame, and the radius of curvature of the ice ball.

2.3 SIMULATED HAIL TESTING BY OTHER INVESTIGATORS

The potential damage which can be caused by hail to exposed portions of buildings and to equipment, such as solar devices, mounted on buildings has made simulated hail testing a subject of interest to a number of investigators. Greenfeld [6], while a Research Associate at the National Bureau of Standards, used an early configuration of the equipment used in the research of this report, and is described later, to study hail resistance of roofing products.

Mathey [7] used basically the same equipment with a modified velocity timer to investigate hail resistance of aluminum skin honeycomb panels. Although details of the current configuration will be presented later, it is noted here for information purposes that this test apparatus uses a compressed air gun for firing an ice ball horizontally at controlled velocity toward the "exposed" surface of a test object. A timer for velocity measurement is included. Ice balls cast in silicone rubber molds are used.

Smith [13], at Texas Tech University, has developed equipment for hail impact testing of solar reflector panel mirror materials and other materials. He also uses a compressed air gun or air cannon with interchangeable barrels to accommodate ice balls of 1.0 in., 1.5 in., 2.0 in., and 2.5 in. diameter. His simulated hailstones or ice balls are cast in a spherical shape by a unique process. In this process, enough water is poured into a rubber balloon for the desired ice ball size. The portion of the balloon containing the water is placed in a spherical mold and then the mold is placed in a freezer. When an ice ball is fired, photoelectric timing gates are actuated by ice ball passage and are used to start and stop an electronic timer. In Smith's test procedure ice balls of a selected size are fired at the target at increasing velocities until failure occurs or until terminal velocity is exceeded by some margin.

Moore, Wilson, and Ross [14, 15], of the Jet Propulsion Laboratory have reported a simulated hail impact apparatus for testing photovoltaic solar panels. Their compressed air gun fires ice balls vertically upward. Interchangeable barrels for various ice ball sizes are employed. A photoelectric velocity measuring system is used. Instead of casting ice balls, Moore, Wilson, and Ross mold pieces of ice into a spherical shape in a hand operated press after which the ice balls are frozen. These authors in addition to observing the type of mechanical failure produced, made high speed movies of ice ball impacts. From an analysis of the individual frames of the high speed movies, they concluded that ice ball deceleration is complete in about 0.001 s after initial contact, that failure initiates in less than 0.002 s after initial contact in glass panels, and that failure is initiated on the back side of a glass panel in a plate bending mode. In most of their tests on glass panels, ice balls shattered on impact. With a view to developing a simpler alternative test method, steel balls of various diameters were dropped from various heights on the cover plate materials and the results of damage were compared with the damage caused by ice balls. It was difficult to find a correlation between the steel and ice ball data for similar kinds of failure but momentum similitude did give agreement for some cover materials.

A somewhat different approach has been taken by F. Rupp [16]. He used a polyamide sphere rather than an ice ball to simulate hail in a test apparatus that was otherwise quite similar to those already described. A compressed air gun with interchangeable barrels for various sizes of spheres was oriented to fire vertically downward. Velocity was measured by a sequence of three electro-optical sensors. The use of the polyamide ball as a simulator for hail was justified by Rupp on the basis that the failure produced in the test apparatus was similar to failure produced by hail in the field. However, polyamide's specific gravity of 1.2 to 1.4 would make it impossible to have both kinetic energy and momentum similitude. Further, the difference in stiffness and

strength between polyamide and ice would make it difficult to simulate all aspects of the impact of failure process.

2.4 LABORATORY TESTING

When it is necessary to evaluate cover performance, decisions regarding the values of the parameters (section 2.1) must be made. Simiu and Cattaneo [1] proposed maximum hailstone sizes corresponding to a 20-year mean recurrence interval for various regions of the United States. An appropriate hailstone size and corresponding velocity can be selected from Reference [1] or a similar governing or advisory document [2]. The collector cover would be expected to sustain an impact or impacts of hail of the selected size for satisfactory service in a given region of the country. Ice balls are good simulators of hailstones and are generally used in laboratory hail impact testing.

The testing apparatus for impact tests should be capable of propelling ice balls of various diameters at various controllable velocities. The system must be capable of being aimed at selected points on a properly mounted solar collector cover. For a given cover material, the initial ice ball size and corresponding velocity should be selected which would not be expected to cause failure. Selected points on the properly supported cover surface should then be impacted. Damage, if any, should be evaluated after selected points have been impacted with the initial size ice balls. To avoid delays, ice balls ranging from 1 in. diameter, in 1/4 in. increments, up to the expected maximum size for the test, possibly up to 2-3/4 in. or 3 in. diameter, should be available. If there has been no damage to the collector cover specimen, it can be impacted with the next larger size ice ball. However, a damaged specimen should be replaced before the next round of impacts. This procedure is repeated with ice balls of increasing size until failure occurs or until a "required" ice ball diameter is exceeded.

3. PREPARATION OF ICE BALLS

3.1 SIMULATION

Ice balls have been used here, and have been used by a number of other investigators, to simulate hailstones in laboratory testing. Hailstones generally consist of layers of ice which may vary in density. It is thought that ice balls are good simulators for hailstones even though the specific gravity of ice is slightly higher than that of actual hail [2, 3]. For example the specific gravity of clear ice is 0.92 as compared to the specific gravities of large hailstones (1 in. diameter or larger) ranging from 0.92 down to 0.82. Mean values of measured specific gravities in relatively large hailstone samples typically are about 0.88.

The selection of ice as a simulator for hail and the attendant use of a higher specific gravity is not a trivial consideration since both terminal velocity and kinetic energy may be influenced. For terminal velocity, T, it is found that

$$T = C_1 (\rho_H D)^{1/2} \quad (4)$$

where: C_1 = Constant
 ρ_H = Hailstone specific gravity
D = Hailstone diameter.

The above equation can be derived from Eq. (6) which is discussed in section 6.2 of this report. With regard to kinetic energy, defined by Eq. (1) of section 2.1, it is found that

$$K.E. = C_2 \rho_H^2 D^4 \quad (5)$$

where: C_2 = Constant.

Since the kinetic energy is a function of the square of ρ_H , an 11 percent change in ρ_H from 0.92 to 0.82 could result in a 24 percent change in kinetic energy. The change in kinetic energy would be 9 percent when comparing the ρ_H of and ice ball of 0.92 to 0.88.

However, clear ice balls can be made reproducibly in the laboratory by techniques described in section 3.3. If a lower specific gravity ball is required, the fabrication process would become more complex and probably less reproducible. In addition, the use of the greater density clear ice tends to be conservative in that for a given diameter of sphere both terminal velocity and kinetic energy are higher for the higher density ice. This means that for criteria based on hailstone size, as proposed by Simiu and Cattaneo [1], the use of solid ice balls in laboratory testing gives a somewhat more severe test than would be true if "actual" air-containing ice balls were used.

3.2 THE SPLIT MOLD APPROACH

The ice balls were cast in silicone rubber split molds. Figure 1 is a cross section sketch of the metal mold pattern which was used for making the silicone

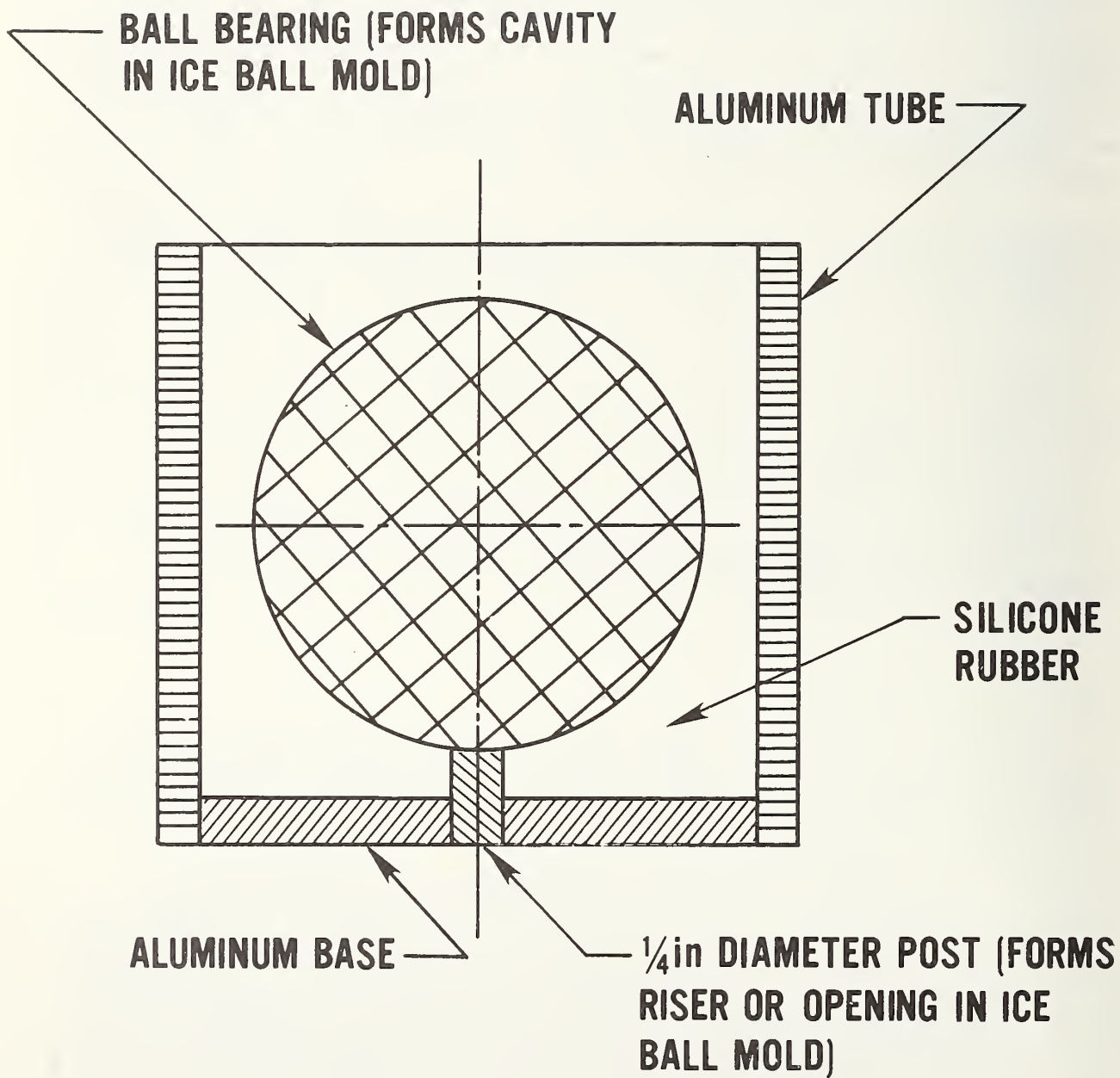


Figure 1. Cross section of metal mold pattern for making rubber molds used to cast ice balls

rubber molds. The metal mold consisted of an external aluminum tube which had an inner diameter at least $3/4$ in. greater than the ice ball cavity.

The ice ball cavity was formed by a steel ball bearing supported on a $1/4$ -in. diameter post which in turn fitted into an aluminum base. The post formed the riser or opening in the silicone rubber mold. A room temperature vulcanizing silicone rubber compound was thoroughly mixed with catalyst, degassed in a vacuum desiccator, and poured into the metal mold. The usual curing procedure was to cure over night at room temperature. The external aluminum tube and the aluminum base plate were removed from the cured silicone rubber casting. The rubber mold was then placed in a lathe and a cut carefully made at the equator of the embedded ball bearing. Index marks were made on the exterior of the halves before the casting was separated into two parts and the ball bearing removed. Figure 2 is a photograph of some of these molds. This procedure produced a mold which provided ice balls with virtually no trace of the parting line in the mold. The molds were stable dimensionally and reusable over an extended period of time.

It is noted that this procedure for mold-making is largely a refinement of the procedure described by Greenfeld [6] and improved by Mathey [7].

3.3 CASTING PROCEDURE

Although the procedure described below may seem tedious, it was found to be necessary if uncracked ice ball castings were to be produced. While it has been the practice at NBS to use individual ice ball molds, gang molds can also be fabricated and used.

The first step was to nearly fill the lower half of the mold with water, assemble the two halves of the mold, and place the assembly in the freezer compartment of a refrigerator at about 0°F . Note that a thin layer of silicone stop cock grease was placed on the mating surfaces of the mold before assembly to prevent water from leaking and to hold the two halves of the molds together. The index marks on the exterior of the molds were lined up to assure that the mold halves were assembled in the same relative orientation in which they were originally formed. This practically assured that there was no offset in the halves of the mold at the parting line.

When the water in the lower half of this mold was frozen, the remaining cavity was filled about one half full. The second step was completed by freezing the added water.

Finally, the third step was to fill the mold with water into the riser or opening. During this step it was very important not to entrap air in the mold while making the final fill. One way to do this was to use a wash bottle with a dispensing tube which was inserted into the mold through the riser so that water entered the mold at the surface of the ice. In this way, air was pushed out of the riser while the mold filled.

This entire procedure required about 24 hours from start to finished ice ball. The ice balls produced using this procedure were of consistent size and mass.

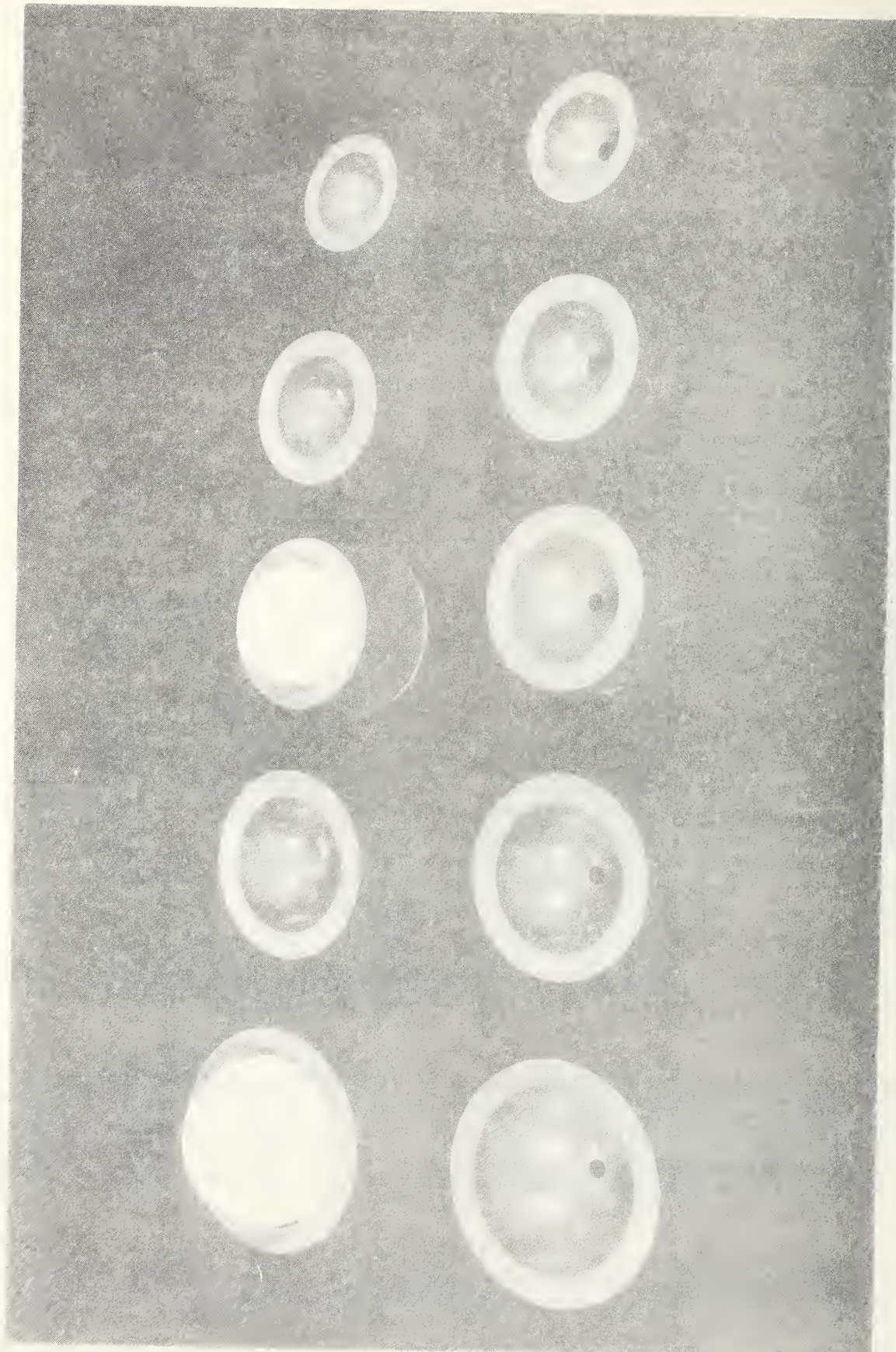


Figure 2. Silicone rubber ice ball molds

Ice balls with diameters of $3/4$ in., 1 in., $1-1/4$ in., $1-1/2$ in., $1-3/4$ in., 2 in., $2-1/4$ in., and $2-1/2$ in. were cast and used in obtaining the test results reported in section 9. Ice balls were stored in plastic bags in a freezer at -20°F . A given bag contained ice balls of the same diameter and was marked with the ball diameter for easy identification.

4. LAUNCHER

The launcher system for ice balls consists of a compressed air gun, a set of interchangeable barrels, a timing range for measuring ice ball velocity, and an optical pointer for alignment on a selected target area. Figure 3 is an overall view of the launcher system, which is very much the same as that used in earlier work [6, 7]. It should be noted that, in the impact tests reported here, the compressed air gun, barrel, and timing range assembly were mounted on a stationary platform.

4.1 COMPRESSED AIR GUN

The compressed air gun, shown in figure 4, is simply a large chamber which can be pressurized and which is connected, through a 2-in. diameter quick release valve to a barrel adapter whose inside diameter is 3-1/4 in. During the work reported here, a 15 psi pressure gage was used although a gage with a lower pressure range could have been used in many cases. Chamber pressures as low as 2 psi were all that was required to achieve resultant velocity (terminal velocity and 66 ft/s horizontal wind component) for 3/4-in. diameter ice balls, for example. The particular gun used at NBS was a commercially available model.

4.2 INTERCHANGEABLE BARRELS

Interchangeable barrels were made of either poly(vinyl chloride), PVC, or acrylic tubing. In the earlier work at NBS, a brass barrel, 3-1/4 in. in diameter, and polyethylene carriers for each ice ball size were used [7]. For the present work, tubing was selected so that the inside diameter was slightly larger than the ice ball diameter. When the inside diameter of the barrel was 0.05 to 0.14 in. larger than the ice ball, the greatest velocity for a particular barrel size and chamber pressure was obtained. If a "tighter" fit was chosen, the ice ball decelerated by contact friction as it passed through the barrel. On the other hand, if a "looser" fit was chosen, pressure did not build up behind the ice ball when the quick release valve was opened and a slower than expected velocity was obtained. Table 1 lists the barrel materials and dimensions for each size of ice ball. Figure 5 shows the assortment of barrels used and figure 6 shows one of the barrels being installed in the compressed air gun. Wooden adapter sleeves were attached to the breech end of each barrel so that a snug fit in the barrel adapter on the compressed air gun was obtained. These adapter sleeves are visible in figure 5.

In our preliminary work, brass tubing was tried for the interchangeable barrels. A note about our negative experience may be in order since other investigators have used metallic barrels with apparent success. Brass barrels with internal diameters 0.05 to 0.10 in. larger than the ice ball diameters resulted in ball velocities much lower (about half) than for plastic barrels for a given air chamber pressure. Also, for a given chamber pressure, the velocities obtained were much more erratic with the brass barrels. Although the reasons for this behavior are not well understood, it is possible that an increased amount of ice ball melting in the brass barrels may be responsible. One mechanism that could be assumed is that there is sufficient melting of the ice ball while pressure is being adjusted and the aiming being checked, to result in a very

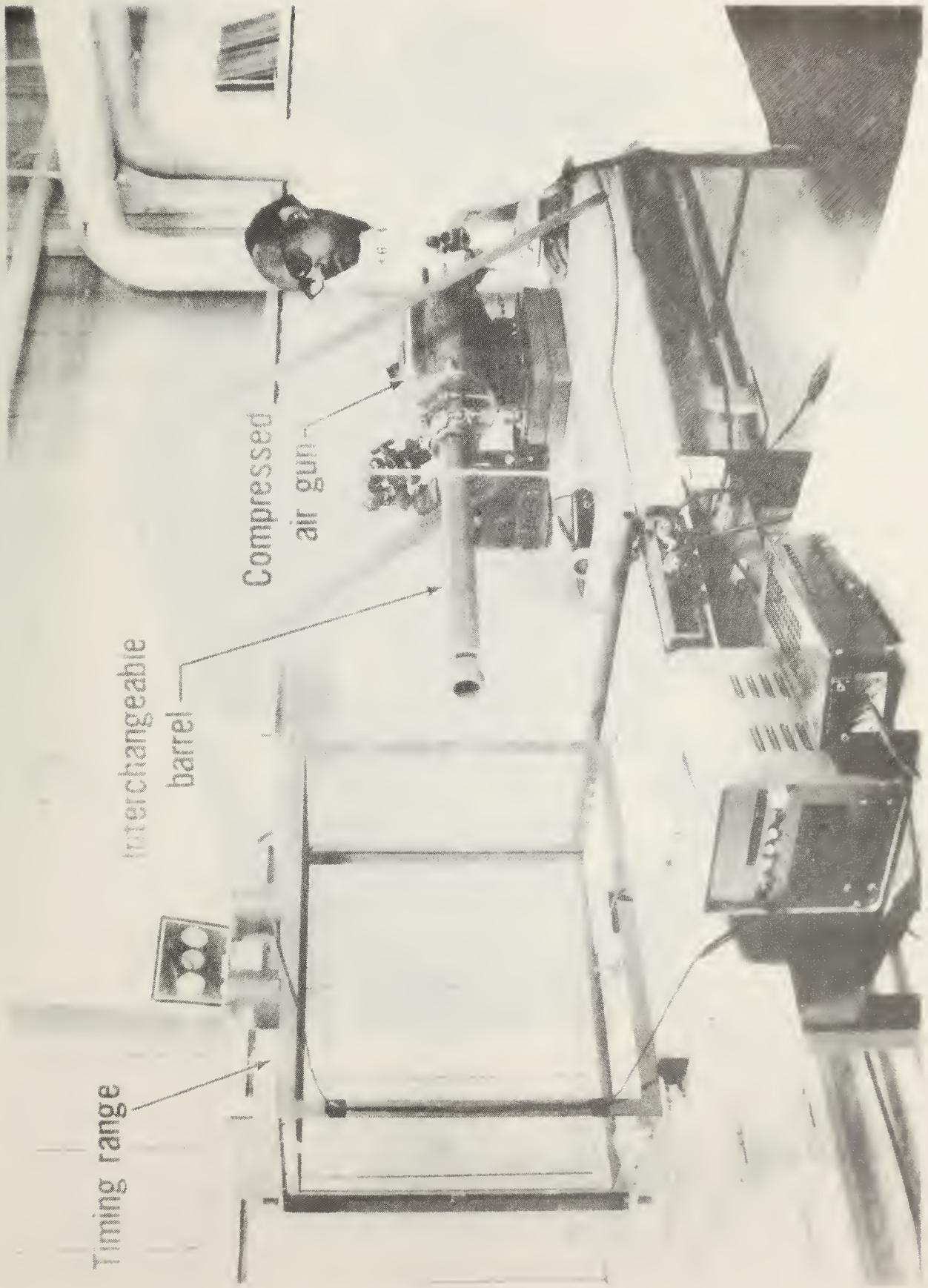


Figure 3. Overall view of launcher system

Pressure gage

Air chamber

Compressed
air cylinder

Barrel adapter

Figure 4. Compressed air gun

Table 1. Interchangeable Barrel Materials and Dimensions

Ice Ball Diameter (in.)	Barrel Material	Nominal Internal Diameter (in.)	Actual Internal Diameter (in.)	Difference Between Actual Barrel Diameter and Ice Ball Diameter (in.)
3/4	3/4-in. PVC Pipe Schedule 40	0.810	0.797	0.047
1	1-in. PVC Pipe Schedule 40	1.033	1.047	0.047
1-1/4	1-1/4-in. PVC Pipe Schedule 80	1.256	1.281	0.031
1-1/2	1-1/2-in. PVC Pipe Schedule 40	1.592	1.594	0.094
1-3/4	2-in. PVC Pipe Schedule 80	1.913	1.891	0.141
2	2-in. PVC Pipe Schedule 40	2.049	2.070	0.070
2-1/4	2-1/2-in. PVC Pipe Schedule 80	2.289	2.328	0.078
2-1/2	Cast Acrylic Tubing	2.625	2.58*	0.080

* Duct tape (one layer) attached to internal surface to reduce diameter.

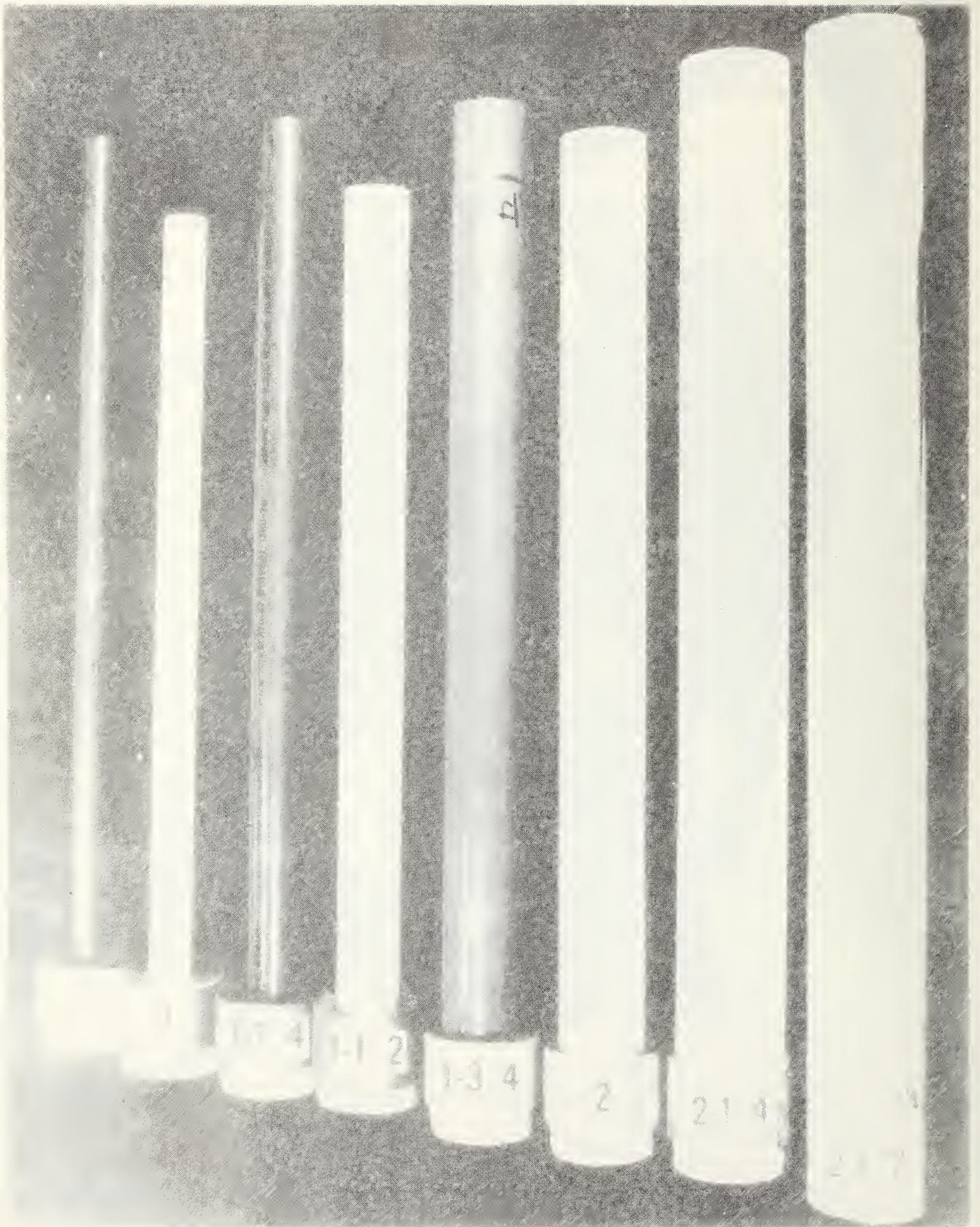


Figure 5. Interchangeable barrels for the compressed air gun



Figure 6. Installation of barrel in the compressed air gun

"loose" fit. Consequently, the released chamber pressure dissipates around the ice ball rather than exerting a force on it. An alternate mechanism would postulate less melting but enough to yield an ice ball that adopts the barrel's cylindrical shape over part of its surface and, thus, does not roll freely as it passes down the barrel. Both of these mechanisms may have some plausibility for the situation where the barrel is horizontal.

4.3 TIMING RANGE

The timing range is the metal framework in the left foreground of figure 3. Each end has an illuminator which projects a 5-in.-wide beam of light in a plane perpendicular to the ice ball path. Each of these beams is focused on a photocell. The beams of light are spaced 2 ft apart and are positioned so that the ice ball interrupts the beams sequentially. When the first beam is interrupted, the photocell output is changed abruptly, this change in output actuates an electronic counter. When the second beam is interrupted, the counter is stopped. The smallest count corresponds to 0.01 millisecond and it is estimated that time measurements are accurate to better than 0.5 percent. This timing range is very dependable and light sources and photocells are protected in such a way that the system is very damage resistant. It was used previously by Mathey [7].

4.4 OPTICAL POINTER

An optical pointer was developed to allow rapid aiming of the system at a selected point on the specimen. Figure 7 shows the pointer mounted in the launcher barrel. During testing the solar collectors and cover support frames, containing the collector covers, were moved to bring different predetermined impact points into alignment with the barrel of the compressed air gun. The method of positioning is described in section 5.3. In operation, the pointer focuses the image of the flashlight bulb filament on the collector cover surface. A sketch showing the various parts of the device is presented in figure 8. During aiming, the unit is mounted in the muzzle end of the barrel. Conventional flashlight batteries in a separate holder are used to illuminate the bulb. As designed, a spot of light lying on the launcher axis was in focus on a plane about 3 ft from the muzzle and facilitated accurate aiming.

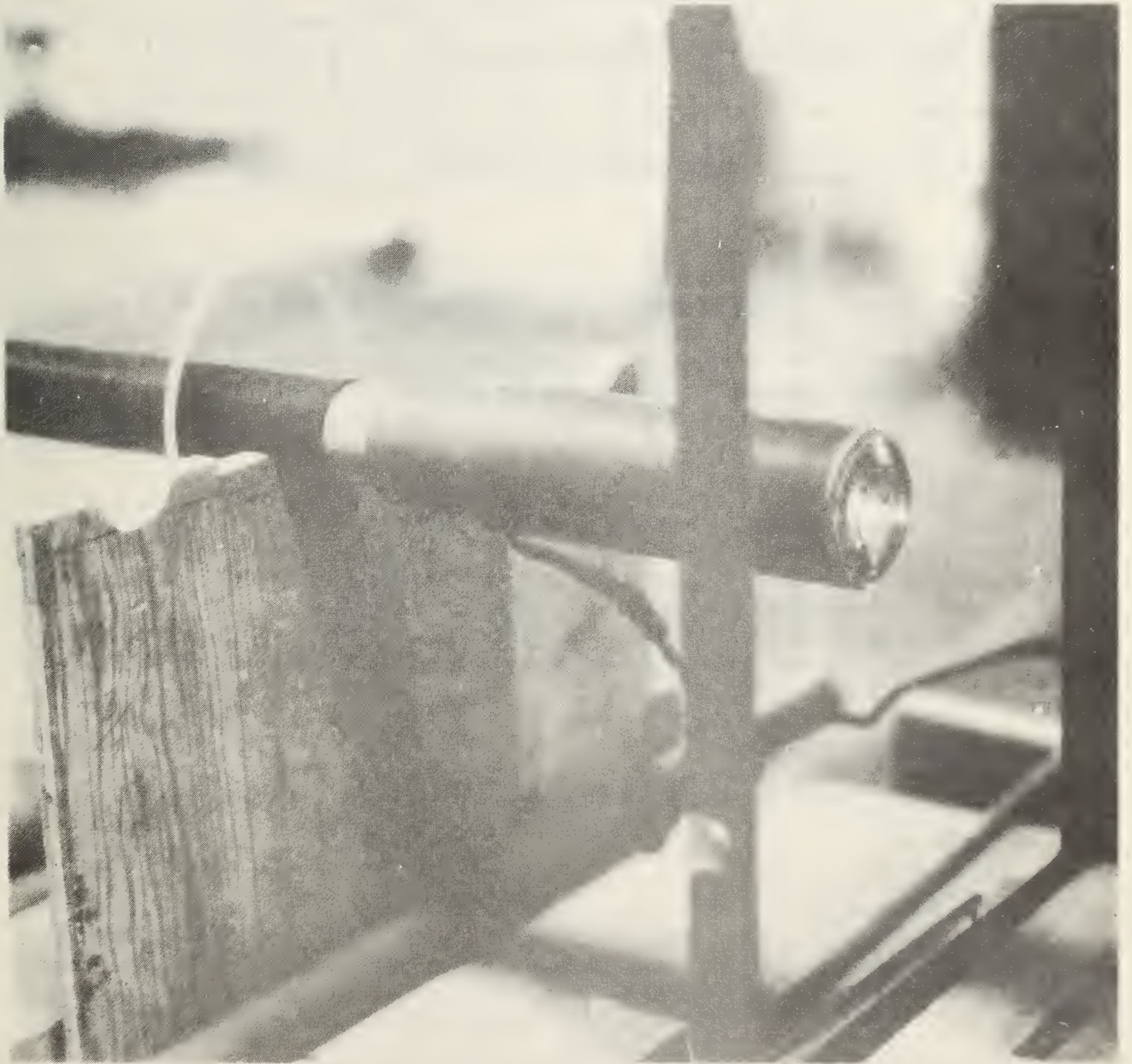


Figure 7. Optical pointer for the hail gun

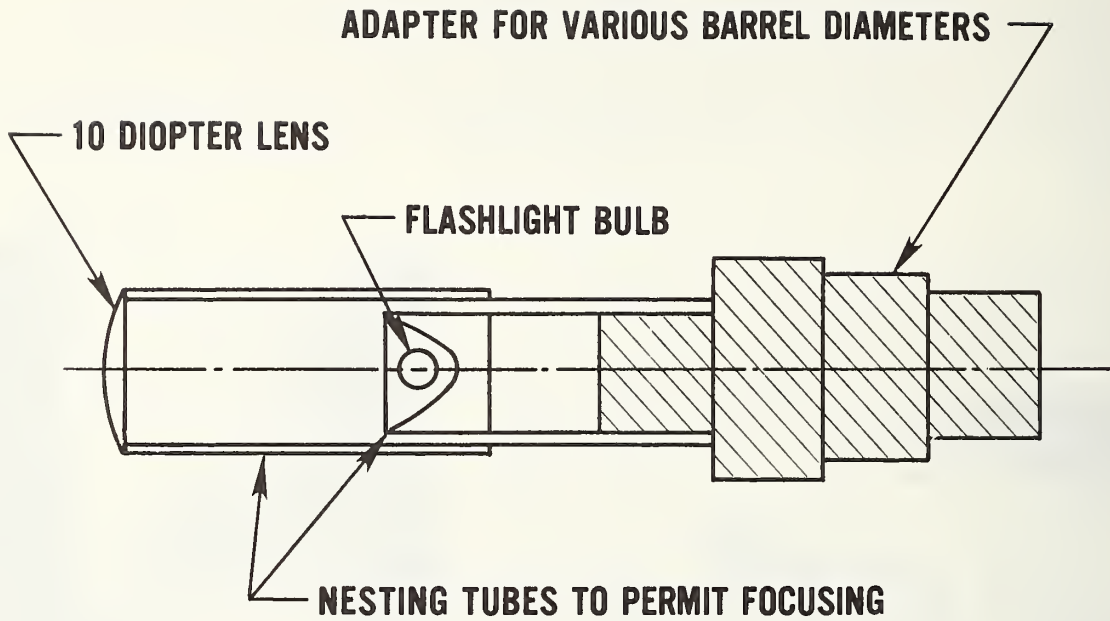


Figure 8. Schematic of optical pointer

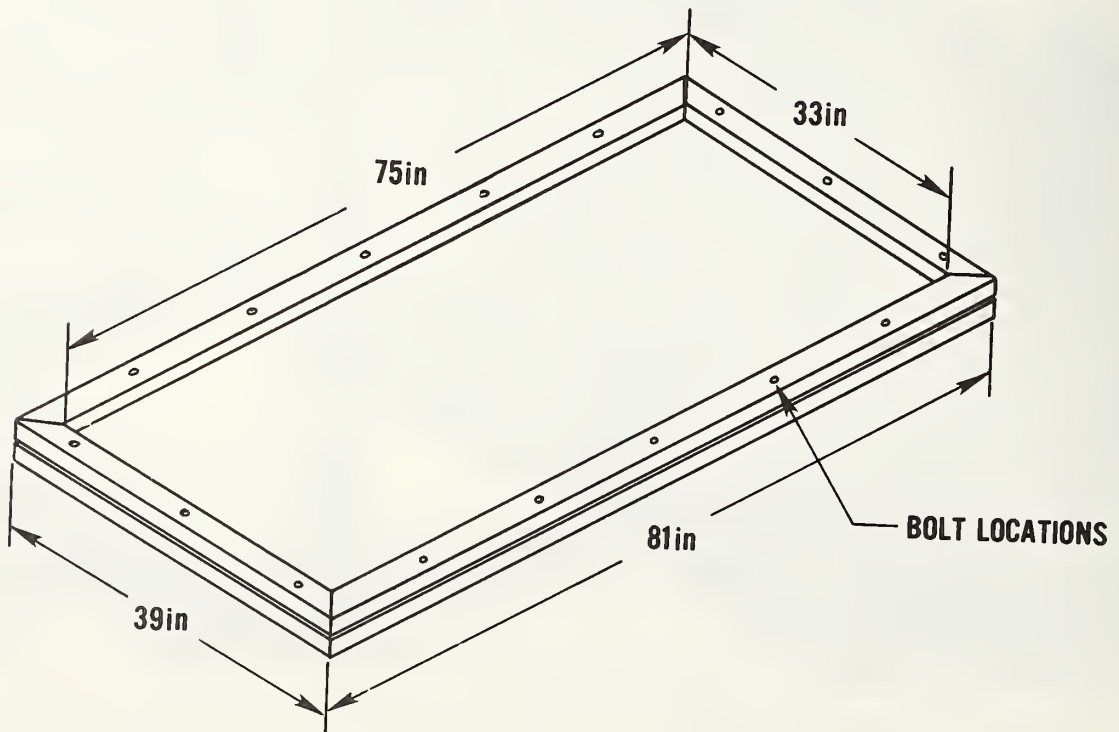


Figure 9. Sketch of assembled support frame

5. MOUNTING OF COVER SPECIMENS

5.1 COVER SUPPORT FRAMES

There are two approaches to mounting solar collector cover materials for hail resistance testing. One of these, the one followed here, is to mount the cover material in a support frame in a consistent manner for all materials of that class. The other approach is to test the cover material as mounted in an assembled collector. The first approach would tend to offer a more objective comparison of cover materials since the support conditions would not vary greatly from specimen to specimen. This approach is preferable even though it would not take into account variations in impact resistance that might occur as a result of collector size or cover mounting configuration. Since full size collector covers are to be investigated, the cover support frames were designed to accommodate 34 in. by 76 in. plates. This is a representative size for flat plate collectors.

For this research, one type of cover support frame was designed to accommodate rigid and semirigid materials while a slightly modified design was used for flexible thin film materials. Basically the cover support frames consist of two halves which are bolted together with the cover specimen between them. In general, the frame simulated to some degree the support conditions found in an assembled solar collector. It is very likely that the resistance to edge rotation is greater for the support frames used here than in many assembled collectors.

Figure 9 gives a simplified sketch of a support frame. The frames used here were rectangular in cross section and were built from solid maple. The inner surfaces of the frames contained strips of neoprene rubber to bear against the edges of the cover specimens. Figure 10 shows typical support frame cross sections with the locations of the neoprene inserts. The neoprene strips, 3/8 in. by 3/4 in., were cemented into slots milled in the frame so that the neoprene compressed about 20 percent when the assembly was complete. To control the amount of compression when rigid or semirigid materials were clamped, a spacer the same thickness as the cover specimen was inserted. The neoprene used here had a Shore A Durometer hardness of 30 to 45. Steel straps such as shown in figure 11, were attached to the exterior of each corner to both stiffen and strengthen the corners of the support frames.

5.2 PLACING SPECIMENS IN THE FRAMES

For rigid and semirigid cover materials, the specimen dimensions were 34 in. by 76 in. so that 1/2 in. of the cover was clamped between the neoprene strips. For thin film covers, the sheet material extended through the support frame so that weights for stretching could be attached outside of the frame. No spacer is used with the thin film cover materials.

In both cases, frames were fastened together with 3/8-in. diameter bolts at locations indicated in figure 9. The bolts were 14 in. on centers and were symmetrically located. Using bolts for fastening was found to be much more convenient than using C-clamps since the bolts interfere a minimum amount with

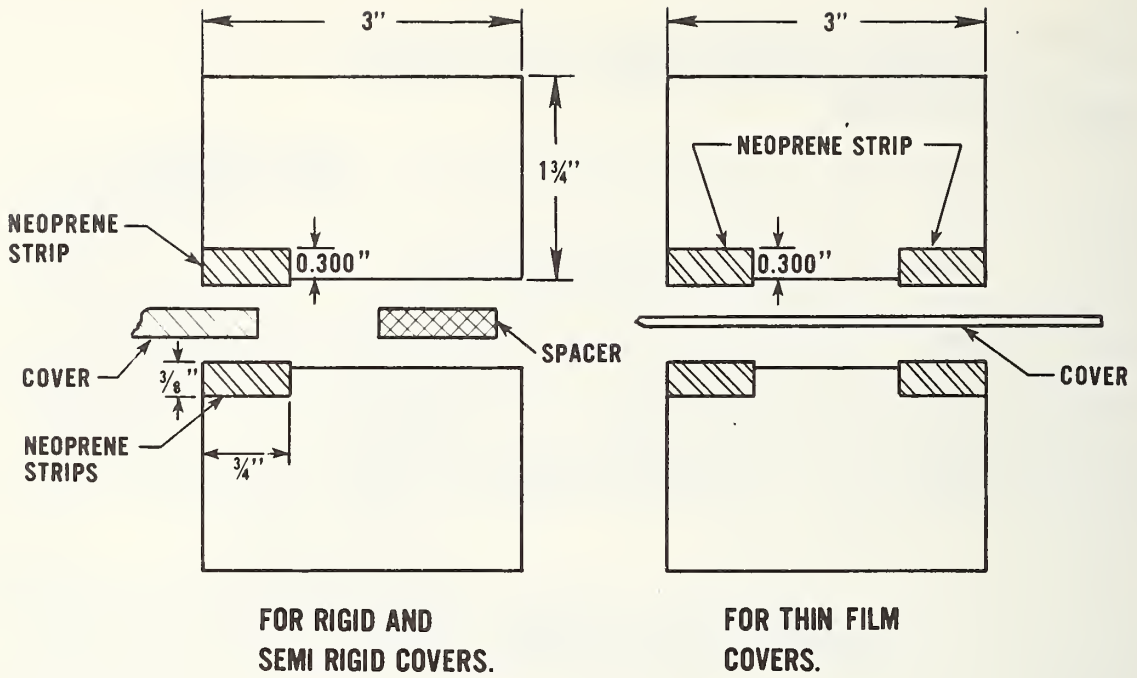


Figure 10. Typical support frame cross sections

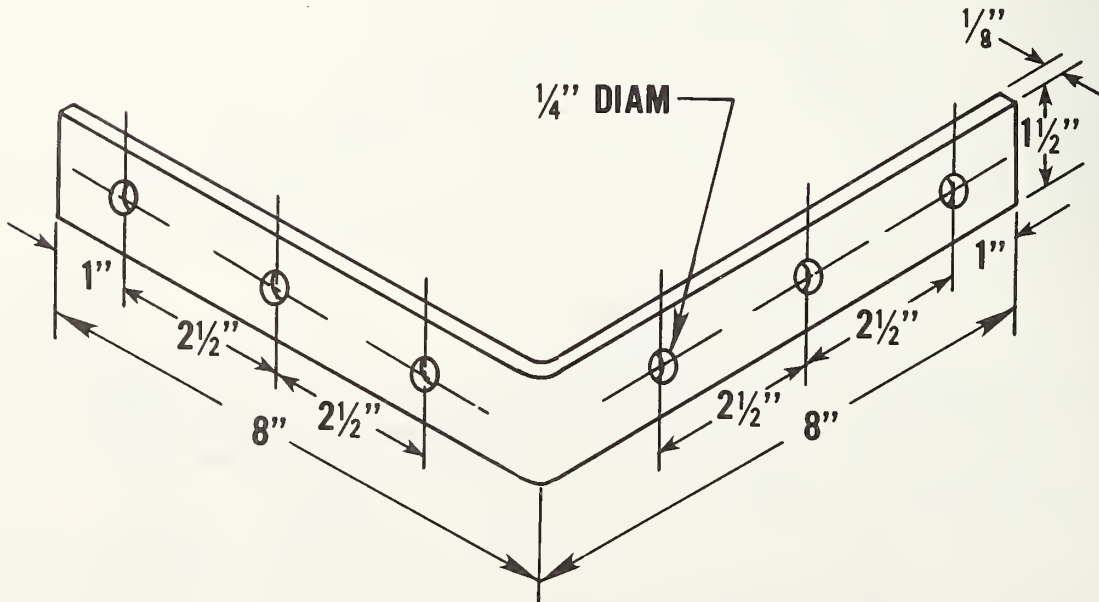


Figure 11. Corner strap for support frames

the mounting of the assembly in the support frame positioner. Further, C-clamps are very difficult to install in the case where thin film cover materials are used since during mounting the material extended outside the frame and had weights attached to it.

It was found that semirigid materials, in particular fiber reinforced plastics, required support during the assembly of the cover support frame. Since assembly was done with the cover in a horizontal plane, the material would sag under its own weight if supported only along the edges. A block of the correct thickness placed under the cover at its center tended to suppress this sagging. However, semirigid materials were not pulled taut during assembly and some deviation from flatness did occur when the cover support frame was raised to a vertical position for testing.

As noted above, thin film cover materials, such as the poly(vinyl fluoride), were tensioned before the halves of the support frame were bolted together. An overall view of this tensioning operation is shown in figure 12. Figure 12, also shows that the specimen was oversize, actually about 50 in. by 92 in., so that the material hung over the frame by about 6 in., on all sides. C-clamps were used as weights for tensioning the flexible material as shown in both figure 12 and in figure 13. In addition, figures 12 and 13 show bolts extending through the cover material. This was facilitated by punching slightly oversize holes in the cover material before the bolts were inserted. This detail is shown in figure 14. It was found that an edge loading of 5.2 lbf/ft to 5.5 lbf/ft used in this study was necessary to achieve moderate tautness of the thin film. The question arises here as to how taut the material needs to be to simulate the "heat stretching" frequently employed. Some film cover materials in an actual collector assembly would probably be "heat stretched" over a frame and then mounted in the collector. A representative edge loading needs to be known. The edge loading values of 5.2 lbf/ft and 5.5 lbf/ft used here produced a tautness in the cover material greater than has been used in some instances to simulate heat "stretched material." The consistency of tensioning of the material by the edge loading was checked by a center deflection measuring technique. This technique was a very simple one in which the horizontally tensioned film was loaded transversely by a 0.1 lbf weight at the center of the specimen and the deflection measured. Fairly consistent results from specimen to specimen were obtained. Figure 15 shows a tensioned film cover loaded by a 0.1 lbf weight.

It should be noted that the thin film material did not always maintain its tautness when the cover-support frame was in the vertical testing configuration.

5.3 SUPPORT FRAME POSITIONER

As noted earlier, the launcher assembly is fixed in position so that the flight path of the ice ball is fixed. The cover frame assembly must be moved to align the selected impact points on the cover specimen with the aimed trajectory of the ice balls. During testing, the cover specimen in its support frame must be held in a vertical plane by a relatively rigid supporting system and that system must be capable of rapid horizontal and vertical positioning of the cover frame assembly.

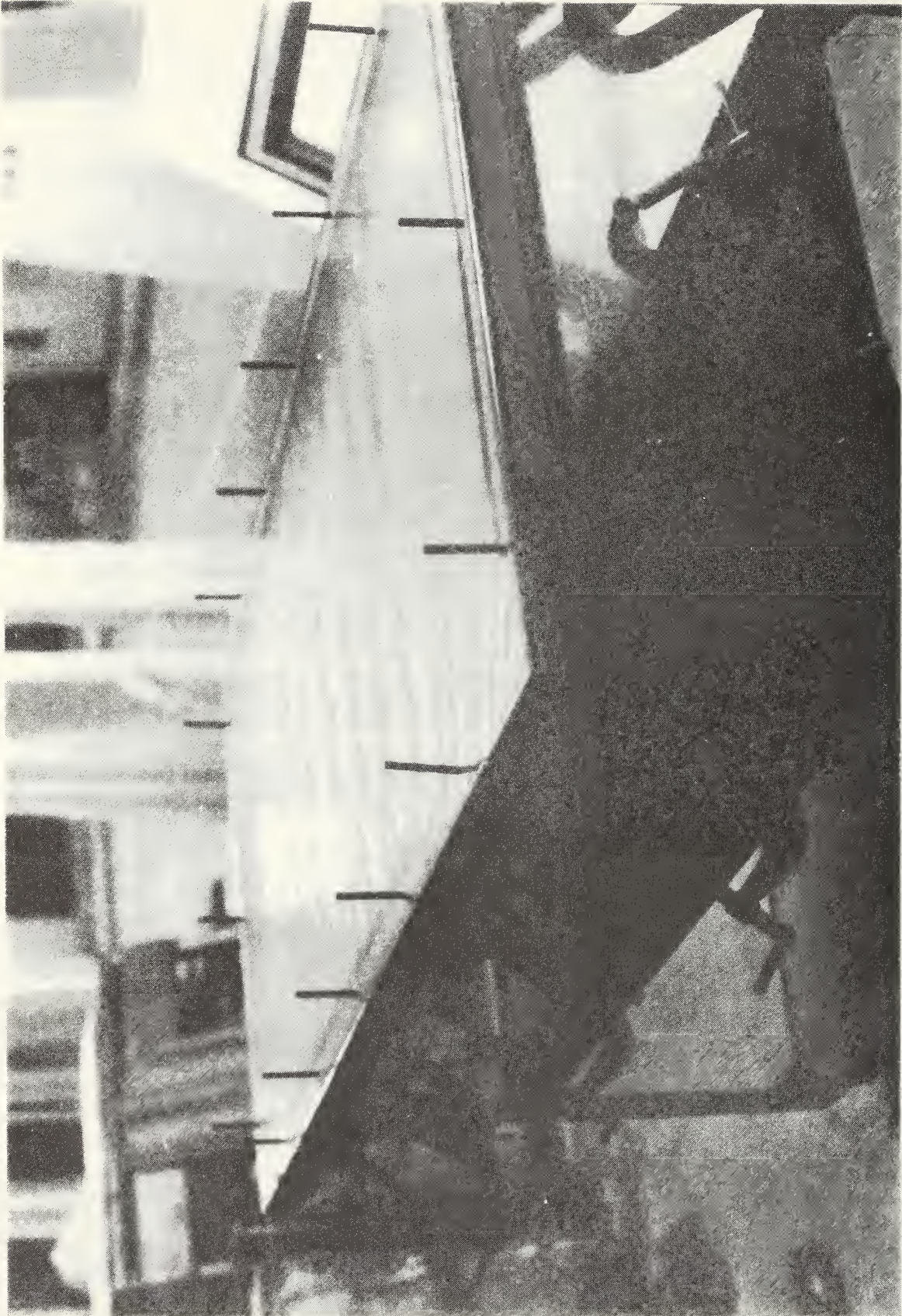


Figure 12. Tensioning of film cover material

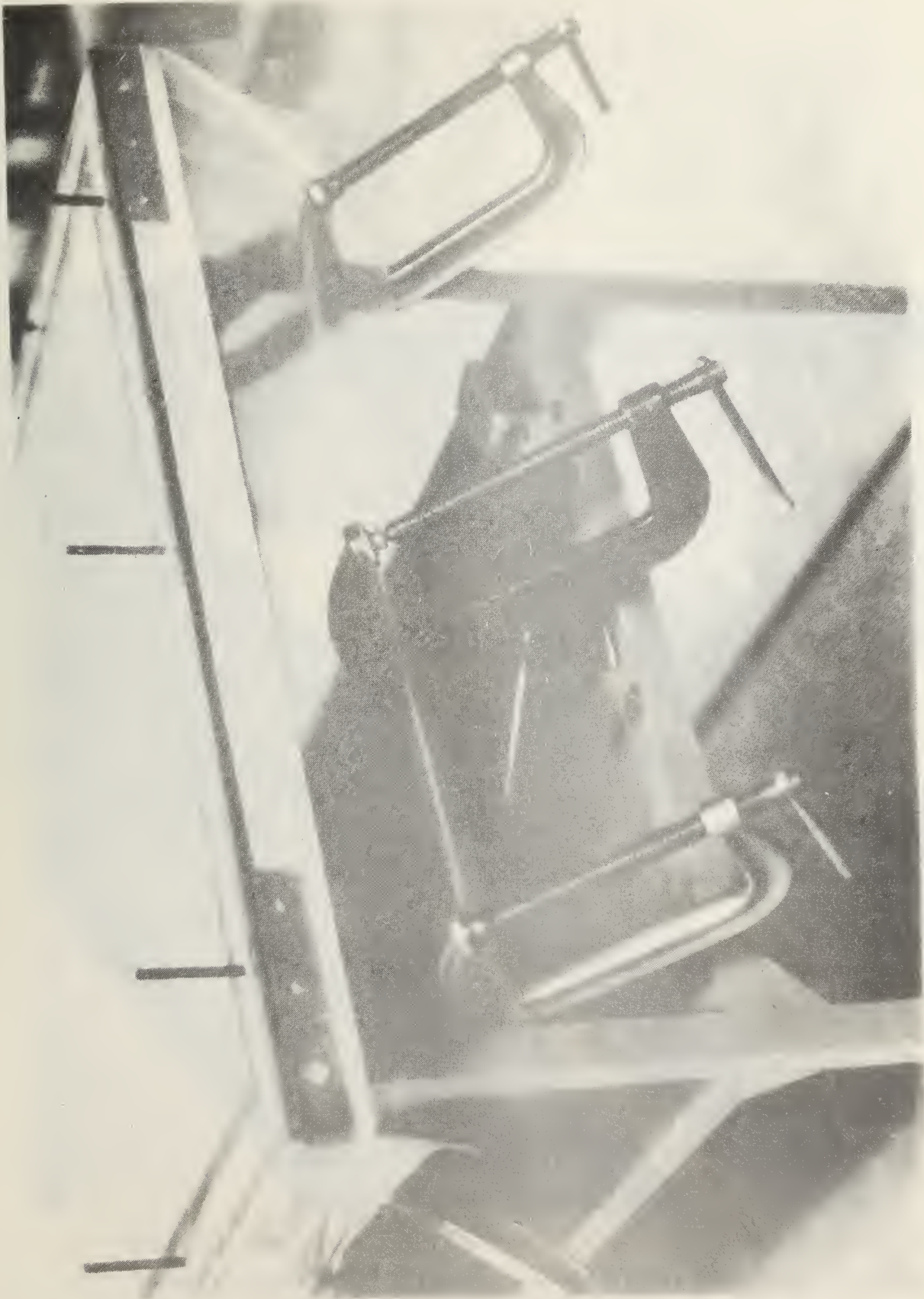


Figure 13. C-clamp weights attached to film cover material

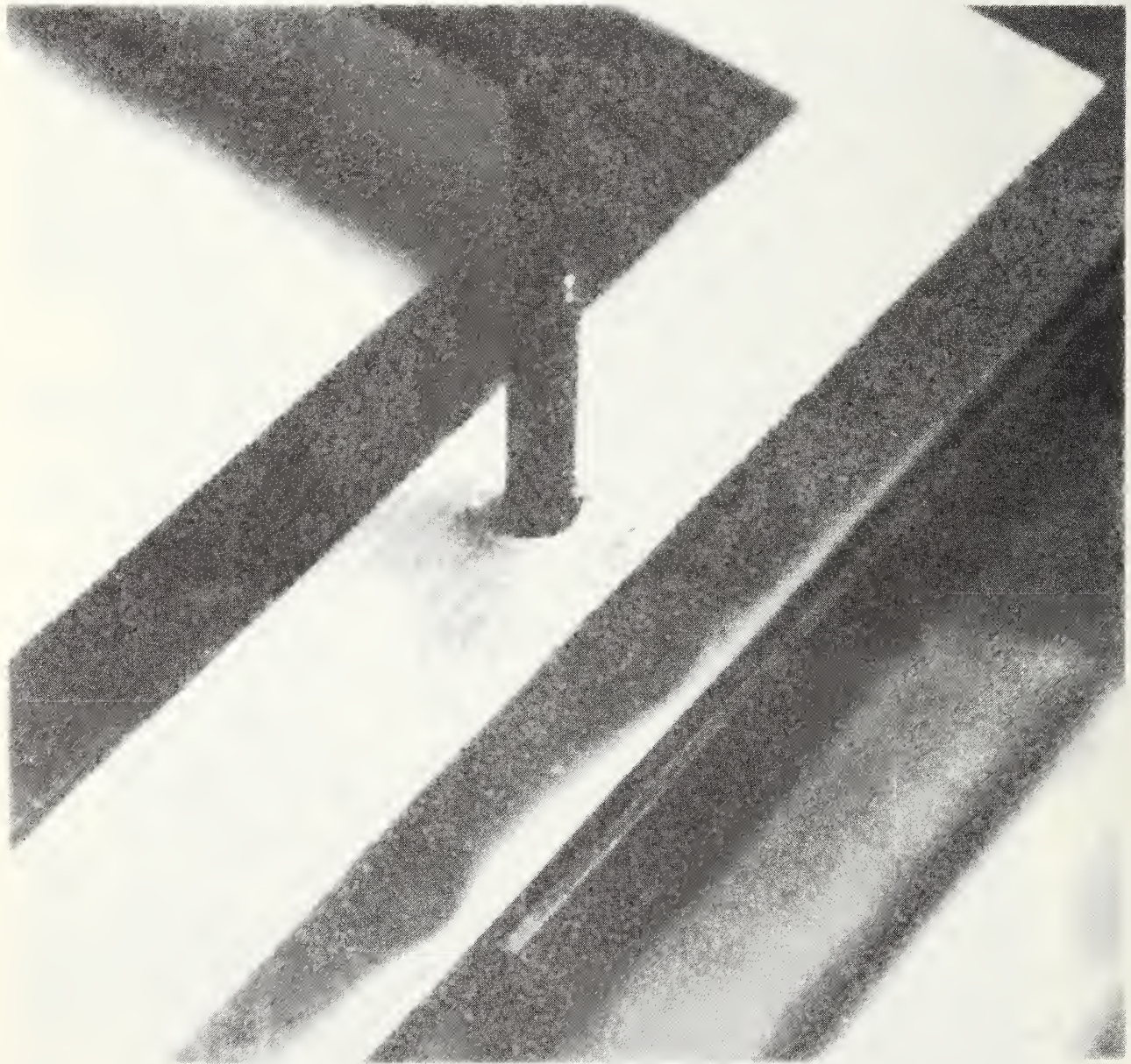


Figure 14. Hole in film cover material to permit bolt passage

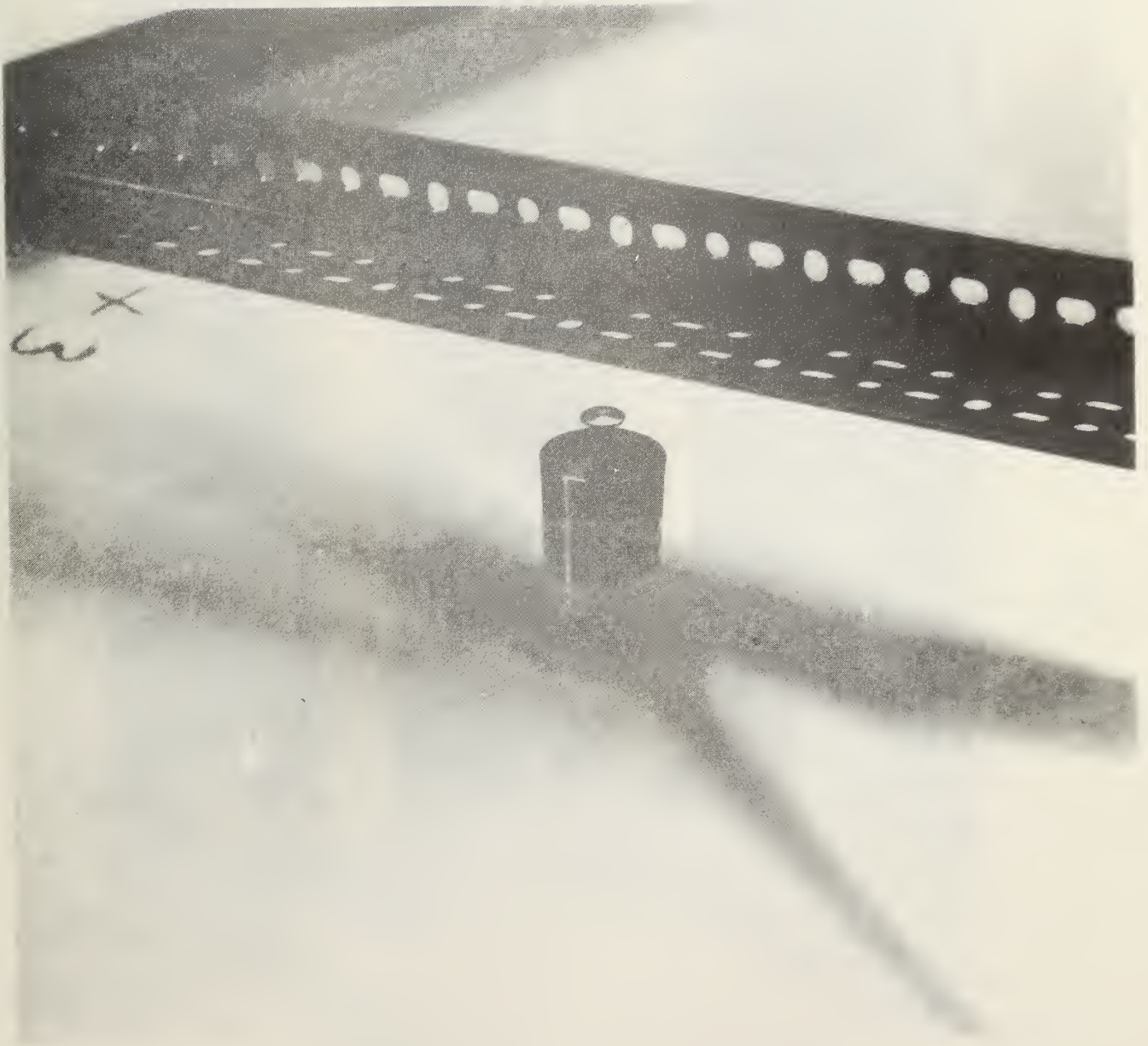


Figure 15. Transverse loading of film cover to check consistency of tensioning

To do this, a battery-operated heavy-duty lift truck was used. Small steel channels were bolted to the uprights of the lift platform and the cover frame assembly was attached to the channels with C-clamps. This is shown in figure 16. The lift mechanism was employed for vertical positioning and horizontal positioning was accomplished by moving the lift truck. Using this technique in combination with the optical pointer, it was possible to reposition the specimen from an impact point at the left end of the exposed area to one at the right end of the exposed area in a few minutes. Clamping and unclamping of the cover support assembly was not necessary as it would had been if a fixed supporting structure had been used.

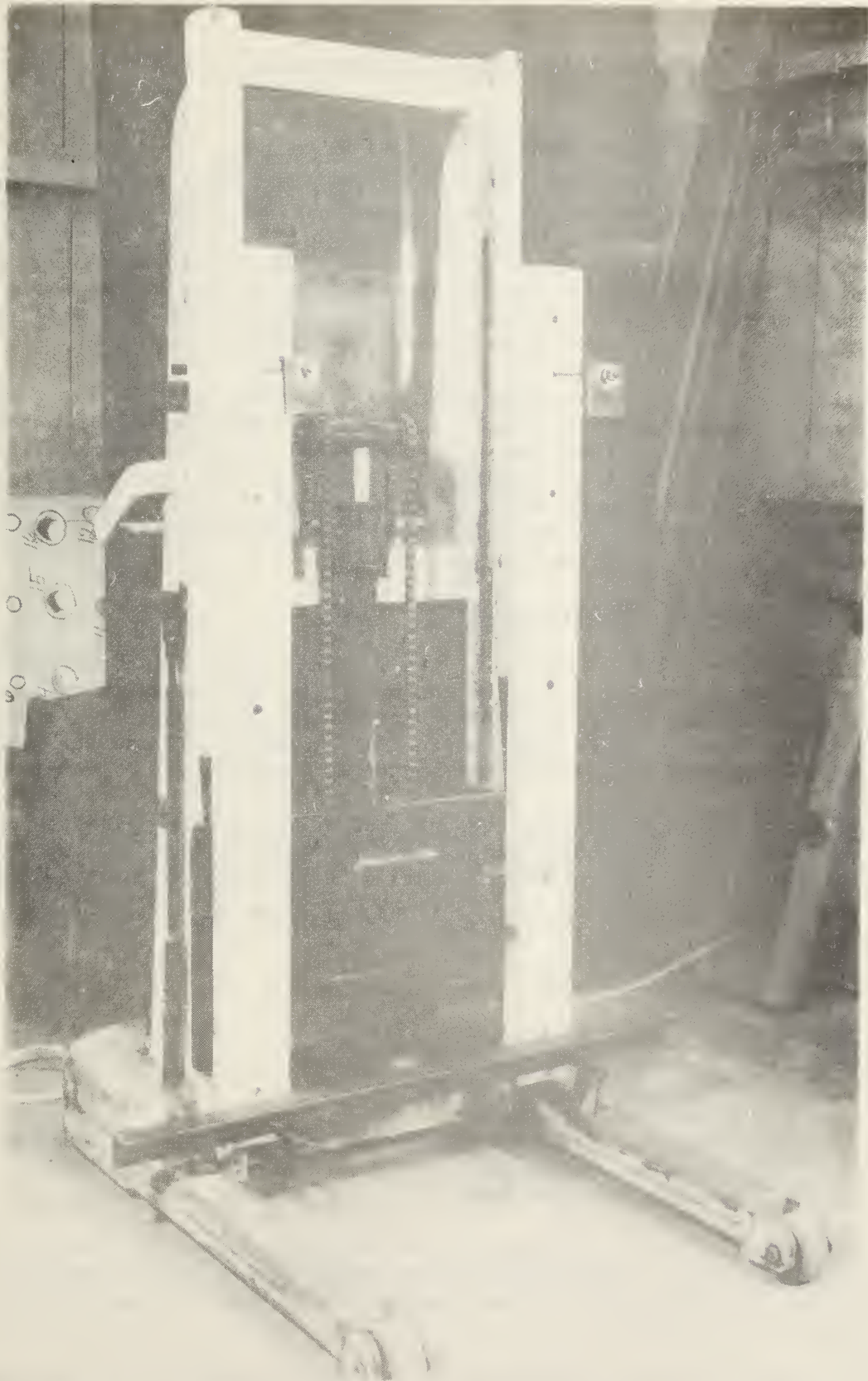


Figure 16. Lift truck modified as a support frame positioner

6. ICE BALL VELOCITY AND IMPACT POINTS

6.1 ALTERNATIVE LABORATORY VELOCITIES

The maximum hailstone sizes which occur in nature have been determined using a statistical approach. The maximum sizes vary with the geographical area and recurrence interval selected. Simiu and Cattaneo [1] have estimated the maximum size hail to be expected under various conditions as already noted in section 2.1. The selection of the velocities of hailstones or ice balls for laboratory testing, if the tests are to simulate extreme but realistic field conditions, is a question that has received considerable attention.

With regard to velocity of the impacting ice ball, there are several questions to consider. First, should the magnitude of the velocity be equal to the terminal velocity or to a resultant of the terminal velocity acting vertically and a wind component acting horizontally? Second, if the laboratory test is to require only normal impact, which seems reasonable to minimize testing costs and testing time, what component of the resultant velocity should one assume acts normal to the laboratory specimen?

6.2 VALUES OF TERMINAL VELOCITY AND WIND VELOCITY

The normal velocity values (ice ball traveling in a direction perpendicular to the plane of impact) used for various ice ball sizes are shown in table 2 along with the corresponding values of kinetic energy and momentum. These data are essentially the same as those reported in 1970 by Mathey [7] and are based on a comprehensive analysis of the relevant technical literature.

As stated earlier in this report, the terminal velocity of a hailstone is the velocity at which the hailstone falls when its weight is equal to the drag force acting upon it. Setting weight equal to drag force in equation form yields

$$\rho_H \cdot g \cdot \frac{1}{6} \pi D^3 = \frac{1}{2} \rho_A T^2 \cdot C_D \cdot \pi D^2 \quad (6)$$

where ρ_H = density of hail stone
 g = acceleration of gravity
 D = hailstone diameter
 ρ_A = density of air at appropriate altitude and temperature
 T = terminal velocity
 C_D = coefficient of drag.

The coefficient of drag, C_D , depends on the Reynolds number in general, but for the flow regime usually experienced by hailstones (i.e., for the range of sizes given in table 2), C_D appears to be constant and to have a value of 0.5 or slightly less.

The data of table 2 were calculated from an equation like Eq. (6) proposed by Bilham and Relf [17]. Clearly there are a number of parameters in Eq. (6) for

Table 2. Ice Ball Parameters for Laboratory Testing

Diameter (in.)	Mass (lbm)	Velocity ^{1/}		Kinetic Energy ^{3/}		Momentum ^{3/}	
		Terminal (ft/s)	Resultant ^{2/} (ft/s)	Terminal (ft-lbf)	Resultant (ft-lbf)	Terminal (lbf-s)	Resultant (lbf-s)
3/4	0.0073	62	91	0.44	0.94	0.014	0.021
1	0.0173	73	98	1.43	2.58	0.039	0.053
1-1/4	0.0337	82	105	3.52	5.77	0.086	0.110
1-1/2	0.0584	90	112	7.35	11.38	0.163	0.203
1-3/4	0.0928	97	117	13.56	19.73	0.280	0.337
2	0.1384	105	124	23.69	33.04	0.451	0.533
2-1/4	0.1971	111	129	37.71	50.93	0.679	0.790
2-1/2	0.2705	117	134	57.50	75.42	0.983	1.126

1/ For laboratory testing, ice balls were propelled in a direction perpendicular to the plane of impact.

2/ Resultant velocity is the vector sum of the terminal velocity and a 66 ft/s horizontal wind component.

3/ Corresponding to the terminal and resultant velocity.

which values must be selected and various investigators have proposed various values. The value of C_D found by Bilham and Relf for ice spheres in their experiments was about 0.5 and other investigators appear to agree with this if the Reynolds number is in the range of 2×10^4 to 2×10^5 . List [18] ran relatively low speed wind tunnel tests on ice spheres and found a C_D of about 0.45. He also points out that the terminal velocities of actual, non-spherical, hailstones will be less than that of a sphere of the same volume and density. Macklin and Ludlam [19] measured C_D values for ice balls in a wind tunnel and measured fall speeds of hailstones dropped from a meteorological balloon. Radar was used for the latter fall speed measurements. Their C_D values ranged from 0.41 to 0.51 at the higher Reynolds numbers. They further showed that the fall speeds of the dropped hailstones could be correlated with the velocity of an equivalent sphere of the same mass and specific gravity of 0.9. Data for the 2-in. diameter equivalent sphere are virtually the same as that in table 2 based on Bilham and Relf's work.

A wind component must be considered when establishing the normal velocity for test purposes since thunderstorms which produce hail are generally accompanied by strong winds. For example, in "Climates of the United States," Baldwin [20] indicates that thunderstorms are occasionally accompanied by hail but most are accompanied by strong wind which can have gusts reaching speeds in excess of 65 mi/h. In connection with a 1961 study in South Africa [21], it was reported that winds having velocities of 30 to 60 mi/h generally are associated with hailstorms and that gust velocities are often 30 to 50 percent higher than the average wind velocity. Finally, Schleusener [22] notes that strong winds aloft have been found to be closely correlated with the occurrence of severe hail. Based upon the evidence of wind accompanying hail, a 45 mi/h horizontal wind component was used in calculating the resultant velocities in table 2. It is noted that in earlier tests on the hail resistance of building materials and products, such as those conducted by Greenfeld [6] and Laurie [23], ice balls were propelled at their terminal velocity. Laurie [23] stated that hailstones can fall at an angle of as much as 45 degrees to the vertical because of high wind.

6.3 MAGNITUDE OF THE NORMAL VELOCITY

A brief discussion of the components of the hailstone velocity vector may clarify the interaction. This discussion will deal with a two-dimensional special case of the actual three-dimensional situation. Considering the latter, for the collector cover shown in figure 17, the normal component N of the resultant velocity, which would be the only component producing a normal impact, makes an angle θ with the vertical or z-axis. This follows since the collector cover is inclined at an angle θ to the x-y or horizontal plane. The resultant velocity of a hailstone does not, in general, coincide with N and in fact does not generally lie in the y-z plane as does N. The resultant vector shown in figure 17 has components in both the x and y horizontal directions as well as the vertical z direction. However, for this orientation of the xyz axes, the x component of the resultant has no effect on the magnitude of N so that the two dimensional analysis of components in the y-z plane is sufficient.

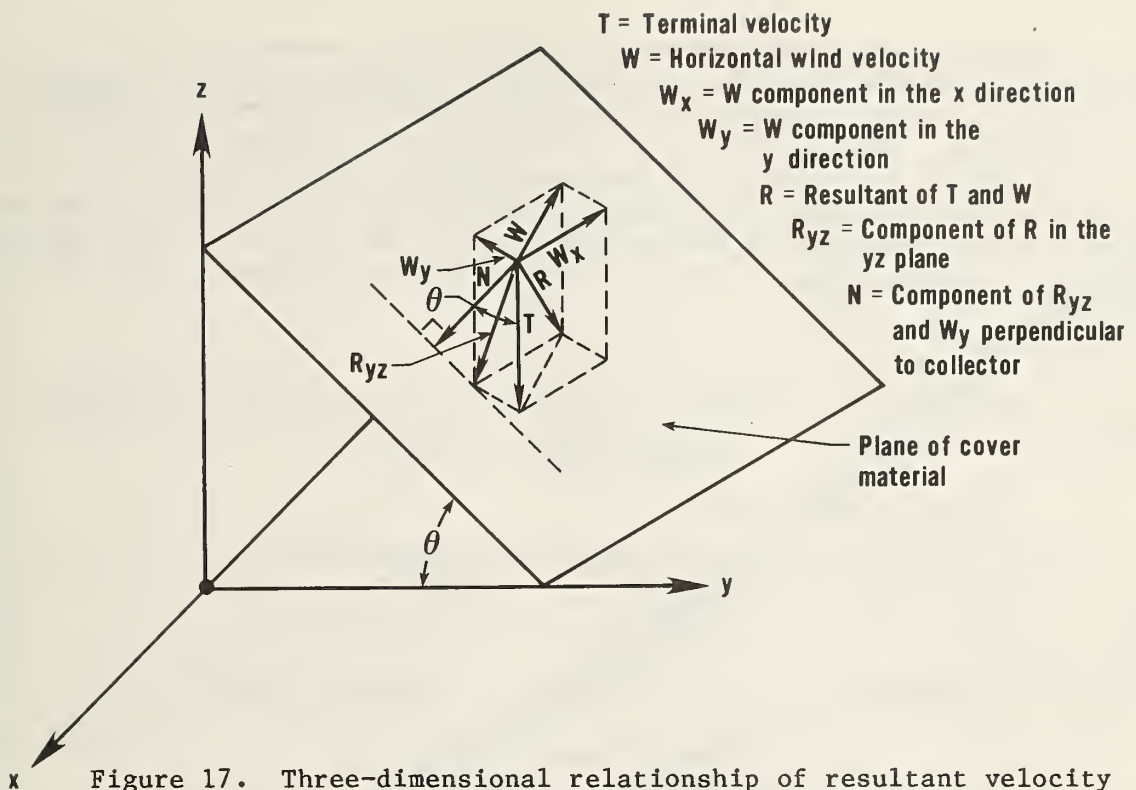


Figure 17. Three-dimensional relationship of resultant velocity and normal component of resultant velocity

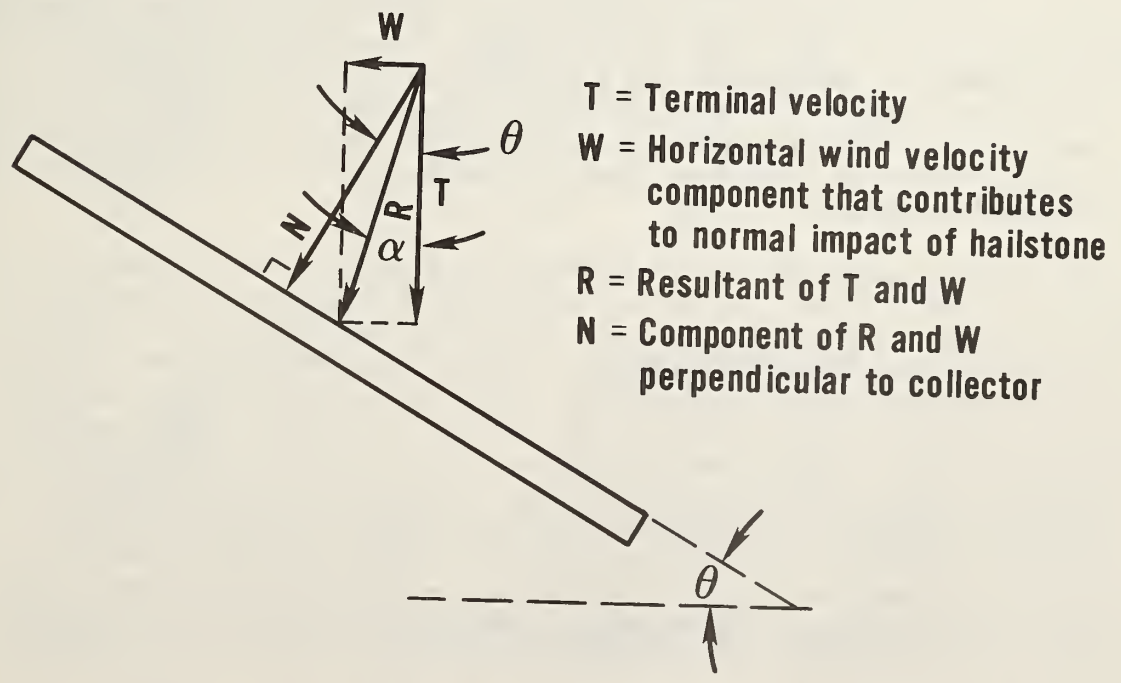


Figure 18. Two-dimensional relationship of the hailstone velocity components and the normal velocity component for wind direction perpendicular to the horizontal edge of an inclined collector

Figure 18 shows a two-dimensional view of the velocity components which contribute to the normal velocity component N. In this figure it is assumed that the wind direction is perpendicular to the lower (horizontal) edge of the inclined collector. This special case will result in a maximum value of N for a given wind velocity. It is noted that the probability of the wind direction and speed must be introduced into occurrence criteria (section 2.1). T represents the terminal velocity of the hailstone, W is the horizontal wind component contributing to normal impact, and R is the resultant of T and W, that is,

$$T^2 + W^2 = R^2. \quad (7)$$

If an angle α is used to designate the direction of the resultant velocity, that is,

$$\tan \alpha = \frac{W}{T}. \quad (8)$$

then, since N can also be considered as a component of R

$$N = R \cos (\theta - \alpha). \quad (9)$$

It can also be shown that

$$N = T \cos \theta + W \sin \theta. \quad (10)$$

Using Eq. (7) and Eq. (10), values of N and R were compared for various values of θ and T. The reason for this comparison was to determine if the normal component, N, could be taken to be equal to the magnitude of R, for the purpose of selecting ice ball velocities for testing of solar collector plates. Clearly, the normal component is equal to the magnitude of R only when $\alpha = \theta$, i.e., when the values of W and T have a particular relationship. In the calculations for N and R, W was taken as equal to 45 mi/h or 66 ft/s, i.e., the full effect of a horizontal wind blowing in a direction perpendicular to a horizontal edge of an inclined collector.

The results of the analyses are presented in figure 19. The uppermost curve in figure 19 is a plot of Eq. (7) or the magnitude of the resultant velocity as a function of terminal velocity, T, and a horizontal wind velocity of 66 ft/s. The straight line plots lying immediately below the R versus T plot represent N versus T for a horizontal wind velocity of 66 ft/s, or Eq. (10), for cover inclination angles, θ , of 30 deg, 40 deg, 50 deg and 60 deg. If attention is confined to terminal velocities, T, ranging from 62 ft/s to 105 ft/s which correspond to ice ball diameters of 3/4 in. to 2 in. respectively, these plots show that the magnitude of R exceeds N at most by 15 ft/s or 13 percent at T = 105 ft/s. Further, this latter N situation occurs for $\theta = 60$ deg which is greater than the angle of inclination for most solar heating systems in the continental United States. Consequently, for testing purposes the magnitude of the normal velocity was taken to be equal to the magnitude of the resultant velocity.

To provide an estimate of the effect of neglecting horizontal wind velocity, W, the dashed lines are presented in the lower part of figure 19. The uppermost

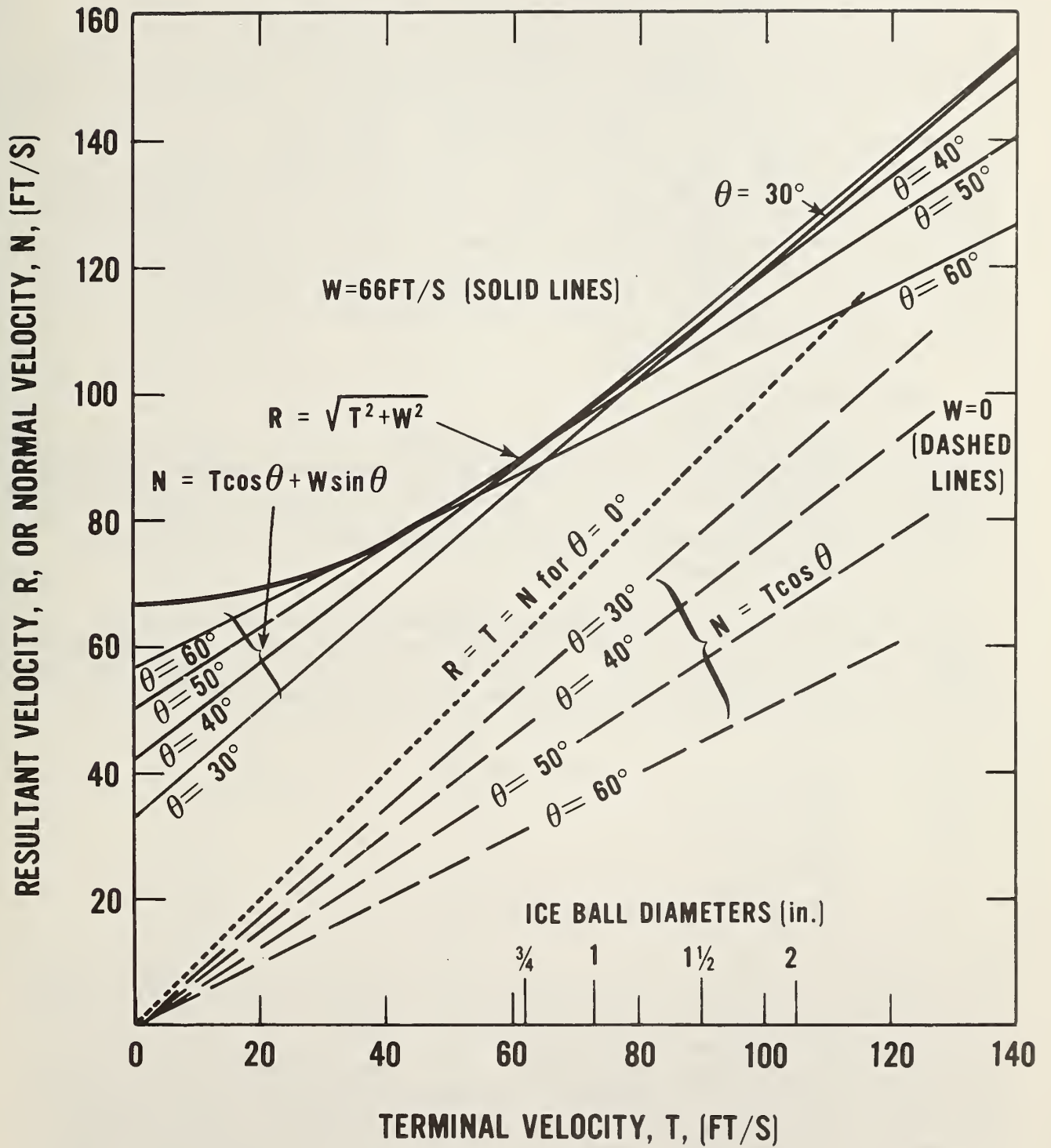


Figure 19. Assumed and actual normal velocity values for various terminal velocities

dashed line represents the resultant velocity R which equals T when $W = 0$. The remaining dashed lines represent the values of N as a function of T , from Eq. (10) with $W = 0$, for various values of θ . It is noted that, for a given value of θ , the solid straight line and the dashed straight line are parallel but that the solid straight line is offset vertically by a distance corresponding to $W \sin \theta$. There is a distinct difference in resultant velocity magnitudes when a wind component is or is not considered. Again looking only at the terminal velocity range from 62 ft/s to 105 ft/s, the greatest difference between R for $W = 66$ ft/s and R for $W = 0$ occurs at 62 ft/s or at the small ice ball diameter end of the range. Here a difference of 29 ft/s or 32 percent occurs. Even the smallest difference between values of R over this terminal velocity range for $W = 66$ ft/s and $W = 0$ which occurs at 105 ft/s or for the 2-in. diameter ice ball is 19 ft/s or 15 percent. These results were taken, in part, to be a justification, for including a wind component in selecting the normal velocity for laboratory testing.

6.4 IMPACT LOCATIONS

A layout of impact points on the mounted collector cover is shown in figure 20. These points were chosen at the outset of the experimental program to determine, in general, the areas of the cover which are more or less susceptible to failure by impact. Locations 6, 7, 8, and 9 which are positioned 6 in. away from the neighboring sides of the support frame have been proposed as preferred test locations in some test methods [2].

It was expected that the "criticality", of an impact location, i.e., the tendency for failure with a given ice ball diameter and velocity, would increase roughly with the location number. Tendency for failure is equated to the strain level at the plate surface on the reverse side at the impact point. Specifically, ascending order of "criticality" were selected as follows:

No. 1	Least Critical
No. 2,3	
No. 4,5	
No. 6,7,8,9	
No. 10,11	
No. 12,13	
No. 14,15,16,17	Most Critical.

This ordering of the criticality of the points was supported in general by the test results. In addition, calculations of the maximum tensile strain in the plane of a simply support plate at the impact location tended to demonstrate that the strain increases in accordance with the order of "criticality" described above. An important parameter is the maximum tensile strain in the plate which from calculation occurs on the back surface of the cover plate at the impact point. The calculation assumed that the nature of the impulse is the same at all locations. However, this may not be entirely correct since the duration of the impulse or the variation of force with time may be different at various locations, due to differences in the effective "stiffness" of the cover at the locations where it is impacted.

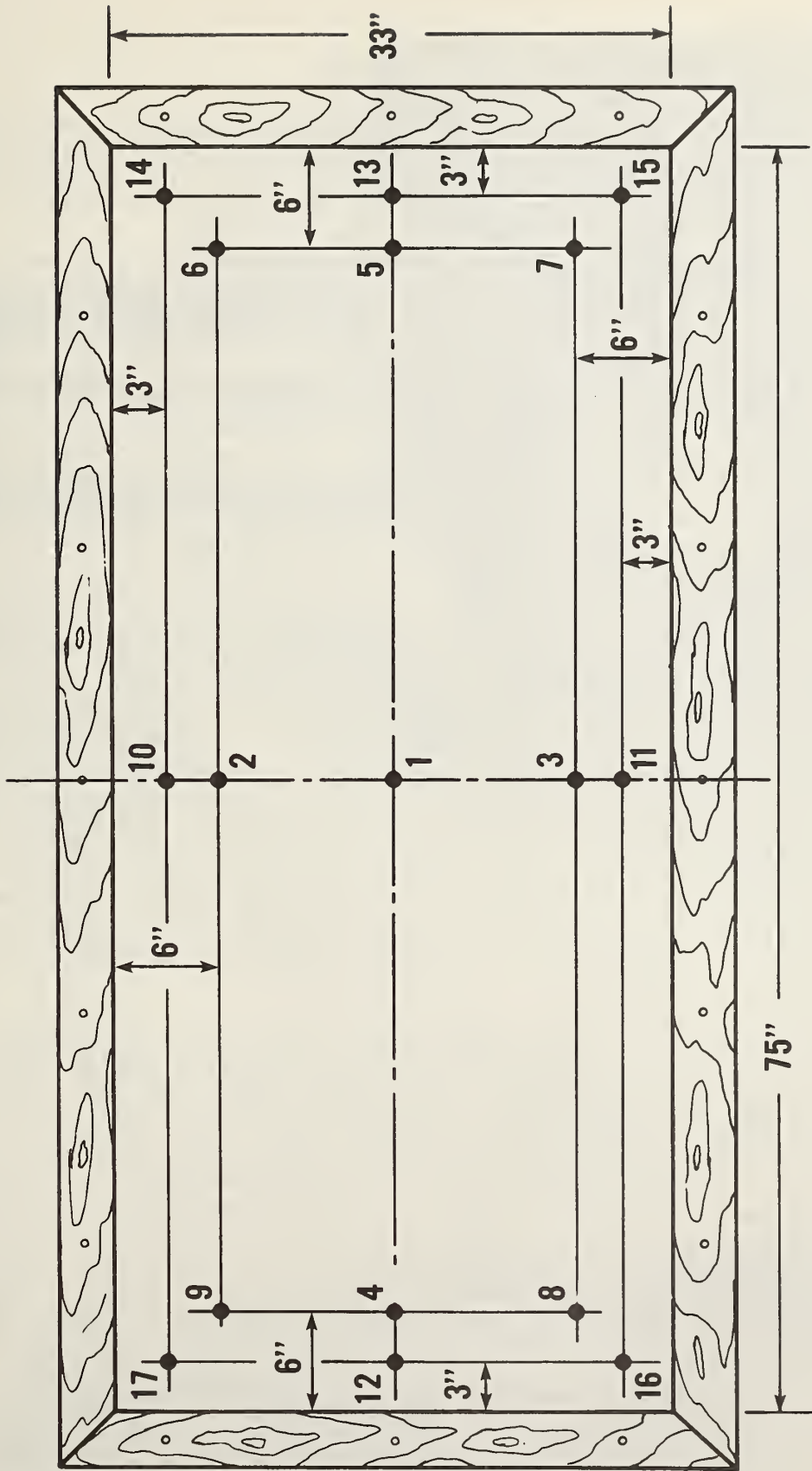


Figure 20. Layout of impact points

7. FAILURE OR DAMAGE ASSESSMENT

Since there are three distinct classes of materials, i.e., rigid, semirigid, and flexible film, used for collector covers, it might be expected that three distinct types of failure behavior may be observed. This will be discussed in terms of the specific cover materials tested in this research program.

Two rigid cover materials were included, namely tempered glass with both surfaces smooth and tempered glass with the exposed surface textured and the other smooth. Failure and/or damage by impact of these materials is quite straightforward to describe because they shatter into small pieces. Tempered glass behaves elastically until the tensile fracture stress is reached. At this point, the tempered glass cover specimen develops a complex crack pattern which, because of the residual stresses due to the tempering, progresses throughout the material in a few minutes. An overall view of a textured surface tempered glass cover specimen after fracture is shown in figure 21. A hole in the cover resulting from the impacting ice ball is shown in figure 22. For impacts which do not produce fracture, there may be some microscopic surface damage but this was not apparent from visual inspection.

One semirigid cover material was tested and this was a polyester resin sheet reinforced with chopped strand glass fiber mat. Sheet thickness was 0.040 in. This class of cover materials is much less brittle than the glasses discussed above. Even at the high strain rates associated with ice ball impact, these reinforced plastic materials exhibited some inelastic deformation before fracture. However when fracture occurred, the crack or cracks were in general confined to the immediate neighborhood of the impact point. This is referred to by some investigators as "starring". A failure of this type is shown in the center of figure 23. Localized failures of this type may or may not be detrimental to solar collector operations. While a relatively small portion of the total surface area is affected and, thus, transmission may not be reduced to any great extent, it is possible that cracking may extend through the specimen thickness. This would allow water penetration which could eventually deteriorate solar collector components.

To check the possibility of water penetration through the area damaged by impact of an ice ball, a leak test procedure was developed. After impact, the reinforced plastic specimen was removed from the support frame and was cut into smaller pieces which contained impacted areas to accomplish the leak testing. The next step was to attach a clear plastic cylinder to the reinforced plastic's surface so that the cracked region was inside the boundary of the cylinder. Melted wax was used to seal the cylinder to the cover surface. Figure 24 shows a cylinder attached in this way. Water was poured into the cylinder to a depth of 1-1/2 in. to give an identical static head for each test. After an arbitrarily selected time period, overnight in our case, the depth of water was recorded and used to indicate water penetration into the specimen at each impact location.

When the reinforced plastic cover material is impacted by large ice balls traveling at relatively high velocities, damage such as tearing and breaks through the cover specimen may occur. Figure 25 shows a failure of this type.

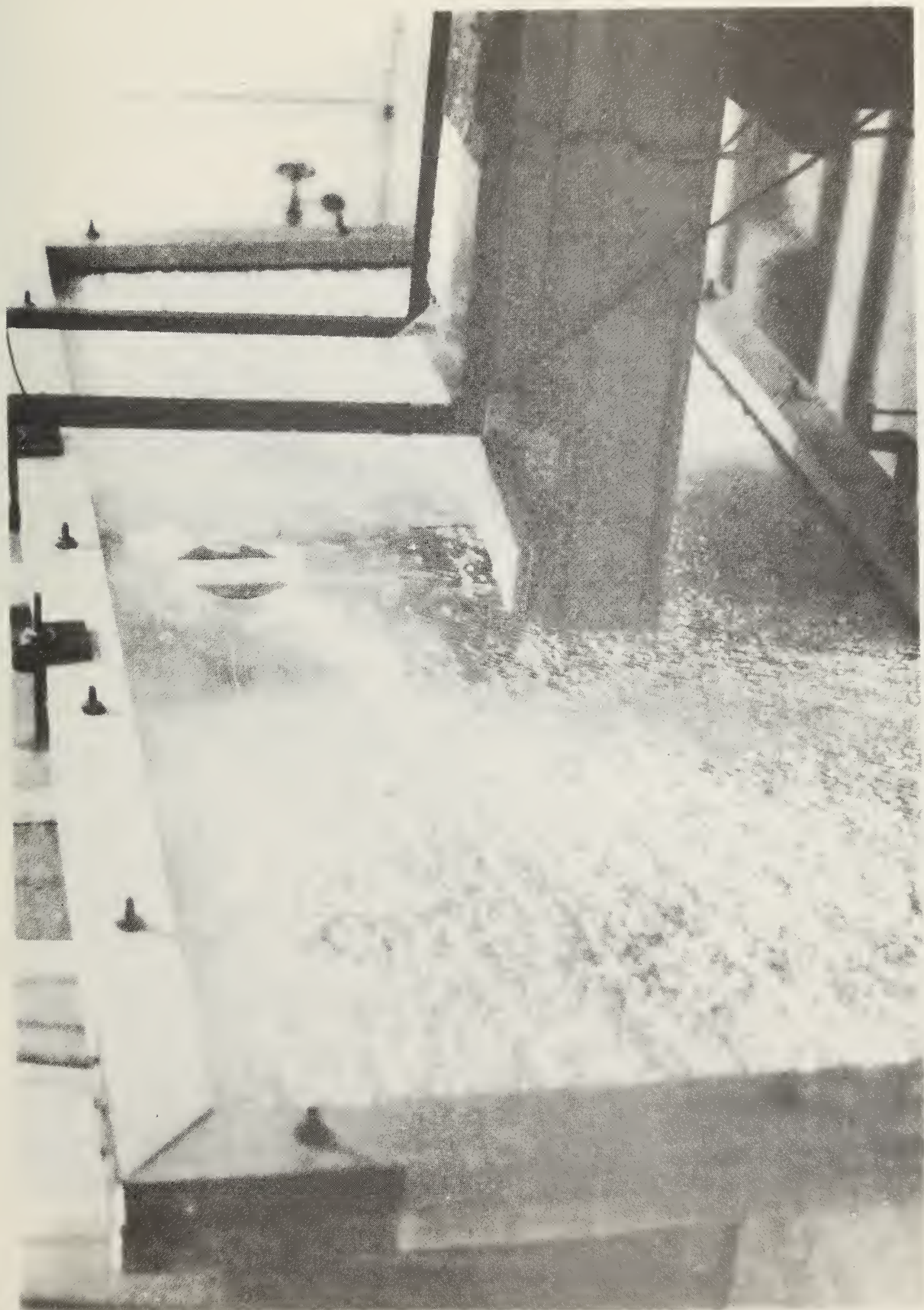


Figure 21. Overall view of a textured surface tempered glass cover specimen after fracture

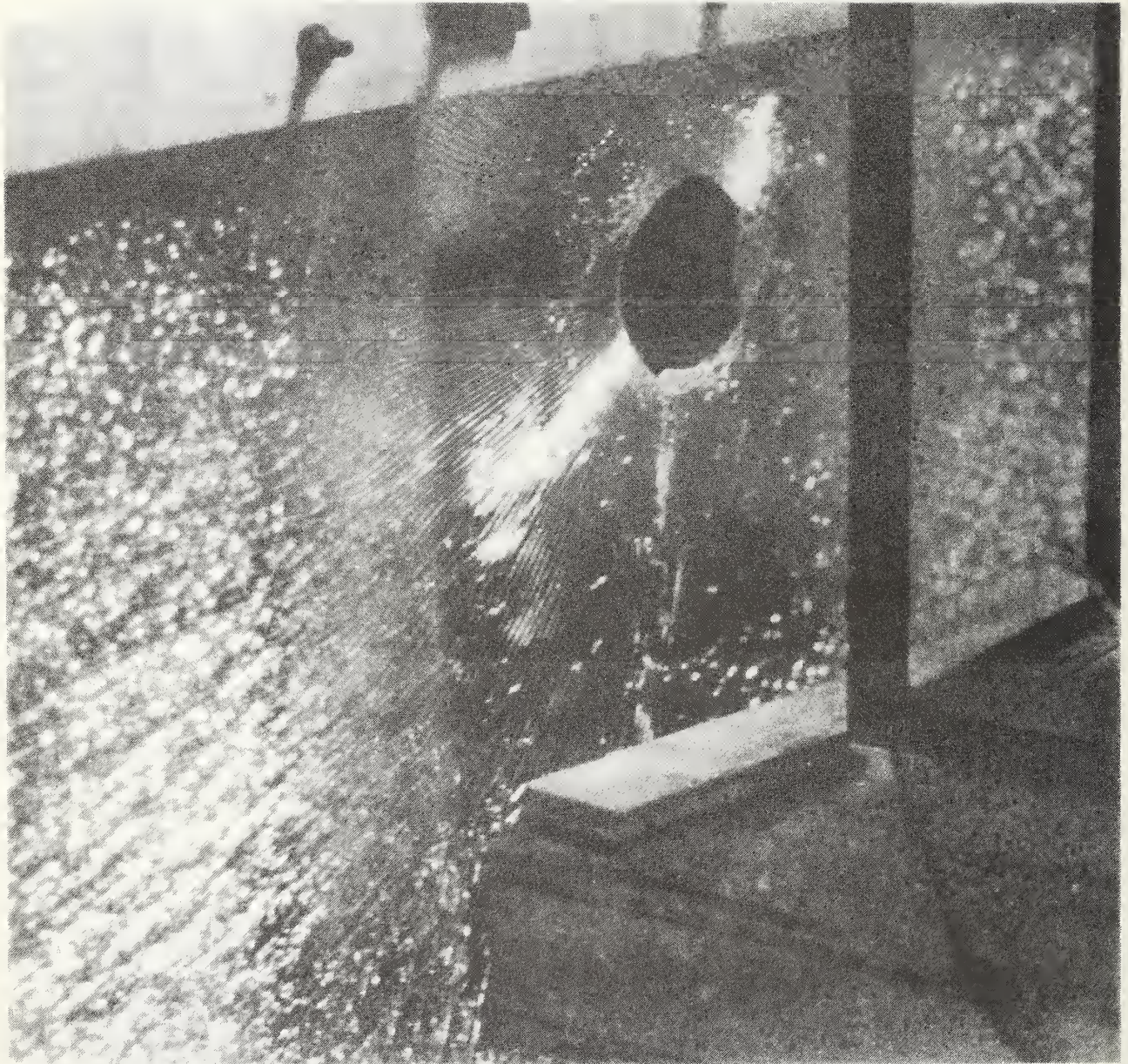


Figure 22. Hole in tempered glass cover specimen caused by impact of ice ball



Figure 23. Localized cracking failure in reinforced plastic cover caused by impacting ice ball

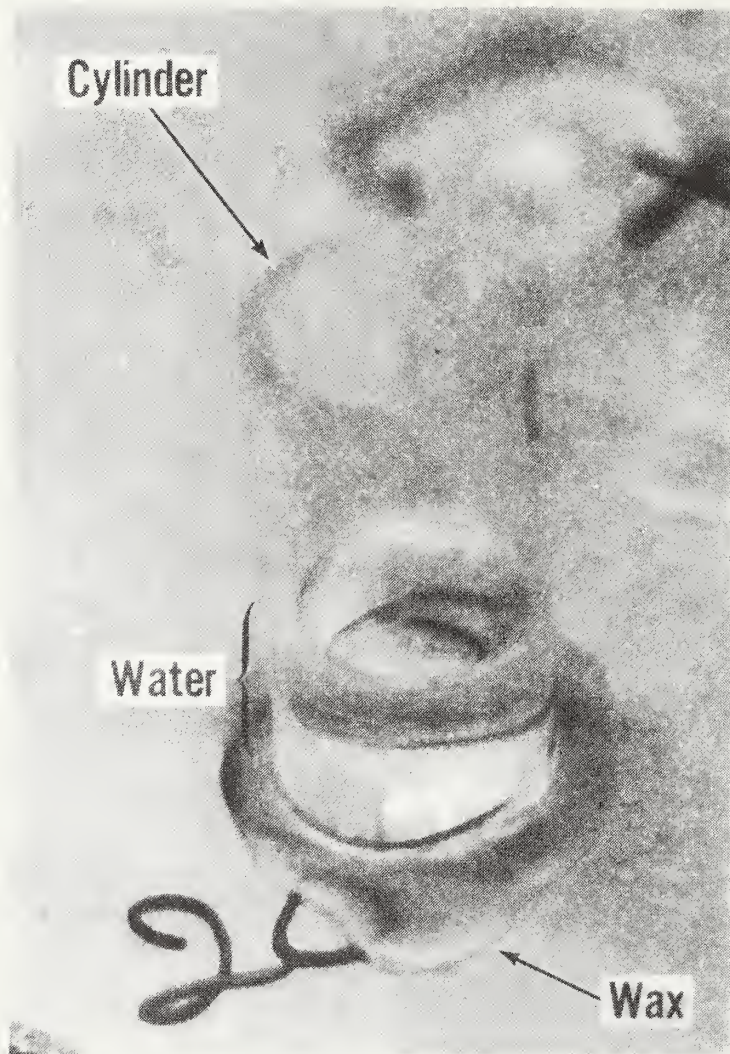


Figure 24. Cylinder sealed to reinforced plastic material for leak testing

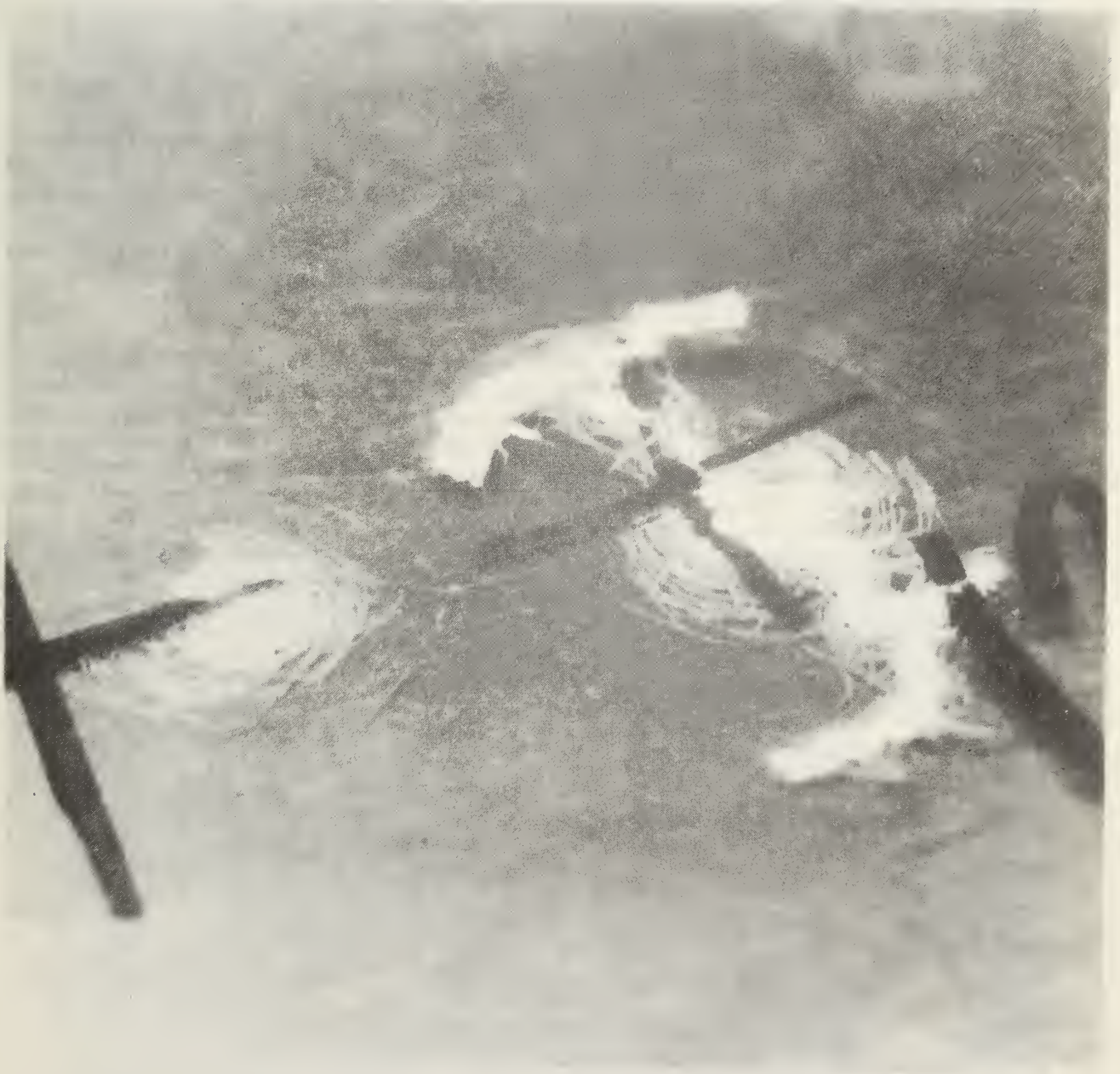


Figure 25. Tearing and penetration through reinforced plastic cover material caused by impacting ice ball

The material is not only cracked but exhibits gross tears through which water or air could flow easily. The area covered by these failures and the ease of water penetration through the damaged area are both much greater than for the localized "starring" type of failure described above. When a penetration or break in the cover material occurred, testing was stopped.

Because localized failure was observed even with relatively small ice balls, points on a given specimen were impacted only once.

The one film cover material tested was 0.004 in. thick poly(vinyl fluoride). This class of cover materials undergoes large deformations before breaking or tearing occurs. It could be characterized as the most ductile of the three classes, although some of this ductility is used up by stretching the film when it is installed in the collector or in the specimen support frame. Local failure in poly(vinyl fluoride) film takes the form of small to large indentations (figure 26) having a depth as much as 70 percent of the impacting ice ball radius. Once the indentations are formed, they persist for long periods of time. Total penetration of the cover material or puncture failure may occur for the larger ice ball sizes, as shown in figure 27.

Punctured film covers would allow much higher convection losses in the space above the absorber than would be the case for undamaged film. Water could also enter the collector through the punctured film. While the large indentations in the cover do not permit water access into the collector interior at the outset, they do contain highly deformed material which may degrade rapidly under typical environmental exposure and thus permit leakage. Another point to consider is that it may be possible where large or deep deformations occur in the film due to impact, that the film may come in contact with the absorber. If this is the case, melting of the film could occur at these locations and also part of the force at impact may be transferred to the absorber.

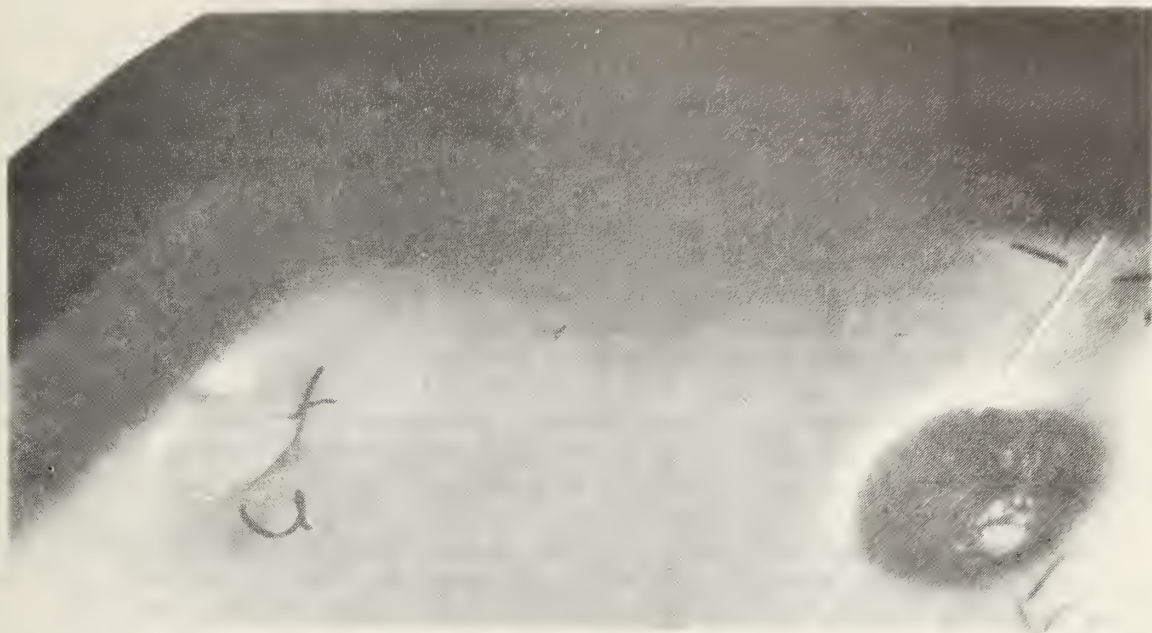


Figure 26. Indentations in plastic film cover

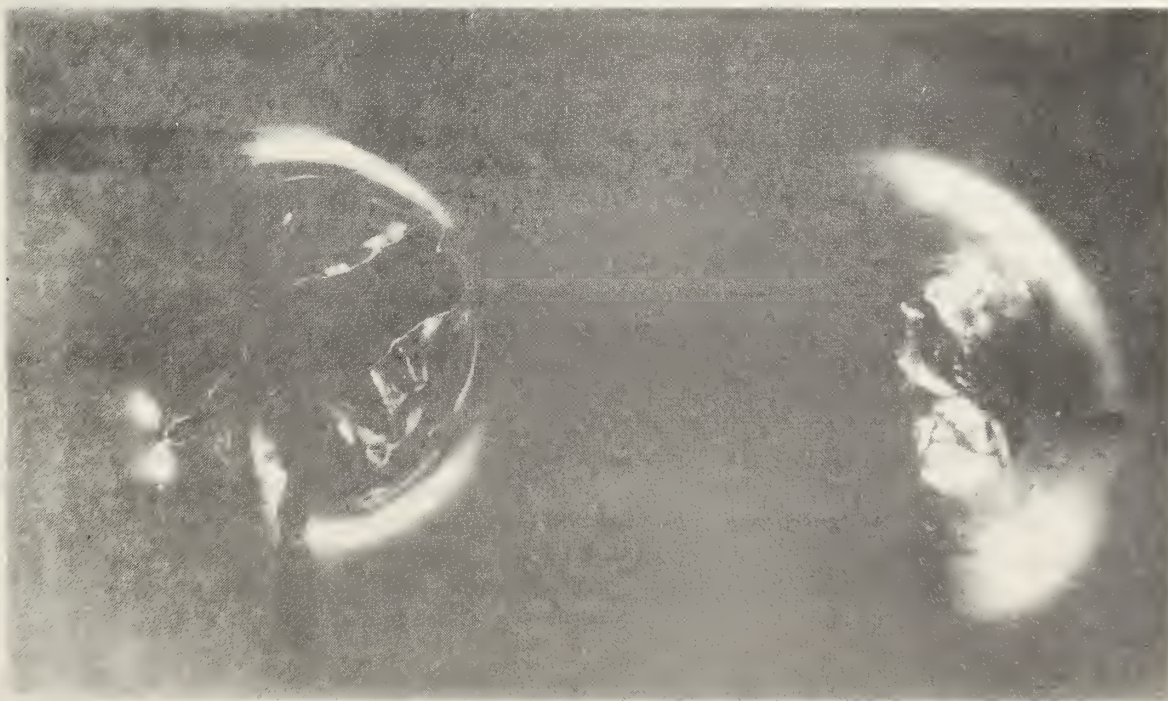


Figure 27. Puncture failures of plastic film cover

8. TEST PROCEDURE

To clarify the use of the various parts of the launcher and to demonstrate how ice ball melting is minimized, the sequence of operation followed during a test run is described.

First, the collector cover material was mounted in the cover support frame following a procedure appropriate to the type of material being tested. This is described in sections 5.1 and 5.2. After mounting, impact points were marked on the specimen surface with a black, felt-tipped pen (see figure 20). The cover support frame assembly was then mounted in the support frame positioner as described in section 5.3. Then the modified lift truck or support frame positioner was moved into position at the end of the launcher system. This location was at the left of the timing range shown in figure 3. Figure 21 shows a mounted specimen in this testing position.

By moving the lift truck laterally and using the forks of the lift truck to raise and lower the cover support frame assembly, a selected impact point was aligned with the compressed air gun with the aid of the optical pointer.

An ice ball size (diameter) and corresponding velocity were selected for the particular test series. The correct barrel was installed on the compressed air gun to match the ice ball diameter. See table 1. In addition, the chamber pressure which would produce the desired velocity was determined from the calibration data for the compressed air gun. The velocity of the ice ball as measured by the timing range was in general not considered valid if it varied more than ± 10 percent from the desired or selected velocity. With regard to ice ball size, the usual approach was to start with a small diameter and increase the selected diameter sequentially until failure occurred.

When the launcher and specimen were ready for firing, an ice ball of the selected size was removed from the freezer. The ice ball was immediately weighed and muzzle-loaded into the barrel of the compressed air gun. Then the timing range was actuated, pressure was introduced into the chamber and the quick-release valve opened to allow the pressure to act on the ice ball. The latter was, in effect, the firing sequence. The ice ball then impacted the cover material at the desired impact point. The velocity of the ice ball was measured using the timing range (section 4.3). Less than one minute elapsed between the time that the ice ball was removed from the freezer and its impact on the specimen.

After firing, the damage caused was evaluated visually and the specimen was indexed to the next impact location. Whenever failure occurred, the testing sequence for that specimen was terminated. Failure or damage assessment is discussed in section 7.

9. TEST RESULTS

9.1 GENERAL

The test results presented here are intended to give an idea of the range of ice ball sizes and corresponding velocities which result in failure for the three class of cover materials. New or unexposed materials were used in the tests and the effect of aging on the impact resistance of the cover materials was not determined. Materials may degrade as a result of environmental exposure and have considerably less impact resistance as compared to new materials. The results are not intended to be a definitive data set which can be used to define the capabilities of a given cover material. Along with this, the data demonstrate the types of failure or damage which are encountered and, consequently, must be evaluated. This has already been discussed to some extent in section 7. Finally, some notion of the degree of variability of the results can be found to the extent this is possible with a limited number of tests. For the tempered glass covers, the effect of damage from previous impacts that did not cause fracture cannot be estimated.

A summary of results from tests on four solar collector cover materials (two types of tempered glass, reinforced plastic, and plastic film) is presented in table 3. In all of these tests, cover materials were mounted in specimen support frames and were impacted by ice balls at either resultant or terminal velocity. Table 3 also contains data from an earlier series of tests, not previously reported, which were conducted on tempered glass (both sides smooth) mounted in solar collector frames. Table 3 reports the diameter, velocity, and kinetic energy of the ice ball causing failure of the cover material; the location of impact and type of failure; prior impact tests on the cover specimen; and the edge loading of plastic film during mounting in the cover support frame.

The information presented in table 3 represents only the final run of impact tests which resulted in fracture or in damage. Prior impact tests which did not result in fracture or other type of failure are listed for the tempered glass cover materials. Consider, for example, the 1/8 in. thick tempered glass with textured side exposed. Specimen No. 1 of that group had been previously subjected to impacts by 1-in. diameter ice balls at resultant velocity and 1-1/2-in. ice balls at resultant velocity. Fracture occurred when a 1-3/4-in. ice ball at resultant velocity impacted the specimen at Point No. 1 or the center of the specimen as indicated in figure 20. For the above specimen, 1 R denotes a 1-in. ice ball fired at resultant velocity and 1-1/2 R denotes a 1-1/2-in. ice ball at resultant velocity. The letter T after the diameter denotes a run at terminal velocity.

Unless noted otherwise, a test run included impacts by ice balls of a given size at either resultant or terminal velocity at all 17 points indicated in figure 20. Fracture in any run precluded further testing.

Data for all impacts during each test run on each specimen are found in appendix A. For example, table A-1 presents the data for tempered glass, textured side exposed, Specimen No. 1 impacted by 1-in. diameter ice balls at

Table 3. Summary of Ice Ball Impact Test Results

Material	Specimen Number	Appendix Table	Ice Ball Causing Failure			Impact Location ^{2/} and Type of Failure	Prior Impact Tests	Edge Loading ^{3/} (lbm/ft)
			Diameter (in.)	Velocity ^{1/} (ft/s)	Kinetic Energy (ft-lbf)			
Tempered glass. Exposed side textured, other side smooth. (1/8 in. thick)	#1	A-3	1-3/4	119 R	20	#1 Fracture	1 R, 1-1/2 R	-
	#2	A-5	1-3/4	115 R	19	#2 Fracture	1-3/4 T	-
	#3	A-6	1-3/4	122 R	20	#2 Fracture	None	-
	#4	A-7	1-3/4	101 R	14	#2 Fracture	None	-
	#5	A-8	1-1/2	95 T	7.5	#2 Fracture	None	-
	#6	A-11	1-3/4	98 T	13	#2 Fracture	1-1/2 T, 1-1/2 R	-
Tempered glass. Both sides smooth. (1/8 in. thick)	#1	A-13	2	129 R	36	#14 Fracture	2 T	-
	#2	A-17	2-1/4	131 R	49	#5 Fracture	2 R, 2-1/4 T	-
	#3	A-18	2-1/4	127 R	47	#3 Fracture	None	-
	#4	A-20	2-1/4	114 T	38	#9 Fracture	2 T	-
	#5	A-21	2	130 R	34	#4 Fracture	None	-
	#6	A-22	2	128 R	33	#1 Fracture	None	-
Tempered glass. Both sides smooth. (1/8 in. thick) Mounted in Solar Collector	A	A-38	2-1/2	135 R	78	#1 Fracture	1-3/4 R, 2 R	-
	F	A-39	1-3/4	119 R	20	#1 Fracture	None	-
	B	A-40	2-1/2	136 R	80	#10 Fracture	2 R	-
	E	A-41	2-1/2	136 R	79	#10 Fracture	2 R	-
	C	A-42	2-1/2	137 R	80	#14 Fracture	1-3/4 R, 2 R	-
D	A-43	1-3/4	115 R	19	#14 Fracture	None	-	
Reinforced plastic. Polyester resin with glass fiber mat. (0.040 in. thick)	#1	A-23	1-1/2	90 T	5.2-9.2	#1 to #11, Leak	None	-
	#1	A-23	1-1/4	82 T	3.1-5.3	#12 to #17, Leak	None	-
	#2	A-24	3/4	62 T	0.38-0.53	#1 to #17, Cracks	None	-
	#3	A-25	1-1/4	82 T	3.0-3.9	#1, #3 to 6, #8 to 11, #13 to 16, Leak	None	-
	#4	A-26	1-1/4	105 R	4.4-5.9	#2 to #12, #14, #15, Leak, #16, #17, Break	None	-
	#5	A-27	1-1/2	98 R	8.3-11.7	#1 to #17, Break	None	-
	#6	A-28	1-1/4	82 T	2.9-3.7	#3 to #9, Leak	None	-
#7	A-29	1-3/4	97 T	12-18	#1 to #9, Break	None	-	
Poly(vinyl fluoride) film. (0.004 in. thick)	#1	A-30	3/4	62 T	0.36-0.49	#1 to #17, Slight damage, small indentations	None	3.3 side 4.2 end
	#1	A-31	3/4	91 R	0.76-1.01	#1 to #17, Slight damage, small indentations	3/4 T	
	#2	A-32	1	73 T	1.1-1.6	#1 to #17, Slight damage, indentations	None	3.6 side 5.3 end
	#2	A-33	1	98 R	2.2-2.7	#1 to #17, Slight damage, indentations	1 T	
	#3	A-34	1-1/4	82 T	2.9-4.0	#1 to #4, #7 to #9, Indentations	None	5.2 side 5.5 end
			1-1/4	105 R	5.0-5.7	#5, #6, #10 to #12, #16, #17, Indentations		
	#3	A-34	1-1/2	90 T	5.8-6.6	#13, #14, Indentations	None	
	#4	A-35	1-1/2	112 R	9.3	#15 Indentation		
			2	105 T	19-24	#2, #6 to #9, Break	None	5.2 side 5.5 end
					18-20	#1, #3 to #5, Indentations		
	#5	A-36	1-3/4	117 R	16	#1, #9, Indentations	None	5.2 side 5.5 end
	#6	A-37	1-3/4	97 T	11-15	#2, #3, #6 to #8, Break		
				12-15	#1 to #9, #11 to #13, Indentations		5.2 side 5.5 end	
					#10, #14 to #17, Break	None		

1/ R = resultant velocity, T = terminal velocity.

2/ Locations are denoted by a number as shown in figure 20.

3/ Edge loading of plastic film during mounting in the cover support frame.

resultant velocity. Some variation in velocity from ice ball to ice ball is apparent in table A-1 and in other tables in appendix A. As indicated in table 2, the nominal resultant velocity for a 1-in. ice ball is 98 ft/s while actual velocities varied from 91 ft/s to 101 ft/s (table A-1). Table A-2 also gives data for Specimen No. 1, but in this case 1-1/2-in. diameter ice balls at resultant velocity were used. The data for the final run on Specimen No. 1 are given in table A-3 which shows that fracture occurred when a 1-3/4-in. ice ball impacted Point No. 1 at resultant velocity.

9.2 TEMPERED GLASS, TEXTURED SIDE EXPOSED

For the two tempered glass cover materials tested, failure implies fracture which eventually results in total destruction of the specimen. As discussed in section 7, the cracking associated with the ice ball impact extends throughout the specimen because of the residual stresses due to tempering. Although the nominal thickness of the textured glass was 1/8 in., areas of this material were thinner due to the texturing. This may account for its impact resistance being lower than the other tempered glass having both sides smooth.

Relatively little specimen-to-specimen variability was displayed by the results for tempered glass with exposed side textured. It is noted, however, that a larger number of tests, which would permit a good statistical treatment of the data, would be preferable even though variability appears to be small in this data set. Some glass cover plate manufacturers often recommend at least 30 individual specimens be tested.

As shown in table 3, all fractures were initiated either at Point No. 1, the center of the specimen, or at Point No. 2, 6 in. from the edge at the center of the long side. Figure 20 gives impact point positions on the specimen. As pointed out in section 6.4, Points 6, 7, 8, and 9 have been recommended as impact points in some test methods [2]. Since Points 6, 7, 8, and 9 have a higher degree of criticality (as described in section 6.4) than Points 1 and 2 it would be expected that smaller ice balls would cause failure at Points 6, 7, 8, and 9 than at Points 1 and 2.

Only one fracture was initiated by a 1-1/2-in. ice ball at terminal velocity. All other fractures required a 1-3/4-in. ice ball at either terminal or resultant velocity. Values of the kinetic energy causing failure ranged from 7.5 ft-lbf to 20 ft-lbf. This is a larger difference in kinetic energy than the limited range of ice ball sizes causing failure that might lead one to expect. It is noted that kinetic energy level is considered by some investigators to be a measure of damage potential.

Damage from prior impact tests did not appear to affect the fracture behavior of Specimen No. 1 and 2 since these specimens and Specimen No. 3, which had no previous impacts, were all fractured by a 1-3/4-in. ice ball at nearly the same (resultant) velocity. Specimen No. 6 which had previous impacts did not perform quite as well as Specimen No. 3, but it did perform better than Specimen No. 5 and about the same as Specimen No. 4. Specimen Nos. 4 and 5 had no previous impacts. Thus, there is no clear evidence of an effect of possible damage from previous impacts.

The data from individual impact tests conducted on tempered glass having one side textured are presented in tables A-1 to A-11 in appendix A.

9.3 TEMPERED GLASS, BOTH SIDES SMOOTH

The results for tempered glass with both sides smooth mounted in a cover support frame showed somewhat greater variability than did the results for tempered glass with exposed side textured. The variety of impact points at which fracture initiated was evidence of this. There was, in fact, no consistent effect of impact location.

All impacts that initiated fracture were caused by at least a 2-in. ice ball at resultant velocity. It should be noted that the reported velocities for the 2-in. ice balls for Specimens Nos. 1, 5, and 6 are somewhat higher than the nominal resultant velocity of 124 ft/s for this size. This accounts for the fact that a 2-1/4-in. ice ball at nominal terminal velocity, (Specimen No. 4) had only slightly higher kinetic energy than the 2-in. ice balls at nominal resultant velocity.

For 2-in. ice balls at resultant velocity, locations of fracture initiation varied from Point No. 1 at the specimen center, to Point No. 4 which is 6 in. from the edge at the center of the short side, to Point No. 14 in the corner 3 in. from each of the adjacent sides. The same situation holds for 2-1/4-in. ice balls. When the 2-1/4-in. ice balls were fired at resultant velocity, fracture was initiated in one case at Point No. 3 which is 6 in. from the edge at the center of the long side or at Point No. 5 which is positioned similarly to Point No. 4. Fracture with a 2-1/4-in. ice ball at terminal velocity occurred at Point No. 9 in a corner at a distance of 6 in. from each of the adjacent sides as might be expected. Here a more critical point should require a lesser velocity for a given size ice ball.

The kinetic energies of ice balls at fracture ranged from 33 ft-lbf to 49 ft-lbf. There seems to be little or no effect of damage from previous impacts for this material since Specimen No. 2 had the highest number of runs prior to fracture but exhibited fracture under the most severe conditions. Similarly, Specimen No. 1 with one previous run performed as well as or better than other specimens impacted by 2-in. ice balls.

Generally, this material displayed better performance than did tempered glass with the exposed side textured. Better performance here implies that impacts by larger sizes of ice balls could be sustained without fracture.

Tables A-12 through A-22 contain the data from the individual runs for this material.

9.4 SEMIRIGID FIBER REINFORCED PLASTIC SHEET

The semirigid material investigated was a polyester resin reinforced with glass fiber mat and was 0.040 in. thick. Covers of this material are much thinner

than tempered glass and the effective Young's Modulus is less than that of tempered glass. Both of these factors would lead to a notably lower plate stiffness in this case. Differences in type and extent of failure have already been discussed in section 7.

Because of possible cumulative damage, unlike glass, multiple runs were not carried out on this material since impacts with small ice balls at terminal velocity produced small regions of localized cracking. Because of this, each specimen was impacted by ice balls of only one size at one velocity.

The regions of localized cracking were larger for the larger ice balls and the cracks in most cases extended through the specimen thickness. A leak test procedure to determine whether cracks extended through the specimen is described in section 7. The onset of this degree of damage occurred with a 1-1/4-in. ice ball impacting at terminal velocity. Both Specimen No. 3 and Specimen No. 6 were subjected to these conditions and, as can be seen from table 3, leakage occurred at 13 of 17 impact points in Specimen No. 3 and at 7 of 9 impact points in Specimen No. 6.

Using a 1-1/4-in. ice ball but increasing the velocity to resultant level as in Specimen No. 4 maintained roughly the portion of impact points that showed a leak or break, i.e., 15 of 17. Going a step further and impacting with a 1-1/2-in. ice ball at terminal velocity at every point of impact up to Point No. 11 produced leaking cracks at all of them as shown in the results for Specimen No. 1 in table A-23. Points 12-17 were then impacted with 1-1/4-in. ice balls at terminal velocity and leakage occurred at all of these points.

The 1-1/2-in. ice balls at resultant velocity were used on Specimen No. 5 and more severe damage began to appear. For this specimen leaks occurred at all impact points and a large number of breaks beginning with Point No. 1 were seen. These breaks are perceptible tears in the cover material through which air or water could easily penetrate.

The progression of increasing impact severity and increasing damage described above suggests relatively consistent behavior by this material. It should be noted that Specimens No. 1 and 2 were "old" material, that is, material that had been on hand for possibly two years while the remainder of the specimens were material which had been purchased recently.

The kinetic energy range of 2.9 ft-lbf to 9.2 ft-lbf was associated with local cracking and leakage. At the upper end of this range more severe damage began to be evident. Large scale tearing or penetration occurred in the kinetic energy range of 13.3 ft-lbf to 14.0 ft-lbf.

Data from individual reinforced plastic specimen runs are presented in tables A-23 to A-29 of appendix A.

9.5 FLEXIBLE THIN PLASTIC FILM

The poly(vinyl fluoride) film cover material which was investigated was only 0.004 in. thick and behaved as a membrane rather than a plate in bending.

When new, the material is very ductile so that impacting ice balls with progressively larger diameters locally deform the film with indentations of increasing size until breaks or penetration through the material occurred.

All poly(vinyl fluoride) specimens were tensioned when mounted in the specimen supported frames and, since the tensioning load was not the same for all specimens, the values used are indicated in table 3. The tensioning procedure is described in section 5.2.

For both Specimen No. 1 and No. 2, two test runs were made with a given ice ball size. In Specimen No. 1, all impact points were subjected to 3/4-in. ice balls at terminal velocity and then the procedure was repeated for points about 1 in. away from the originals with 3/4-in. ice balls at resultant velocity. Specimen No. 2 was tested the same way but with 1-in. ice balls. In both cases, small indentations which only slightly damaged the cover sheet were produced.

In Specimen No. 3, Point Nos. 1-4 and 7-9 were impacted with 1-1/4-in. ice balls at terminal velocity while Point Nos. 5, 6, 10, 11, and 12 were impacted at resultant velocity. See table A-34. A maximum indentation depth of 0.22 in. occurred at Point No. 10. Points 13 and 14 were then impacted with 1-1/2-in. ice balls traveling at terminal velocity. A maximum indentation depth of 0.34 in. was found at Point No. 13. The indentation depth was 0.19 in. at Point No. 12, a point of identical criticality. Thus, a step change in material response occurs between 1-1/4 in. ice balls at resultant velocity and 1-1/2-in. ice balls at terminal velocity.

When larger size ice balls were used, breaks or penetration through the material occurred. This began with 1-3/4-in. ice balls at terminal velocity, Specimen No. 6, in which breaks appeared at 5 of 17 points impacted. When Specimen No. 5, was impacted with 1-3/4-in. ice balls at resultant velocity, 5 of 7 impacted points displayed breaks and the other two, large indentations. Increasing the ice ball size to 2 in. and firing at terminal velocity did not greatly increase the proportion of breaks at impact points. However, the depth of indentation at points that did not break increased as shown by Specimen 4 (table A-35). Again, the increasing damage associated with increasing impact severity tended to indicate consistent specimen-to-specimen behavior of this material.

For this thin film material, only slight damage occurred for kinetic energy levels up to 2.7 ft-lbf. When the kinetic energy was in the range 5.0 to 6.6 ft-lbf, rather large, permanent, indentations occurred which may be detrimental to collector performance depending on the number of indentations and other environmental factors. However, for kinetic energy levels greater than about 12 ft-lbf, ice balls may penetrate through the cover material. The latter phenomenon occurred for kinetic energies ranging from 12 to 24 ft-lbf, while in some cases the material did not break at an energy level of as much as 20 ft-lbf.

9.6 TEMPERED GLASS MOUNTED IN SOLAR COLLECTORS

These data were obtained by Mathey in 1976 and have not been reported previously in the open literature. Testing conditions were very similar to those which

have been described in this report and previously by Mathey [7]. The tempered glass cover material, both sides smooth, was also very similar to the material described in section 9.3.

In table 3, impact locations for this data set are reported in terms of the points shown in figure 20. Data from the individual runs for the six specimens are presented in tables A-38 to A-43 in appendix A.

The major difference between these tests and the ones reported in section 9.3 lies in the edge conditions or support conditions. A detail of the solar collector construction as it relates to support of the cover plate is shown in figure 28.

When fracture results are compared for specimens mounted in the specimen support frames and specimens in solar collectors, very little difference is seen. Two of the six specimens in the solar collectors were fractured by 1-3/4-in. ice balls at the resultant velocity (Point Nos. 1 and 14, specimens F and D, respectively). The other four specimens were fractured by 2-1/2-in ice balls at the resultant velocity.

Specimens mounted in the support frames were fractured by a 2-in. ice ball at resultant velocity. For impacts in the corner, Points No. 14-17, the same situation applied. The cover material mounted in the solar collector appeared to have greater resistance to ice ball impacts but the variability was greater than was found for cover specimens mounted in the support frames.

This suggests that the specimen support frames described in section 5.1 provide adequate simulation of the edge conditions in solar collectors. Conservative test results appear to be produced.

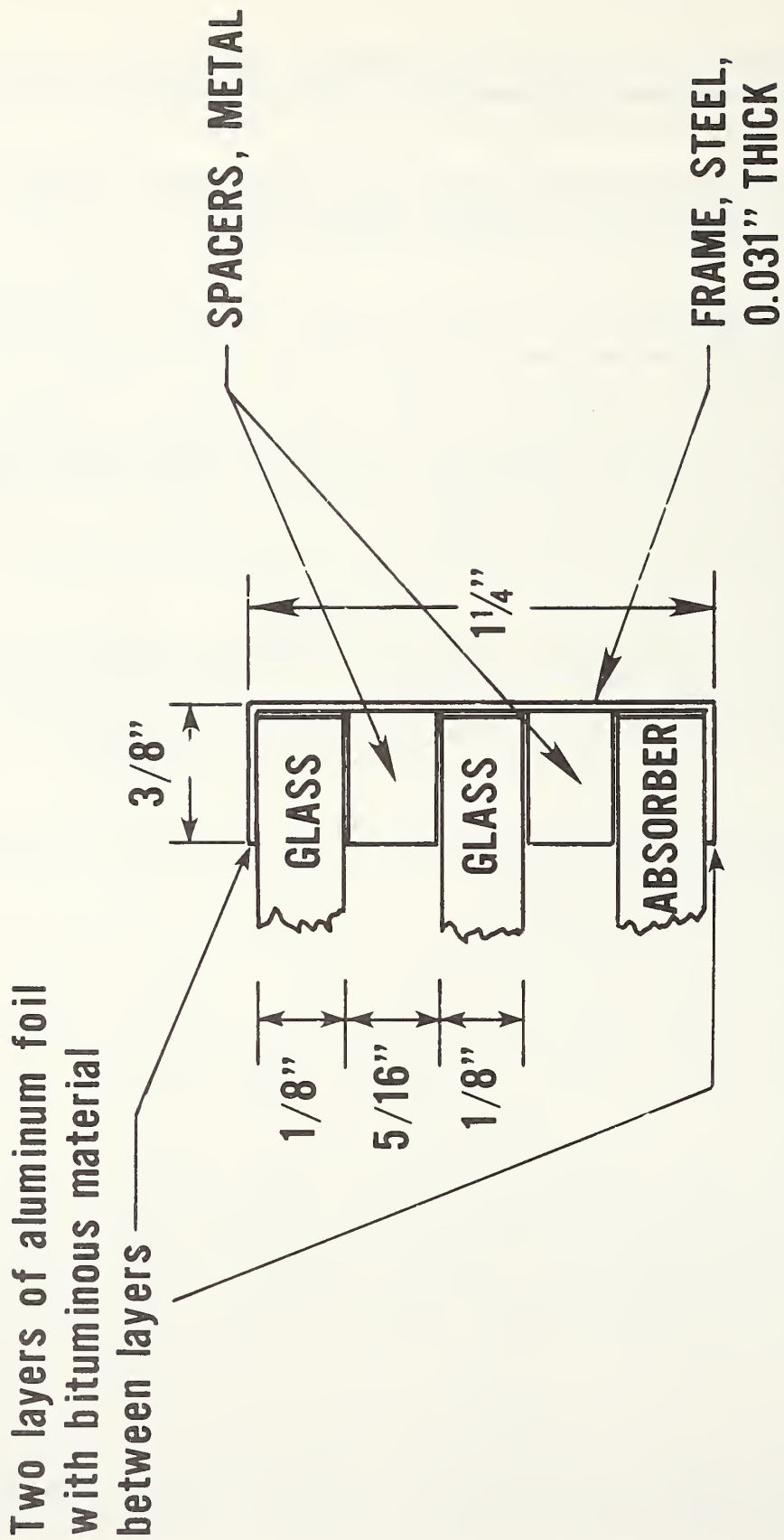


Figure 28. Detail of solar collector edge support

10. CONCLUSIONS

This report has presented a discussion of important parameters and testing considerations which relate to laboratory testing of solar collector covers for determining their resistance to hail impact. In addition to this, a fully detailed experimental procedure for performing such testing is described. This includes the preparation of ice balls, the launching or propulsion of ice balls, a method for appropriately mounting cover specimens, the selection of ice ball velocity and impact location, and various aspects of failure or damage assessment. Finally, results of simulated hail impact tests on four typical solar collector cover materials are presented and evaluated.

It was intended that the results of this research would contribute to the development of a general test method for simulating hail impact on solar collector covers.

The data and analysis presented in this report appear to support the following conclusions:

1. Ice spheres or ice balls provide good simulation of hailstones. Clear ice balls, without cracks and with consistent diameter and mass, can be readily prepared in laboratory. Modifying the clear ice density is judged to be unnecessary.
2. Ice balls should impact a specimen along a path perpendicular to the specimen surface at a resultant velocity which is the vector sum of the hailstone terminal velocity and a horizontal wind velocity component corresponding to 45 mi/h or 66 ft/s.
3. A compressed air launcher with interchangeable plastic barrels of different diameters for propelling the ice balls offers a safe and readily controllable propulsion system. This is based on the authors' experience and that of other investigators.
4. A system for accurate velocity measurement (within about 2 percent) of ice balls in flight is essential. The velocity data were in general not considered valid if they varied more than ± 10 percent from the desired or selected values.
5. A support frame for collector cover materials was found to offer good simulation of support conditions as compared to actual collectors.
6. The preference for various impact locations and their influence on test results is difficult to define. Arbitrarily selected points near the cover plate boundaries appear to be a satisfactory compromise. Plate bending response is not the only structural behavior mode present, particularly near the corners.
7. Several kinds of failure must be considered when evaluating test results, one of which is fracture or rupture of the cover plate. Others include localized cracking which may permit water penetration and localized regions of severe deformation which may alter optical properties.

11. REFERENCES

1. Cattaneo, L. E., Harris, J. R., Reinhold, T. A., Simiu, E., and Yancey, C. W. C., Wind, Earthquake, Snow, and Hail Loads on Solar Collectors, NBSIR 81-2199, National Bureau of Standards, Washington, DC, January 1981. (See, in particular, Part IV).
2. Waksman, D., Streed, E., R., Reichard, T. W., and Cattaneo, L. E., Provisional Flat Plate Solar Collector Testing Procedures: First Revision, NBSIR 78-1305 A, National Bureau of Standards, Washington, DC, June 1978.
3. Intermediate Minimum Property Standards Supplement, Solar Heating and Domestic Hot Water Systems, 1977 Edition, HUD 4930.2, prepared for HUD by NBS.
4. Interim Performance Criteria for Solar Heating and Cooling Systems in Commercial Buildings, NSIR 76-1187, National Bureau of Standards, Washington, DC, November 1976.
5. Interim Performance Criteria for Solar Heating and Combined Heating/Cooling Systems and Dwellings, January 1975, prepared for HUD by NBS.
6. Greenfeld, S. N., Hail Resistance of Roofing Products, Building Science Series 23, National Bureau of Standards, Washington, DC, August 1969.
7. Mathey R. G., Hail Resistance Tests of Aluminum Skin Honeycomb Panels for the Relocatable Lewis Building, Phase II, NBS Report 10193, National Bureau of Standards, Washington, DC, April 1970.
8. List, R., Cantin, J. G., and Ferland, M. G., "Structural Properties of Two Hailstone Samples," Journal of the Atmospheric Sciences, Vol. 27, pp. 1080-1090, October 1970.
9. Macklin, W. C., Strauch, E., and Ludlam, F. N., "The Density of Hailstones Collected from a Summer Storm", Nubila, Vol. 3, pp. 12-17, 1960.
10. Clough, R. W., and Penzien, J., Dynamics of Structures, McGraw-Hill, 1975.
11. Meirovich, L., Analytical Methods in Vibrations, Macmillan, 1967.
12. Hertz, H. (See Timoshenko, S. and Goodier, J. N., Theory of Elasticity, McGraw-Hill, 1951, Sec 125)
13. Smith, M. L., Hail Testing of Solar Reflector Panels, Preprint: Solar Reflector Materials Technology Workshop, Texas Tech University, Lubbock, TX, 1978.

14. Moore, D., Wilson, A., and Ross, R., "Simulated Hail Impact Testing of Photovoltaic Solar Panels", Proceedings - Institute of Environmental Sciences, pp. 419-430, 1978.
15. Moore, D., and Wilson, A., "Photovoltaic Solar Panel Resistance to Simulated Hail", DOE/JPL-1012-78/6 (Low-Cost Solar Array Project 5101-62), Jet Propulsion Laboratory, Pasadena, CA, October 15, 1978.
16. Rupp, R., "Structure and Mode of Operation of a Tester for Investigation of the Resistance of Roofing Materials Against Simulated Hail-Impact", Material and Technik, No. 4, pp. 198-201, 1976 (In German).
17. Bilham, E. G., and Relf, E. F., "The Dynamics of Large Hailstones" Quarterly Journal of the Royal Meteorological Society, Vol. 63, pp. 149-162, 1937.
18. List, R., "The Aerodynamics of Hailstones" Zeitschrift für angewandte Mathematik and Physik, Vol. 10, No. 2, pp. 143-159, 1959, Research Translation T-G-244, Air Force Cambridge Research Laboratories, Bedford, MA, September 1965.
19. Macklin, W. C. and Ludlam, F. N., "The Fallspeeds of Hailstones," Quarterly Journal of the Royal Meteorological Society, Vol. 87, No. 371, 1961.
20. Baldwin, J. L., Climates of the United States, National Oceanic and Atmospheric Administration, Environmental Data Service, Washington, DC, 1973.
21. Technical Support Package for Tech. Brief 68-10552, Simulated Hailstone Fabrication, PB 183 582, Office of Technology Utilization, National Aeronautics and Space Administration, Washington, DC.
22. Schleusener, R. A., "Hailstorm Characterization and the Crystal Structure of Hail," Meteorological Monographs, Vol. 5, No. 27, pp. 173-176, September 1963.
23. Laurie, J. A. P., "Hail and Its Effects on Buildings," Bulletin 21, National Building Research Institute, Pretoria, South Africa, August 1960.

APPENDIX A. IMPACT TEST DATA

The tables (A-1 to A-43) presented in this appendix contain data from each ice ball impact on each specimen of the collector cover material. In a given, table, data are in general presented for one ice ball size corresponding to either terminal or resultant velocity. Exceptions to this are tables A-23, A-34, A-38, A-40, A-41, and A-42 where more than one ice ball size and velocity were tried on a given specimen. Measured ice ball mass, velocities, and observed damage states are listed. The kinetic energy calculated for each ice ball is also listed.

The tables are arranged with data from tempered glass, exposed side textured, mounted in a cover support frame, listed first. This is followed by data for tempered glass, both sides smooth, then fiber reinforced plastic sheet and finally poly(vinyl fluoride) film materials mounted in a cover support frame. The last six tables contain data from tempered glass mounted in solar collectors.

The numerical designation of the impact locations are shown in figure 20.

Table A-1
Tempered Glass
Exposed Side Textured
1/8 in. Thick

Specimen No. 1

Impact Location*	Desired Resultant Velocity (ft/s)	Ice Ball				Results of Impact
		Nominal Diameter (in.)	Weight Mass (lbm)	Velocity (ft/s)	Kinetic Energy (ft-lbf)	
1	98	1	0.018	96	2.5	No visible damage
2	98	1	0.016	92	2.2	No visible damage
3	98	1	0.016	99	2.5	No visible damage
4	98	1	0.018	98	2.6	No visible damage
5	98	1	0.016	96	2.4	No visible damage
6	98	1	0.018	93	2.4	No visible damage
7	98	1	0.016	92	2.2	No visible damage
8	98	1	0.018	99	2.7	No visible damage
9	98	1	0.016	94	2.3	No visible damage
10	98	1	0.016	95	2.3	No visible damage
11	98	1	0.018	91	2.3	No visible damage
12	98	1	0.018	100	2.7	No visible damage
13	98	1	0.016	101	2.6	No visible damage
14	98	1	0.015	95	2.2	No visible damage
15	98	1	0.018	100	2.7	No visible damage
16	98	1	0.018	98	2.6	No visible damage
17	98	1	0.016	95	2.3	No visible damage

* Impact locations are shown in figure 20.

Table A-2
Tempered Glass
Exposed Side Textured
1/8 in. Thick

Specimen No. 1

Impact Location	Desired Resultant Velocity (ft/s)	Ice Ball				Results of Impact
		Nominal Diameter (in.)	Weight Mass (lbm)	Velocity (ft/s)	Kinetic Energy (ft-lbf)	
1	112	1-1/2	0.060	120	13	No visible damage
2	112	1-1/2	0.060	118	13	No visible damage
3	112	1-1/2	0.060	114	12	No visible damage
4	112	1-1/2	0.060	104	10	No visible damage
5	112	1-1/2	0.060	116	12	No visible damage
6	112	1-1/2	0.060	112	12	No visible damage
7	112	1-1/2	0.060	110	11	No visible damage
8	112	1-1/2	0.060	111	11	No visible damage
9	112	1-1/2	0.060	106	10	No visible damage
10	112	1-1/2	0.060	115	12	No visible damage
11	112	1-1/2	0.060	110	11	No visible damage
12	112	1-1/2	0.060	111	11	No visible damage
13	112	1-1/2	0.060	111	11	No visible damage
14	112	1-1/2	0.060	113	12	No visible damage
15	112	1-1/2	0.058	110	11	No visible damage
16	112	1-1/2	0.060	112	12	No visible damage
17	112	1-1/2	0.060	114	12	No visible damage

Table A-3
Tempered Glass
Exposed Side Textured
1/8 in. Thick

Specimen No. 1

Impact Location	Desired Resultant Velocity (ft/s)	Ice Ball				Results of Impact
		Nominal Diameter (in.)	Weight Mass (lbm)	Velocity (ft/s)	Kinetic Energy (ft-lbf)	
1	117	1-3/4	0.093	119	20	Fracture

Table A-4
Tempered Glass
Exposed Side Textured
1/8 in. Thick

Specimen No. 2

Impact Location	Desired Terminal Velocity (ft/s)	Ice Ball				Results of Impact
		Nominal Diameter (in.)	Weight Mass (lbm)	Velocity (ft/s)	Kinetic Energy (ft-lbf)	
1	97	1-3/4	0.093	114	19	No visible damage
2	97	1-3/4	0.090	97	13	No visible damage
3	97	1-3/4	0.090	107	16	No visible damage
4	97	1-3/4	0.089	99	14	No visible damage
5	97	1-3/4	0.093	96	13	No visible damage
6	97	1-3/4	0.088	100	14	No visible damage
7	97	1-3/4	0.089	108	16	No visible damage
8	97	1-3/4	0.090	102	15	No visible damage
9	97	1-3/4	0.090	106	16	No visible damage
10	97	1-3/4	0.088	116	18	No visible damage
11	97	1-3/4	0.088	101	14	No visible damage
12	97	1-3/4	0.090	100	14	No visible damage
13	97	1-3/4	0.099	96	13	No visible damage
14	97	1-3/4	0.089	98	13	No visible damage
15	97	1-3/4	0.088	107	16	No visible damage
16	97	1-3/4	0.088	99	13	No visible damage
17	97	1-3/4	0.088	97	13	No visible damage

Table A-5
Tempered Glass
Exposed Side Textured
1/8 in. Thick

Specimen No. 2

Impact Location	Desired Resultant Velocity (ft/s)	Ice Ball				Results of Impact
		Nominal Diameter (in.)	Weight Mass (lbm)	Velocity (ft/s)	Kinetic Energy (ft-lbf)	
1	117	1-3/4	0.090	129	24	No visible damage
2	117	1-3/4	0.090	115	19	Fracture

Table A-6
Tempered Glass
Exposed Side Textured
1/8 in. Thick

Specimen No. 3

Impact Location	Desired Resultant Velocity (ft/s)	Ice Ball				Results of Impact
		Nominal Diameter (in.)	Weight Mass (lbm)	Velocity (ft/s)	Kinetic Energy (ft-lbf)	
1	117	1-3/4	0.090	119	20	No visible damage
2	117	1-3/4	0.090	122	20	Fracture

Table A-7
Tempered Glass
Exposed Side Textured
1/8 in. Thick

Specimen No. 4

Impact Location	Desired Terminal Velocity (ft/s)	Ice Ball				Results of Impact
		Nominal Diameter (in.)	Weight Mass (lbm)	Velocity (ft/s)	Kinetic Energy (ft-lbf)	
1	97	1-3/4	0.086	100	14	No visible damage
2	97	1-3/4	0.086	101	14	Fracture

Table A-8
Tempered Glass
Exposed Side Textured
1/8 in. Thick

Specimen No. 5

Impact Location	Desired Terminal Velocity (ft/s)	Ice Ball			Kinetic Energy (ft-lbf)	Results of Impact
		Nominal Diameter (in.)	Weight Mass (lbm)	Velocity (ft/s)		
1	90	1-1/2	0.051	80	5.1	No visible damage
2	90	1-1/2	0.053	95	7.5	Fracture

Table A-9
Tempered Glass
Exposed Side Textured
1/8 in. Thick

Specimen No. 6

Impact Location	Desired Terminal Velocity (ft/s)	Ice Ball			Kinetic Energy (ft-lbf)	Results of Impact
		Nominal Diameter (in.)	Weight Mass (lbm)	Velocity (ft/s)		
1	90	1-1/2	0.051	89	6.3	No visible damage
2	90	1-1/2	0.051	87	5.9	No visible damage
3	90	1-1/2	0.051	83	5.4	No visible damage
4	90	1-1/2	0.051	91	6.5	No visible damage
5	90	1-1/2	0.053	88	6.3	No visible damage
6	90	1-1/2	0.053	90	6.7	No visible damage
7	90	1-1/2	0.051	90	6.4	No visible damage
8	90	1-1/2	0.053	96	7.6	No visible damage
9	90	1-1/2	0.053	87	6.2	No visible damage

Table A-10
Tempered Glass
Exposed Side Textured
1/8 in. Thick

Specimen No. 6

Impact Location	Desired Resultant Velocity (ft/s)	Ice Ball			Kinetic Energy (ft-lbf)	Results of Impact
		Nominal Diameter (in.)	Weight Mass (lbm)	Velocity (ft/s)		
1	112	1-1/2	0.053	104	8.9	No visible damage
2	112	1-1/2	0.053	111	10.1	No visible damage
3	112	1-1/2	0.051	98	7.5	No visible damage
4	112	1-1/2	0.055	115	11.4	No visible damage
5	112	1-1/2	0.053	105	9.1	No visible damage
6	112	1-1/2	0.055	122	12.8	No visible damage
7	112	1-1/2	0.055	116	11.6	No visible damage
8	112	1-1/2	0.057	115	11.8	No visible damage
9	112	1-1/2	0.055	113	11.0	No visible damage

Table A-11
Tempered Glass
Exposed Side Textured
1/8 in. Thick

Specimen No. 6

Impact Location	Desired Terminal Velocity (ft/s)	Ice Ball			Kinetic Energy (ft-lbf)	Results of Impact
		Nominal Diameter (in.)	Weight Mass (lbm)	Velocity (ft/s)		
1	97	1-3/4	0.086	101	14	No visible damage
2	97	1-3/4	0.086	98	13	Fracture

Table A-12
Tempered Glass
Both Sides Smooth
1/8 in. Thick

Specimen No. 1

Impact Location	Desired Terminal Velocity (ft/s)	Ice Ball			Kinetic Energy (ft-lbf)	Results of Impact
		Nominal Diameter (in.)	Weight Mass (lbm)	Velocity (ft/s)		
1	105	2	0.141	104	24	No visible damage
2	105	2	0.139	106	24	No visible damage
3	105	2	0.139	120	31	No visible damage
4	105	2	0.138	107	24	No visible damage
5	105	2	0.138	108	25	No visible damage
6	105	2	0.139	109	26	No visible damage
7	105	2	0.138	103	23	No visible damage
8	105	2	0.138	107	24	No visible damage
9	105	2	0.140	109	25	No visible damage
10	105	2	0.138	113	27	No visible damage
11	105	2	0.138	101	21	No visible damage
12	105	2	0.139	111	27	No visible damage
13	105	2	0.141	113	28	No visible damage
14	105	2	0.138	118	30	No visible damage
15	105	2	0.138	113	27	No visible damage
16	105	2	0.138	94	19	No visible damage
17	105	2	0.138	110	26	No visible damage

Table A-13
Tempered Glass
Both Sides Smooth
1/8 in. Thick

Specimen No. 1

Impact Location	Desired Resultant Velocity (ft/s)	Ice Ball			Kinetic Energy (ft-lbf)	Results of Impact
		Nominal Diameter (in.)	Weight Mass (lbm)	Velocity (ft/s)		
1	124	2	0.139	121	32	No visible damage
2	124	2	0.133	126	33	No visible damage
3	124	2	0.137	135	39	No visible damage
4	124	2	0.138	125	33	No visible damage
5	124	2	0.134	130	35	No visible damage
6	124	2	0.139	128	35	No visible damage
7	124	2	0.136	126	34	No visible damage
8	124	2	0.137	128	35	No visible damage
9	124	2	0.138	120	31	No visible damage
10	124	2	0.136	122	31	No visible damage
11	124	2	0.139	129	36	No visible damage
12	124	2	0.138	130	36	No visible damage
13	124	2	0.137	130	36	No visible damage
14	124	2	0.137	129	36	Fracture

Table A-14
Tempered Glass
Both Sides Smooth
1/8 in. Thick

Specimen No. 2

Impact Location	Desired Resultant Velocity (ft/s)	Ice Ball			Kinetic Energy (ft-lbf)	Results of Impact
		Nominal Diameter (in.)	Weight Mass (lbm)	Velocity (ft/s)		
10	124	2	0.137	126	34	No visible damage
11	124	2	0.134	121	30	No visible damage
12	124	2	0.136	128	34	No visible damage
13	124	2	0.139	123	33	No visible damage
14	124	2	0.137	131	36	No visible damage
15	124	2	0.139	117	30	No visible damage
16	124	2	0.139	113	38	No visible damage
17	124	2	0.137	131	37	No visible damage

Table A-15
Tempered Glass
Both Sides Smooth
1/8 in. Thick

Specimen No. 2

Impact Location	Desired Resultant Velocity (ft/s)	Ice Ball				Results of Impact
		Nominal Diameter (in.)	Weight Mass (lbm)	Velocity (ft/s)	Kinetic Energy (ft-lbf)	
10	124	2	0.139	128	35	No visible damage
11	124	2	0.138	122	32	No visible damage
12	124	2	0.136	123	32	No visible damage
13	124	2	0.137	126	33	No visible damage
14	124	2	0.138	125	33	No visible damage
15	124	2	0.139	133	38	No visible damage
16	124	2	0.140	132	38	No visible damage
17	124	2	0.138	120	31	No visible damage

Table A-16
Tempered Glass
Both Sides Smooth
1/8 in. Thick

Specimen No. 2

Impact Location	Desired Terminal Velocity (ft/s)	Ice Ball				Results of Impact
		Nominal Diameter (in.)	Weight Mass (lbm)	Velocity (ft/s)	Kinetic Energy (ft-lbf)	
1	111	2-1/4	0.187	114	38	No visible damage
2	111	2-1/4	0.187	119	41	No visible damage
3	111	2-1/4	0.187	117	40	No visible damage
4	111	2-1/4	0.190	120	43	No visible damage
5	111	2-1/4	0.190	114	39	No visible damage
6	111	2-1/4	0.187	114	38	No visible damage
7	111	2-1/4	0.190	114	39	No visible damage
8	111	2-1/4	0.190	111	36	No visible damage
9	111	2-1/4	0.190	113	37	No visible damage
10	111	2-1/4	0.190	112	37	No visible damage
11	111	2-1/4	0.190	111	36	No visible damage
12	111	2-1/4	0.190	113	37	No visible damage
13	111	2-1/4	0.190	112	37	No visible damage
14	111	2-1/4	0.190	116	40	No visible damage
15	111	2-1/4	0.190	113	38	No visible damage
16	111	2-1/4	0.190	112	37	No visible damage
17	111	2-1/4	0.186	111	36	No visible damage

Table A-17
Tempered Glass
Both Sides Smooth
1/8 in. Thick

Specimen No. 2

Impact Location	Desired Resultant Velocity (ft/s)	Ice Ball				Results of Impact
		Nominal Diameter (in.)	Weight Mass (lbm)	Velocity (ft/s)	Kinetic Energy (ft-lbf)	
1	129	2-1/4	0.186	127	46	No visible damage
2	129	2-1/4	0.187	127	47	No visible damage
3	129	2-1/4	0.190	134	53	No visible damage
4	129	2-1/4	0.187	129	49	No visible damage
5	129	2-1/4	0.185	131	49	Fracture

Table A-18
Tempered Glass
Both Sides Smooth
1/8 in. Thick

Specimen No. 3

Impact Location	Desired Resultant Velocity (ft/s)	Ice Ball				Results of Impact
		Nominal Diameter (in.)	Weight Mass (lbm)	Velocity (ft/s)	Kinetic Energy (ft-lbf)	
1	129	2-1/4	0.187	131	50	No visible damage
2	129	2-1/4	0.190	127	47	No visible damage
3	129	2-1/4	0.187	127	47	Fracture

Table A-19
Tempered Glass
Both Sides Smooth
1/8 in. Thick

Specimen No. 4

Impact Location	Desired Terminal Velocity (ft/s)	Ice Ball				Results of Impact
		Nominal Diameter (in.)	Weight Mass (lbm)	Velocity (ft/s)	Kinetic Energy (ft-lbf)	
1	105	2	0.126	112	25	No visible damage
2	105	2	0.128	112	25	No visible damage
3	105	2	0.126	102	20	No visible damage
4	105	2	0.126	116	26	No visible damage
5	105	2	0.126	117	27	No visible damage
6	105	2	0.126	98	19	No visible damage
7	105	2	0.128	102	21	No visible damage
8	105	2	0.126	92	18	No visible damage
9	105	2	0.126	103	21	No visible damage

Table A-20
Tempered Glass
Both Sides Smooth
1/8 in. Thick

Specimen No. 4

Impact Location	Desired Terminal Velocity (ft/s)	Ice Ball				Results of Impact
		Nominal Diameter (in.)	Weight Mass (lbm)	Velocity (ft/s)	Kinetic Energy (ft-lbf)	
1	111	2-1/4	0.185	107	33	No visible damage
2	111	2-1/4	0.192	117	41	No visible damage
3	111	2-1/4	0.190	116	40	No visible damage
4	111	2-1/4	0.192	114	38	No visible damage
8	111	2-1/4	0.190	113	37	No visible damage
9	111	2-1/4	0.190	114	38	Fracture

Table A-21
Tempered Glass
Both Sides Smooth
1/8 in. Thick

Specimen No. 5

Impact Location	Desired Resultant Velocity (ft/s)	Ice Ball				Results of Impact
		Nominal Diameter (in.)	Weight Mass (lbm)	Velocity (ft/s)	Kinetic Energy (ft-lbf)	
1	124	2	0.129	123	30	No visible damage
2	124	2	0.123	121	28	No visible damage
3	124	2	0.126	127	32	No visible damage
4	124	2	0.128	130	34	Fracture

Table A-22
Tempered Glass
Both Sides Smooth
1/8 in. Thick

Specimen No. 6

Impact Location	Desired Resultant Velocity (ft/s)	Ice Ball				Results of Impact
		Nominal Diameter (in.)	Weight Mass (lbm)	Velocity (ft/s)	Kinetic Energy (ft-lbf)	
1	124	2	0.129	128	33	Fracture

Table A-23
Reinforced Plastic
Polyester Resin With Glass Fiber Mat
0.040 in. Thick

Specimen No. 1 ("Old" Material)

Impact Location	Desired Terminal Velocity (ft/s)	Ice Ball				Results of Impact
		Nominal Diameter (in.)	Weight Mass (lbm)	Velocity (ft/s)	Kinetic Energy (ft-lbf)	
1	90	1-1/2	0.058	101	9.2	Leaked
2	90	1-1/2	0.060	101	9.5	Leaked
3	90	1-1/2	0.057	76	5.2	Leaked
4	90	1-1/2	0.058	100	9.0	Leaked
5	90	1-1/2	0.057	97	8.4	Leaked
6	90	1-1/2	0.057	101	9.1	Leaked
7	90	1-1/2	0.057	97	8.3	Leaked
8	90	1-1/2	0.057	93	7.7	Leaked
9	90	1-1/2	0.057	77	5.3	Leaked
10	90	1-1/2	0.057	91	7.4	Leaked
11	90	1-1/2	0.058	99	8.9	Leaked
12	82	1-1/4	0.033	101	5.3	Leaked
13	82	1-1/4	0.031	81	3.1	Leaked
14	82	1-1/4	0.031	85	3.4	Leaked
15	82	1-1/4	0.032	86	3.7	Leaked
16	82	1-1/4	0.032	82	3.3	Leaked
17	82	1-1/4	0.032	88	3.8	Leaked

Table A-24
Reinforced Plastic
Polyester Resin With Glass Fiber Mat
0.040 in. Thick

Specimen No. 2 ("Old" Material)

Impact Location	Desired Terminal Velocity (ft/s)	Ice Ball				Results of Impact
		Nominal Diameter (in.)	Weight Mass (lbm)	Velocity (ft/s)	Kinetic Energy (ft-lbf)	
1	62	3/4	0.007	69	0.50	Fine cracking
2	62	3/4	0.007	70	0.51	Fine cracking
3	62	3/4	0.007	67	0.46	Fine cracking
4	62	3/4	0.007	60	0.37	Fine cracking
5	62	3/4	0.007	72	0.53	Fine cracking
6	62	3/4	0.007	70	0.50	Fine cracking
7	62	3/4	0.007	66	0.45	Fine cracking
8	62	3/4	0.007	61	0.38	Fine cracking
9	62	3/4	0.007	62	0.39	Fine cracking
10	62	3/4	0.007	61	0.39	Smaller cracked area
11	62	3/4	0.007	64	0.42	Smaller cracked area
12	62	3/4	0.007	63	0.40	Fine cracking
13	62	3/4	0.007	61	0.39	Fine cracking
14	62	3/4	0.007	61	0.39	Fine cracking
15	62	3/4	0.007	64	0.42	Fine cracking
16	62	3/4	0.007	61	0.38	Fine cracking
17	62	3/4	0.007	64	0.42	Fine cracking

Table A-25
Reinforced Plastic
Polyester Resin With Glass Fiber Mat
0.040 in. Thick

Specimen No. 3

Impact Location	Desired Terminal Velocity (ft/s)	Ice Ball				Results of Impact
		Nominal Diameter (in.)	Weight Mass (lbm)	Velocity (ft/s)	Kinetic Energy (ft-lbf)	
1	82	1-1/4	0.029	82	3.0	Leaked
2	82	1-1/4	0.029	85	3.2	Fine cracking
3	82	1-1/4	0.029	82	3.0	Leaked
4	82	1-1/4	0.031	88	3.7	Leaked
5	82	1-1/4	0.031	82	3.1	Leaked
6	82	1-1/4	0.031	81	3.1	Leaked
7	82	1-1/4	0.031	83	3.3	Fine cracking
8	82	1-1/4	0.031	86	3.5	Leaked
9	82	1-1/4	0.031	84	3.4	Leaked
10	82	1-1/4	0.031	81	3.1	Leaked
11	82	1-1/4	0.031	90	3.9	Leaked
12	82	1-1/4	0.031	86	3.6	Fine cracking
13	82	1-1/4	0.031	83	3.4	Leaked
14	82	1-1/4	0.031	81	3.1	Leaked
15	82	1-1/4	0.031	81	3.2	Leaked
16	82	1-1/4	0.031	82	3.2	Leaked
17	82	1-1/4	0.031	82	3.2	Fine cracking

Table A-26
Reinforced Plastic
Polyester Resin With Glass Fiber Mat
0.040 in. Thick

Specimen No. 4

Impact Location	Desired Resultant Velocity (ft/s)	Ice Ball				Results of Impact
		Nominal Diameter (in.)	Weight Mass (lbm)	Velocity (ft/s)	Kinetic Energy (ft-lbf)	
1	105	1-1/4	0.031	111	5.9	Fine cracking
2	105	1-1/4	0.031	108	5.5	Leaked
3	105	1-1/4	0.031	105	5.3	Leaked
4	105	1-1/4	0.031	101	4.9	Leaked
5	105	1-1/4	0.031	103	5.1	Leaked
6	105	1-1/4	0.031	108	5.6	Leaked
7	105	1-1/4	0.031	104	5.1	Leaked
8	105	1-1/4	0.031	104	5.2	Leaked
9	105	1-1/4	0.031	107	5.5	Leaked
10	105	1-1/4	0.031	101	4.9	Leaked
11	105	1-1/4	0.031	105	5.3	Leaked
12	105	1-1/4	0.031	97	4.4	Leaked
13	105	1-1/4	0.031	106	5.4	Cracking
14	105	1-1/4	0.031	107	5.5	Leaked
15	105	1-1/4	0.031	99	4.7	Leaked
16	105	1-1/4	0.031	110	5.8	Break through
17	105	1-1/4	0.031	108	5.6	Break through

Table A-27
Reinforced Plastic
Polyester Resin With Glass Fiber Mat
0.040 in. Thick

Specimen No. 5

Impact Location	Desired Resultant Velocity (ft/s)	Ice Ball				Results of Impact
		Nominal Diameter (in.)	Weight Mass (lbm)	Velocity (ft/s)	Kinetic Energy (ft-lbf)	
1	112	1-1/2	0.055	98	8.3	Break through
2	112	1-1/2	0.055	107	9.7	Break through
3	112	1-1/2	0.055	117	11.7	Break through
4	112	1-1/2	0.055	106	9.7	Break through
5	112	1-1/2	0.055	110	10.3	Break through
6	112	1-1/2	0.055	110	10.4	Break through
7	112	1-1/2	0.054	112	10.6	Break through
8	112	1-1/2	0.055	111	10.6	Break through
9	112	1-1/2	0.055	111	10.6	Break through
10	112	1-1/2	0.055	109	10.2	Break through
11	112	1-1/2	0.055	116	11.5	Break through
12	112	1-1/2	0.054	111	10.3	Break through
13	112	1-1/2	0.055	116	11.6	Break through
14	112	1-1/2	0.055	113	11.0	Break through
15	112	1-1/2	0.055	113	11.0	Break through
16	112	1-1/2	0.055	111	10.6	Break through
17	112	1-1/2	0.055	114	11.2	Break through

Table A-28
Reinforced Plastic
Polyester Resin With Glass Fiber Mat
0.040 in. Thick

Specimen No. 6

Impact Location	Desired Terminal Velocity (ft/s)	Ice Ball				Results of Impact
		Nominal Diameter (in.)	Weight Mass (lbm)	Velocity (ft/s)	Kinetic Energy (ft-lbf)	
1	82	1-1/4	0.029	79	2.8	Fine cracking
2	82	1-1/4	0.029	82	3.0	Fine cracking
3	82	1-1/4	0.031	84	3.4	Leaked
4	82	1-1/4	0.029	91	3.7	Leaked
5	82	1-1/4	0.029	82	3.0	Leaked
6	82	1-1/4	0.031	83	3.3	Leaked
7	82	1-1/4	0.031	89	3.8	Leaked
8	82	1-1/4	0.029	81	2.9	Leaked
9	82	1-1/4	0.031	81	3.1	Leaked

Table A-29
Reinforced Plastic
Polyester Resin With Glass Fiber Mat
0.040 in. Thick

Specimen No. 7

Impact Location	Desired Terminal Velocity (ft/s)	Ice Ball				Results of Impact
		Nominal Diameter (in.)	Weight Mass (lbm)	Velocity (ft/s)	Kinetic Energy (ft-lbf)	
1	97	1-3/4	0.086	115	18	Break through
2	97	1-3/4	0.088	102	14	Break through
3	97	1-3/4	0.088	99	14	Break. Large deformation
4	97	1-3/4	0.086	97	12	Break through
5	97	1-3/4	0.088	100	14	Break through
6	97	1-3/4	0.088	101	14	Full Penetration
7	97	1-3/4	0.088	98	13	Break through
8	97	1-3/4	0.086	97	12	Break. Large deformation
9	97	1-3/4	0.088	99	13	Break through

Table A-30
Poly(Vinyl Fluoride) Film
0.004 in. Thick

Specimen No. 1

Impact Location	Desired Terminal Velocity (ft/s)	Ice Ball				Results of Impact
		Nominal Diameter (in.)	Weight Mass (lbm)	Velocity (ft/s)	Kinetic Energy (ft-lbf)	
1	62	3/4	0.007	61	0.38	Slight damage
2	62	3/4	0.007	63	0.41	Slight damage
3	62	3/4	0.007	67	0.46	Slight damage
4	62	3/4	0.007	69	0.49	Slight damage
5	62	3/4	0.007	64	0.42	Slight damage
6	62	3/4	0.007	61	0.38	Slight damage
7	62	3/4	0.007	62	0.40	Slight damage
8	62	3/4	0.007	59	0.36	Slight damage
9	62	3/4	0.007	67	0.46	Slight damage
10	62	3/4	0.007	66	0.45	Slight damage
11	62	3/4	0.007	60	0.37	Slight damage
12	62	3/4	0.007	59	0.36	Slight damage
13	62	3/4	0.007	66	0.45	Slight damage
14	62	3/4	0.007	68	0.47	Slight damage
15	62	3/4	0.007	63	0.41	Slight damage
16	62	3/4	0.007	62	0.39	Slight damage
17	62	3/4	0.007	60	0.37	Slight damage

Table A-31
Poly(Vinyl Fluoride) Film
0.004 in. Thick

Specimen No. 1

Impact Location	Desired Resultant Velocity (ft/s)	Ice Ball			Kinetic Energy (ft-lbf)	Results of Impact
		Nominal Diameter (in.)	Weight Mass (lbm)	Velocity (ft/s)		
1	91	3/4	0.007	98	0.90	Slight damage
2	91	3/4	0.007	86	0.76	Slight damage
3	91	3/4	0.007	97	0.97	Slight damage
4	91	3/4	0.007	97	0.97	Slight damage
5	91	3/4	0.007	91	0.84	Slight damage
6	91	3/4	0.007	98	0.99	Slight damage
7	91	3/4	0.007	98	0.98	Slight damage
8	91	3/4	0.007	97	0.97	Slight damage
9	91	3/4	0.007	96	0.95	Slight damage
10	91	3/4	0.007	96	0.95	Slight damage
11	91	3/4	0.007	113	1.32	Slight damage
12	91	3/4	0.007	112	1.29	Slight damage
13	91	3/4	0.007	94	0.91	Slight damage
14	91	3/4	0.007	99	1.01	Slight damage
15	91	3/4	0.007	93	0.90	Slight damage
16	91	3/4	0.007	92	0.87	Slight damage
17	91	3/4	0.007	91	0.85	Slight damage

Table A-32
Poly(Vinyl Fluoride) Film
0.004 in. Thick

Specimen No. 2

Impact Location	Desired Resultant Velocity (ft/s)	Ice Ball			Kinetic Energy (ft-lbf)	Results of Impact
		Nominal Diameter (in.)	Weight Mass (lbm)	Velocity (ft/s)		
1	73	1	0.015	81	1.6	Slight damage
2	73	1	0.015	69	1.1	Slight damage
3	73	1	0.015	72	1.2	Slight damage
4	73	1	0.015	76	1.4	Slight damage
5	73	1	0.015	71	1.2	Slight damage
6	73	1	0.015	72	1.3	Slight damage
7	73	1	0.015	75	1.3	Slight damage
8	73	1	0.015	75	1.4	Slight damage
9	73	1	0.015	74	1.3	Slight damage
10	73	1	0.015	73	1.3	Slight damage
11	73	1	0.015	74	1.3	Slight damage
12	73	1	0.015	74	1.3	Slight damage
13	73	1	0.015	77	1.4	Slight damage
14	73	1	0.015	80	1.5	Slight damage
15	73	1	0.015	79	1.5	Slight damage
16	73	1	0.015	72	1.2	Slight damage
17	73	1	0.015	74	1.3	Slight damage

Table A-33
Poly(Vinyl Fluoride) Film
0.004 in. Thick

Specimen No. 2

Impact Location	Desired Resultant Velocity (ft/s)	Ice Ball			Kinetic Energy (ft-lbf)	Results of Impact
		Nominal Diameter (in.)	Weight Mass (lbm)	Velocity (ft/s)		
1	98	1	0.015	99	2.3	Slight damage
2	98	1	0.015	103	2.6	Slight damage
3	98	1	0.015	95	2.2	Slight damage
4	98	1	0.015	101	2.5	Slight damage
5	98	1	0.015	103	2.6	Slight damage
6	98	1	0.015	107	2.7	Slight damage
7	98	1	0.015	99	2.4	Slight damage
8	98	1	0.015	101	2.4	Slight damage
9	98	1	0.015	97	2.2	Slight damage
10	98	1	0.015	99	2.4	Slight damage
11	98	1	0.015	101	2.4	Slight damage
12	98	1	0.015	95	2.2	Slight damage
13	98	1	0.015	100	2.4	Slight damage
14	98	1	0.015	105	2.6	Slight damage
15	98	1	0.015	98	2.3	Slight damage
16	98	1	0.015	95	2.2	Slight damage
17	98	1	0.015	98	2.3	Slight damage

Table A-34
Poly(Vinyl Fluoride) Film
0.004 in. Thick

Specimen No. 3

Impact Location	Desired Velocity (ft/s)	Ice Ball			Kinetic Energy (ft-lbf)	Results of Impact
		Nominal Diameter (in.)	Weight Mass (lbm)	Velocity (ft/s)		
1	82	1-1/4	0.031	91	4.0	0.13 in. indent.
2	82	1-1/4	0.031	80	3.1	
3	82	1-1/4	0.031	81	3.2	
4	82	1-1/4	0.031	78	2.9	
5	105	1-1/4	0.031	104	5.1	
6	105	1-1/4	0.031	109	5.7	
7	82	1-1/4	0.031	82	3.3	
8	82	1-1/4	0.031	82	3.2	
9	82	1-1/4	0.031	77	2.9	
10	105	1-1/4	0.031	107	5.5	
11	105	1-1/4	0.031	108	5.6	
12	105	1-1/4	0.031	102	5.0	0.19 in. indent.
13	90	1-1/2	0.055	88	6.6	0.34 in. indent.
14	90	1-1/2	0.055	82	5.8	0.34 in. indent.
15	112	1-1/2	0.055	104	9.3	
16	105	1-1/4	0.031	107	5.5	
17	105	1-1/4	0.031	108	5.6	

Table A-35
Poly(Vinyl Fluoride) Film
0.004 in. Thick

Specimen No. 4

Impact Location	Desired Terminal Velocity (ft/s)	Ice Ball			Kinetic Energy (ft-lbf)	Results of Impact
		Nominal Diameter (in.)	Weight Mass (lbm)	Velocity (ft/s)		
1	105	2	0.130	95	18	0.50 in. indent.
2	105	2	0.130	91	19	Break
3	105	2	0.130	100	20	0.70 in. indent.
4	105	2	0.130	95	18	0.70 in. indent.
5	105	2	0.130	99	20	0.72 in. indent.
6	105	2	0.132	108	24	Break
7	105	2	0.132	107	23	Break
8	105	2	0.132	105	23	Break
9	105	2	0.132	106	23	Break

Table A-36
Poly(Vinyl Fluoride) Film
0.004 in. Thick

Specimen No. 5

Impact Location	Desired Resultant Velocity (ft/s)	Ice Ball			Kinetic Energy (ft-lbf)	Results of Impact
		Nominal Diameter (in.)	Weight Mass (lbm)	Velocity (ft/s)		
1	117	1-3/4	0.086	109	16	0.60 in. indent.
2	117	1-3/4	0.086	113	17	Break
3	117	1-3/4	0.086	117	18	Break
6	117	1-3/4	0.086	115	18	Break
7	117	1-3/4	0.086	116	18	Break
8	117	1-3/4	0.086	117	18	Break
9	117	1-3/4	0.086	109	16	0.60 in. indent.

Table A-37
Poly(Vinyl Fluoride) Film
0.004 in. Thick

Specimen No. 6

Impact Location	Desired Terminal Velocity (ft/s)	Ice Ball				Results of Impact
		Nominal Diameter (in.)	Weight Mass (lbm)	Velocity (ft/s)	Kinetic Energy (ft-lbf)	
1	97	1-3/4	0.086	92	11	0.40 in. indent.
2	97	1-3/4	0.088	105	15	0.55 in. indent.
3	97	1-3/4	0.086	97	12	0.45 in. indent.
4	97	1-3/4	0.086	100	13	0.48 in. indent.
5	97	1-3/4	0.086	103	14	0.55 in. indent.
6	97	1-3/4	0.086	101	14	0.52 in. indent.
7	97	1-3/4	0.088	105	15	0.55 in. indent.
8	97	1-3/4	0.086	100	14	0.50 in. indent.
9	97	1-3/4	0.086	100	13	0.55 in. indent.
10	97	1-3/4	0.086	96	12	Break
11	97	1-3/4	0.086	98	13	0.52 in. indent.
12	97	1-3/4	0.086	98	13	0.65 in. indent.
13	97	1-3/4	0.086	97	13	0.65 in. indent.
14	97	1-3/4	0.086	104	15	Break
15	97	1-3/4	0.086	100	13	Break
16	97	1-3/4	0.086	107	15	Break
17	97	1-3/4	0.086	101	14	Break

Table A-38
Tempered Glass
Both Sides Smooth
1/8 in. Thick
Mounted in Solar Collector

Specimen No. A

Impact Location	Desired Resultant Velocity (ft/s)	Ice Ball				Results of Impact
		Nominal Diameter (in.)	Weight Mass (lbm)	Velocity (ft/s)	Kinetic Energy (ft-lbf)	
1 (4 in. right)	117	1-3/4	0.095	130	25	No visible damage
1 (4 in. right)	117	1-3/4	0.095	128	24	No visible damage
1 (4 in. right)	117	1-3/4	0.095	129	25	No visible damage
1 (6 in. left)	124	2	0.141	130	37	No visible damage
1 (6 in. left)	124	2	0.141	132	38	No visible damage
1 (6 in. left)	124	2	0.143	128	36	No visible damage
1	134	2	0.141	132	38	No visible damage
1 (4 in. right)	134	2-1/2	0.276	135	78	Fracture

Table A-39
Tempered Glass
Both Sides Smooth
1/8 in. Thick
Mounted in Solar Collector

Specimen No. F

Impact Location	Desired Resultant Velocity (ft/s)	Ice Ball				Results of Impact
		Nominal Diameter (in.)	Weight Mass (lbm)	Velocity (ft/s)	Kinetic Energy (ft-lbf)	
1 (4 in. right)	117	1-3/4	0.093	129	24	No visible damage
1 (4 in. right)	117	1-3/4	0.093	119	20	Fracture

Table A-40
Tempered Glass
Both Sides Smooth
1/8 in. Thick
Mounted in Solar Collector

Specimen No. B

Impact Location	Desired Resultant Velocity (ft/s)	Ice Ball				Results of Impact
		Nominal Diameter (in.)	Weight Mass (lbm)	Velocity (ft/s)	Kinetic Energy (ft-lbf)	
11	124	2	0.134	133	37	No visible damage
11	124	2	0.143	127	36	No visible damage
11	124	2	0.141	122	33	No visible damage
11	124	2	0.139	127	35	No visible damage
11	124	2	0.141	125	34	No visible damage
10	134	2-1/2	0.276	136	79	No visible damage
10	134	2-1/2	0.276	136	79	No visible damage
10	134	2-1/2	0.276	136	79	No visible damage
10	134	2-1/2	0.273	137	80	No visible damage
10	134	2-1/2	0.278	136	80	Fracture

Table A-41
Tempered Glass
Both Sides Smooth
1/8 in. Thick
Mounted in Solar Collector

Specimen No. E

Impact Location	Desired Resultant Velocity (ft/s)	Ice Ball				Results of Impact
		Nominal Diameter (in.)	Weight Mass (lbm)	Velocity (ft/s)	Kinetic Energy (ft-lbf)	
11	124	2	0.137	128	35	No visible damage
11	124	2	0.137	125	34	No visible damage
11	124	2	0.134	129	35	No visible damage
11	124	2	0.134	125	33	No visible damage
11	124	2	0.134	132	36	No visible damage
10	124	2-1/2	0.273	136	79	Fracture

Table A-42
Tempered Glass
Both Sides Smooth
1/8 in. Thick
Mounted in Solar Collector

Specimen No. C

Impact Location	Desired Resultant Velocity (ft/s)	Ice Ball				Results of Impact
		Nominal Diameter (in.)	Weight Mass (lbm)	Velocity (ft/s)	Kinetic Energy (ft-lbf)	
11	117	1-3/4	0.093	119	20	No visible damage
14	117	1-3/4	0.093	118	20	No visible damage
15	124	2	0.139	130	36	No visible damage
15	124	2	0.141	132	38	No visible damage
15	124	2	0.141	129	36	No visible damage
15	124	2	0.139	126	34	No visible damage
15	124	2	0.139	130	36	No visible damage
14	124	2-1/2	0.280	138	83	No visible damage
14	124	2-1/2	0.273	137	80	Fracture

Table A-43
Tempered Glass
Both Sides Smooth
1/8 in. Thick
Mounted in Solar Collector

Specimen No. D

Impact Location	Desired Resultant Velocity (ft/s)	Ice Ball				Results of Impact
		Nominal Diameter (in.)	Weight Mass (lbm)	Velocity (ft/s)	Kinetic Energy (ft-lbf)	
14	117	1-3/4	0.093	121	21	No visible damage
14	117	1-3/4	0.093	115	19	Fracture

U.S. DEPT. OF COMM. BIBLIOGRAPHIC DATA SHEET <i>(See Instructions)</i>	1. PUBLICATION OR REPORT NO. NBSIR 82-2487	2. Performing Organ. Report No.	3. Publication Date March 1982
4. TITLE AND SUBTITLE <p>Hail Impact Testing Procedure for Solar Collector Covers</p>			
5. AUTHOR(S) David R. Jenkins and Robert G. Mathey			
6. PERFORMING ORGANIZATION <i>(If joint or other than NBS, see instructions)</i> NATIONAL BUREAU OF STANDARDS DEPARTMENT OF COMMERCE WASHINGTON, D.C. 20234		7. Contract/Grant No. 8. Type of Report & Period Covered	
9. SPONSORING ORGANIZATION NAME AND COMPLETE ADDRESS <i>(Street, City, State, ZIP)</i> U.S. Department of Energy Office of Solar Heat Technologies Active Heating and Cooling Division Washington, DC 20585			
10. SUPPLEMENTARY NOTES <input type="checkbox"/> Document describes a computer program; SF-185, FIPS Software Summary, is attached.			
11. ABSTRACT <i>(A 200-word or less factual summary of most significant information. If document includes a significant bibliography or literature survey, mention it here)</i> <p>This report presents laboratory test results which simulate hail impact on solar collector covers. The general objective of the work is to contribute to the development of a test method for evaluating the resistance of solar collector covers to this type of loading. A procedure for such testing is described as well as results obtained with ice balls impacting four typical collector cover materials. Aspects which are discussed include the preparation of ice balls, the design and operation of a launcher for ice ball propulsion, the method of mounting cover panel specimens, the selection of ice ball velocity and impact location, and techniques for failure or damage assessment.</p> <p>The research results show that ice balls of consistent diameter and mass can be prepared in the laboratory. Further, both analysis and results tend to show that acceptable simulation for evaluation or testing can be achieved with normal impacts of ice balls traveling at a resultant velocity which is the vector sum of the terminal velocity and a horizontal wind component. Results for a variety of impact locations are presented and for comparison purposes, arbitrarily selected points near the collector cover boundaries appear to be a reasonable choice. Finally, it is shown that for some collector cover materials, more than one kind of failure must be considered when evaluating test results. Test data for two types of tempered glass, semirigid fiber reinforced plastic, and flexible thin plastic film covers are presented.</p>			
12. KEY WORDS <i>(Six to twelve entries; alphabetical order; capitalize only proper names; and separate key words by semicolons)</i> hail damage; hail impact testing; hail launcher; simulated hail testing; solar collector covers; test method development			
13. AVAILABILITY <input checked="" type="checkbox"/> Unlimited <input type="checkbox"/> For Official Distribution. Do Not Release to NTIS <input type="checkbox"/> Order From Superintendent of Documents, U.S. Government Printing Office, Washington, D.C. 20402. <input checked="" type="checkbox"/> Order From National Technical Information Service (NTIS), Springfield, VA. 22161		14. NO. OF PRINTED PAGES 86 15. Price \$10.50	

